PROCESS SYSTEM REQUIREMENTS OF THE MIT REACTOR AT FIVE MEGAWATTS

WILLIAM R. DEVOTO

AUGUST 1962

MIT-NE-23

MIT RESEARCH REACTOR

DEPARTMENT OF NUCLEAR ENGINEERING

MASSACHUSETTS INSTITUTE OF TECHNOLOGY

CAMBRIDGE , MASSACHUSETTS

PROCESS SYSTEM REQUIREMENTS OF THE MIT REACTOR AT FIVE MEGAWATTS

by

WILLIAM ROBERT DEVOTO
B.S., United States Military Academy
(1956)

Submitted in partial fulfillment
of the requirements for
the degrees of
NUCLEAR ENGINEER
and
MASTER OF SCIENCE
at the
MASSACHUSETTS INSTITUTE OF TECHNOLOGY
August 1962

ABSTRACT

PROCESS SYSTEM REQUIREMENTS OF THE MIT REACTOR

AT FIVE MEGAWATTS

BY

William Robert Devoto

Submitted to the Department of Nuclear Engineering on August 20, 1962, in partial fulfillment of the requirements for the degrees of Nuclear Engineer and Master of Science.

Operating ranges of the major process systems of the MIT Reactor are projected to a power level of five megawatts. Reasonable limitations are set on the maximum fuel plate temperature and the bulk temperature of the D_2O primary coolant. A lower limit is placed on the flow rate of the primary coolant. Consistent with these limitations, the fuel loading per element is limited according to the amount of excess reactivity in the core.

The flow rate of the H_2O secondary coolant necessary to remove the heat load from the primary system under the above limitations is investigated. The efficiency of the cooling tower which cools the secondary coolant is evaluated and projected to five megawatts. The shield coolant system is examined under five megawatt conditions. Recommendations are made as to additional equipment necessary to provide adequate, compatible process systems for operation of the MITR at a power level of five megawatts.

Thesis Supervisor: Theos J. Thompson
Title: Professor of Nuclear Engineering
Director of the MIT Reactor

ACKNOWLEDGEMENTS

The author is indebted to his thesis supervisor, Prof. T.J. Thompson, for his guidance and constructive comments on all phases of this work. The author also wishes to thank Prof. D.D. Lanning for helpful discussions and useful suggestions concerning many of the problems encountered.

Many members of the operating and maintenance staff of the MITR contributed valuable assistance with the experimental portions of this work. Their efforts are sincerely appreciated.

Calculations of axial flux distributions were carried out on the IBM 7090 at the MIT Computation Center. The author wishes to thank Mr. E. Pilat for his invaluable assistance with this program. The courtesy of Brookhaven National Laboratories in supplying the code deck is appreciated.

TABLE OF CONTENTS

LIST OF FIGURES

TABLES

SECTION I

INTRODUCTION

The objective of this study was to predict, on the basis of experiments and theoretical calculations, the process requirements of the M I T Reactor at a power level of five megawatts. The original nuclear design of the system envisioned operating powers of five megawatts or greater, however, the associated cooling equipment was designed to serve primarily during the initial phases of operation, and expanded capacity was planned for higher power operation. Initial space provisions were made for the necessary equipment.

This study began inside the fuel element itself. Nuclear, as well as thermal properties, predicted the hottest element and, further, which plate would sustain the highest temperatures. An analysis depending on the rate of flow of the cooling fluid predicted the point of highest surface temperature. The temperature at this point was limited by the requirement that no surface boiling occur in the facility.

Two separate series of experiments at operating powers up to two megawatts produced a well-correlated value for the coefficient of convective heat transfer on the surface of the fuel element plates which was used

in this analysis. A limitation was then placed on the maximum bulk temperature of the coolant under the most severe operating conditions. With these restrictions the necessary flow rate was evolved.

Attention was next given to the main heat exchanger. The general plan indicated the need for another heat exchanger of the required capacity to be installed in parallel with the existing system. This concept of parallel circuits is employed throughout the reactor facility whenever possible both for reasons of safety and to insure at least limited operation in the event of the failure of any component. It was, therefore, necessary to investigate the capabilities of the installed heat exchanger and to arrive at a theoretical model of its performance at current operating levels. On the basis of this model a prediction was made of the heat exchanger limitations at the five megawatt operating conditions.

Two separate experiments were conducted on the system primarily to establish the variation in overall coefficient of heat transfer with flow rate on the secondary side of the exchanger. These studies also produced an approximate value for the resistance to heat flow due to scaling on the outside of the tubes of the heat exchanger. A third result of these experiments was temperature corrections

which were applied to the convective heat transfer coefficients on the inside and outside of the heat exchanger tubes. These temperature corrections were later confirmed by a separate experiment.

Knowing the variation of the overall coefficient of heat transfer with flow rate and knowing the amount of heat it was necessary to transfer, the flow rate on the secondary side of the heat exchanger necessary to maintain the correct reactor operating conditions under the most severe limitations on heat removal was calculated. Through the above method the present heat exchanger was found to be adequate to remove one half of the heat load at five megawatts. A heat exchanger identical to the installed one has been ordered to be placed in the above-mentioned parallel circuit to remove the remainder of the heat load.

Although most of the heat generated in the MITR is removed by the primary coolant, a small percentage of the heat is carried away by the distilled H_2O in the shield coolant system. This system has its own separate heat exchanger, therefore, calculations were necessary to evaluate the impact of the increased heat load on these components.

The first information necessary for this analysis was the exact amount of heat carried away by the shield

at present operating levels. This quantity was readily calculated from corrected operating data. The assumption was then made that the percentage of heat carried by the shield coolant will be the same at five megawatts as it is at two megawatts. The reasons for this assumption are stated. With this information the heat load on the shield coolant system at five megawatts was predicted.

The next step was to perform a heat exchanger experiment on Heat Exchanger No. 3 similar to the one used on Heat Exchanger No. 1. The resulting plot of $1/UA$ vs. $1/w_o^{.6}$ gave a means of predicting the resistance to heat flow in the heat exchanger at five megawatts.

Since there is no pump on the secondary side of the shield heat removal system, and since Heat Exchanger No. 3 is in parallel with Heat Exchanger No. 1 secondary, the flow rate is determined by pressure drop considerations. A method was, therefore, evolved to calculate the secondary flow rate in Heat Exchanger No. 3 under the five megawatt operating conditions. With this information the temperature of the primary shield coolant at five megawatts can be predicted or conversely, the temperature of the shield coolant can be limited and the flow rates necessary to maintain these limits can be calculated. From these studies recommendations were made as to the addition of new equipment to the system.

The last experimental section deals with the cooling tower. Neither the total amount of water flowing through the facility nor its entering temperature are accurately known. Exact calculations involving this structure were, therefore, unwarranted and proved to be unnecessary. An experiment was devised to approximate the performance of the cooling tower under diverse conditions of temperature, relative humidity, and power level.

The wet-bulb temperature of the air in the vicinity of the cooling tower was plotted against the temperature of the outlet water from the cooling tower during a period of approximately two months during midsummer. Using the results of this study, the maximum temperature of the water to be supplied to the secondary cooling system at five megawatts was predicted.

The first section of this paper summarizes the principal experimental results and theoretical predictions. On this basis conclusions are drawn and recommendations are made.

It should be emphasized at the outset that this is essentially a limiting study. In all assumptions and calculations the safest or most conservative alternative has been selected. The most severe hazards of weather and operating conditions have been envisioned and employed as routine. As an example, in the limiting calculation

of the heat generation in the hottest element a very compact core arrangement was employed that utilized no elements in the outside ring. Six elements are presently placed in this ring for two-megawatt operation. For five-megawatt operation, it is highly unlikely (although theoretically possible) that the reactor core would be further compacted. This compact core resulted in greater flux peaking and ultimately meant a higher rate of heat generation in the hottest element. Enlarged cores were also calculated to prove the validity of this statement.

As more fuel is loaded into the core and excess reactivity is present in varying amounts, there are times when the reactor will be at power with the control rod bank inserted as much as 10 inches into the core. The effect of the control rods in varying the flux shape in the core has been taken into account wherever applicable. Some calculations also employed a fresh 162-gram element in the hottest position. Operating rules of the MITR provide that fresh elements are always inserted in the edge of the core and partially burned elements moved toward the center with the result that the element occupying the center (hottest) position is always partially burned out.

Extending this philosophy into process system operating conditions required the use of the hottest

summer day for the calculation of the cooling requirements. For this investigation a wet-bulb temperature of 78°F was employed. This corresponds to an air temperature of 78°F at 100 per cent relative humidity, or 96°F at 50 per cent relative humidity. Even in the unlikely event that these liberal limiting temperatures were exceeded, any resulting operating time at reduced power would be very short indeed.

Experimental errors and their propagation through the calculations were examined. They were particularly investigated in the case of the H_2O requirements where a complete error analysis was carried through the entire calculation.

It is believed that the results of this study define the operating limits for five megawatts and that planning based on these figures will provide adequate process systems for operation at that power level.

SECTION II

DESCRIPTION OF THE MIT REACTOR

[2-1] GENERAL

The MITR is a heavy water cooled and moderated reactor used for research and educational purposes at the Massachusetts Institute of Technology. It is presently being operated at a power of two thermal megawatts, although the nuclear and structural design anticipates operation at power levels in excess of five megawatts. The inherent safety of a long thermal neutron lifetime combined with the utility of a large and versatile research volume characterize a reactor of this type.

[2-2] CORE

The fuel, moderator, and control rods of the MITR are contained in an aluminum core tank four ft. in diameter and approximately seven ft. high. The tank is filled with heavy water to a depth of approximately six ft., and the water surface is blanketed with helium. The active section of the fuel plates, which contains the uranium, is 23.375 ± .5 in. long. This gives a core height of about two ft. The fuel elements are suspended from the lower shield plug, which forms the lid of the core tank, so that approximately two ft. of heavy water remain both

above and below the core forming upper and lower reflectors.

Lateral stability is afforded by the nozzles in the plenum head below the core into which the lower extensions of the fuel elements fit. The plenum head is a sheet of aluminum curved and placed with its convex side upwards for strength, and it contains holes for each fuel element and control rod. The plenum's major function is to distribute the D_2O flow to the fuel elements. A section through the reactor in figure 1. indicates vertical positioning. The central fuel element position is located at the radial center of the tank. Positions 2 through 7 are equally spaced on a circle of radius 6.375 in. from the center. Positions 8 through 19 are equally spaced on a circle of radius 13.25 in. from the center. Positions 20 through 30 are irregularly spaced on a circle of radius 20.94 in. Fuel element positions are shown as squares in figure 2. Positions 20 through 30 may accommodate either fuel elements, arranged so as to enhance the fast flux in certain experimental ports, or sample irradiation thimbles, depending on experimental needs and fuel requirements.

The six control rods are equally spaced on a circle of radius 9.25 in. from the center of the reactor. A fine regulating rod is located 19.5 in. from the center of the core and on the centerline of the thermal column.

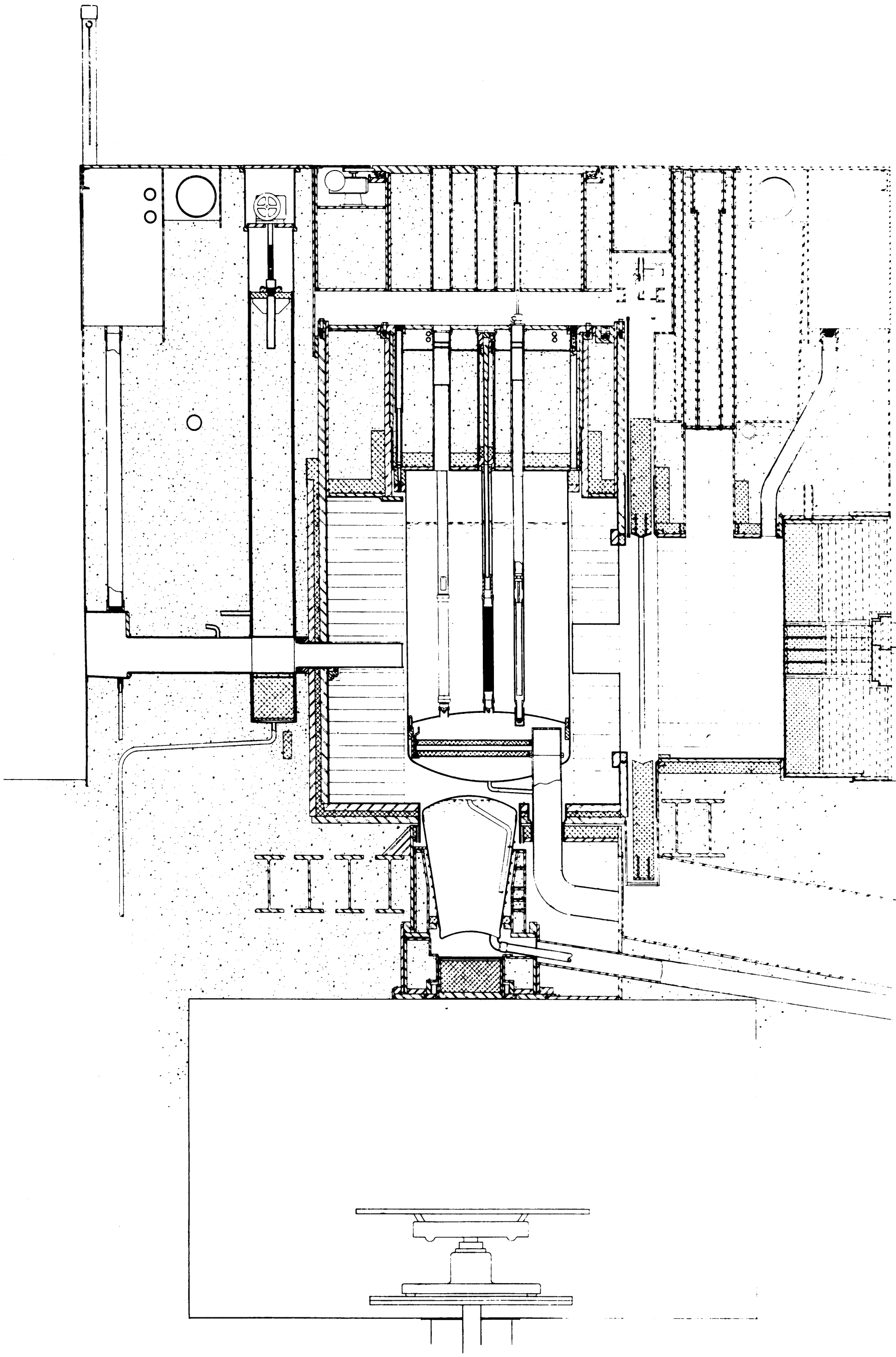

FIGURE 1

VERTICAL SECTION

THROUGH MITR

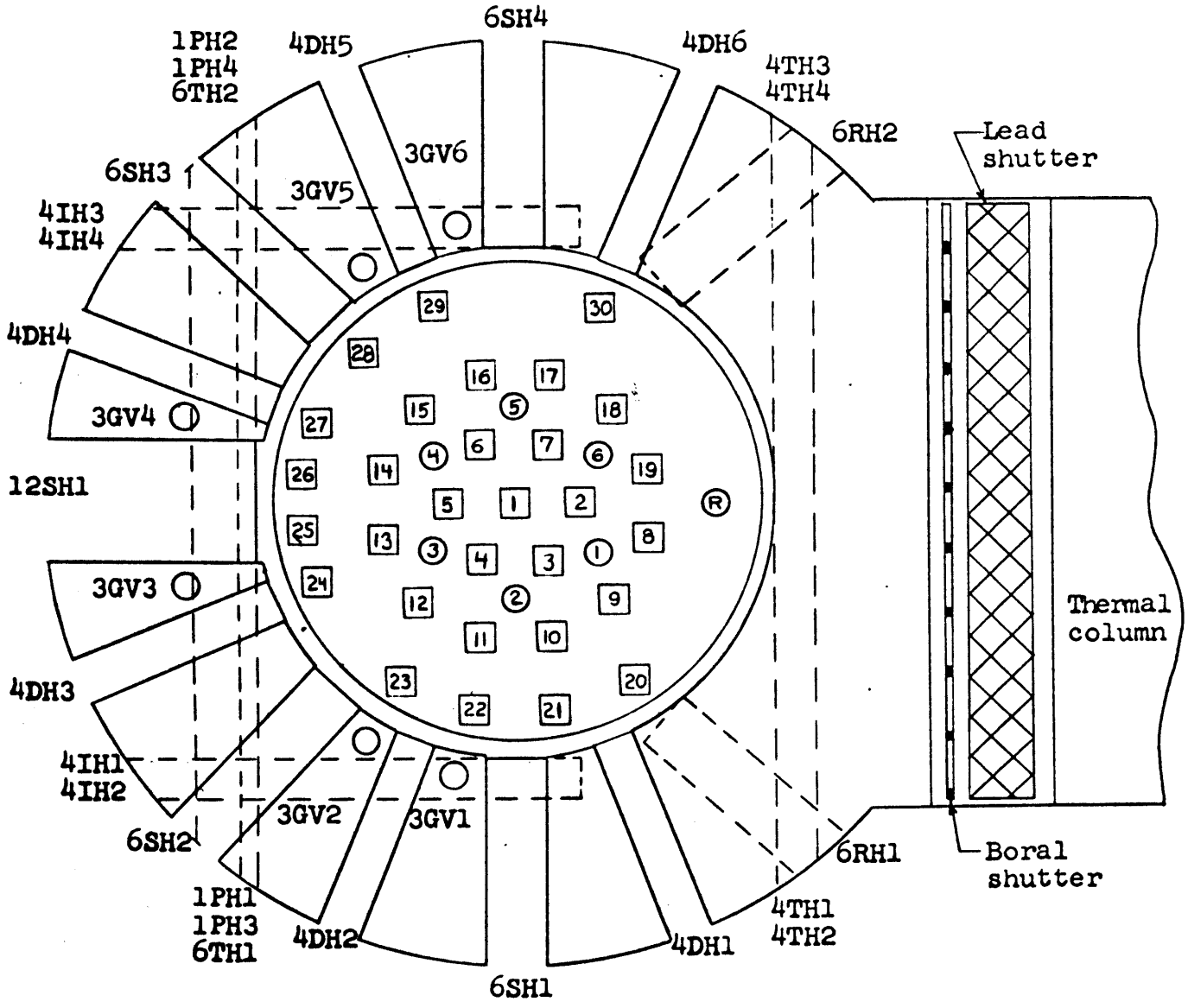

FIGURE 2

HORIZONTAL SECTION

THROUGH MITR

The control and regulating rods are shown as circles in figure 2.

In addition to the top and bottom reflectors previously discussed, the heavy water outside the 19 primary fuel positions can essentially be considered to be an 8-in. thick inner radial reflector. Outside the aluminum core tank there is a 1-in. helium-filled gap surrounded by a 2-ft. thick graphite radial reflector. Surrounding the graphite reflector is the thermal shield. This component is constructed of two concentric steel cylinders, each two in. thick. The inner cylinder has an inside diameter of eight feet and its inner surface is lined with 1/4 in. of boral. There is a one and one-half in. space between the cylinders which contains two sets of cooling coils. The remainder of the space between the cylinders has been filled with lead. Five and one-half feet of high density concrete complete the shielding of the MITR.

[2-3] FUEL ELEMENTS

The MITR fuel element is constructed of 18 plates 24.625 in. long and 2.996 in. wide curved on a radius of 5.5 in. The inner 16 plates contain uranium enriched to 94 per cent and alloyed with aluminum over 23.375 in. of their length. The uranium-aluminum alloy forms the center

.020 in. of each plate. This "meat" is then clad with .020-in. thick aluminum plates on each face to make a total "sandwich" thickness of .060 in. The outer two plates are of pure aluminum. These eighteen plates are then fastened to grooved aluminum side plates to form the fuel element box. The side plates maintain a plate spacing of .117 in. and form approximately rectangular channels through which the primary coolant flows. Further mechanical rigidity is assured through the use of plate-spacing combs at each end of the element. The outer plates do not contain fuel, therefore, all fuel-bearing surfaces are cooled by forced convection of the heavy water coolant. A fuel element cross section is shown in figure 3.

Standard fuel elements contain 160 $\pm$ 3 grams of uranium 235. In any one fuel plate the quantity of U-235 does not exceed 10 $\pm$ .3 grams. Some of the fuel elements from the initial fuel loading containing 104 $\pm$ 2 grams were still in use at the time of this work but were gradually being phased out. A few fractionally loaded elements containing 2/3 and 1/3 the standard amount of U-235 are available for special experiments.

The fuel element assembly consists of a shielding plug, an upper adaptor, the fuel element box itself, and

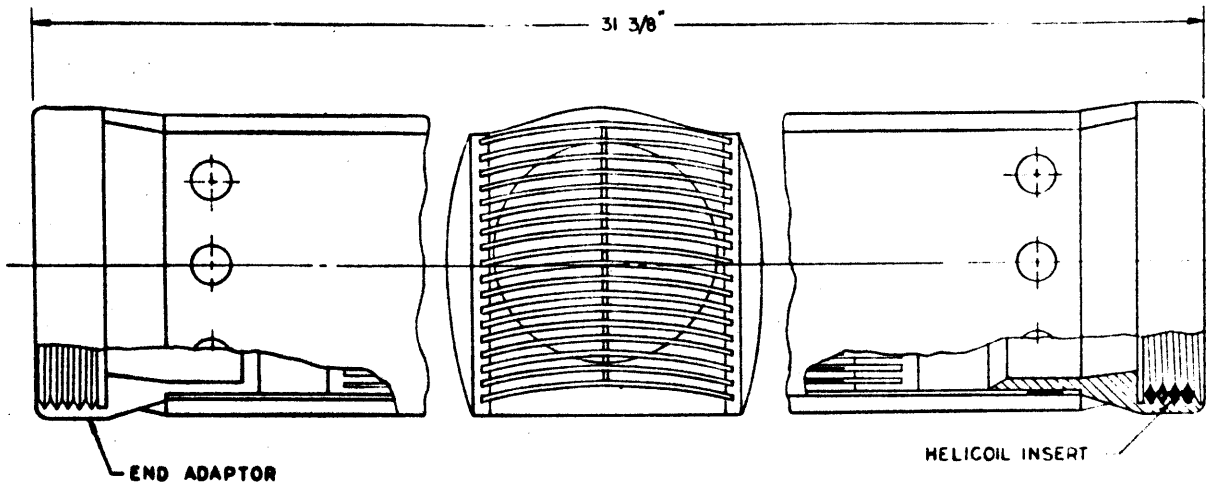

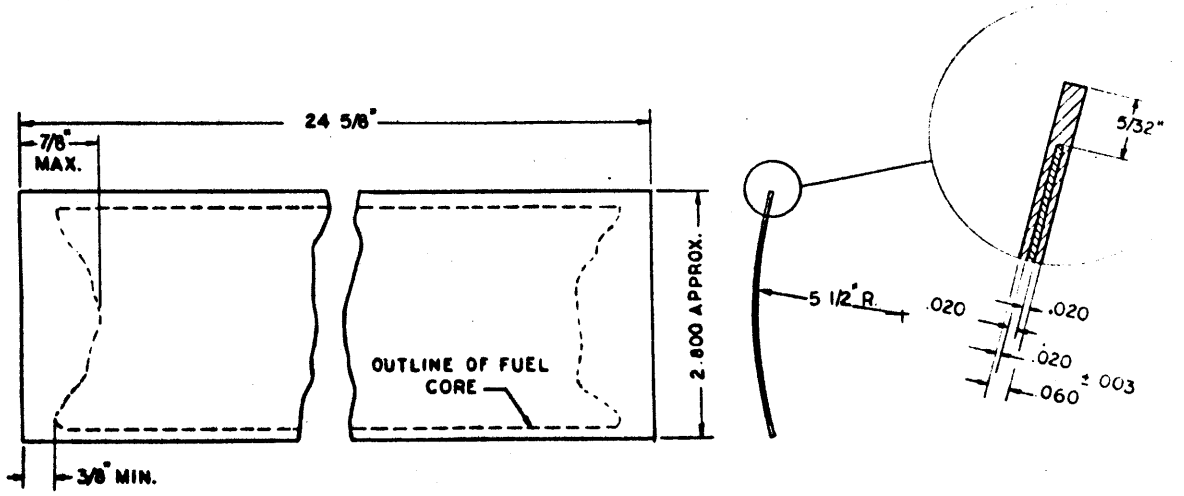

FUEL PLATE

MITR FUEL ELEMENT

FIGURE 3

the lower adaptor as shown in figure 4. As its name implies, the shielding plug fills the hole in the top shielding through which the element is inserted and withdrawn. Two serpentine holes in the shield plug provide for such things as thermocouple leads to the fuel plate surfaces and for gravity flow of D_2O from an emergency cooling tank down into the upper adaptor. This water then flows down through spray plates in the adaptor and onto the fuel plates in the event that the primary coolant is suddenly lost or dumped.

The upper adaptor is a 3-in. O. D. aluminum tube which connects the fuel element box to the lower shield plug and provides flow space for the emergency cooling water. The lower adaptor is a short nozzle which assists in seating the fuel element in the plenum head.

[2-4] CONTROL RODS

The six MITR control rods are combination shim and safety rods. The absorber section of each rod is a hollow cadmium cylinder .040 in. thick, 2.15 in. O.D., and 26.125 in. long sandwiched between two .050 in.layers of aluminum. Attached to the upper end of the absorber is an armature which may be magnetically coupled to the movable shim magnets. To lift the absorbers out of the core, current is applied to the magnet coupling the arma-

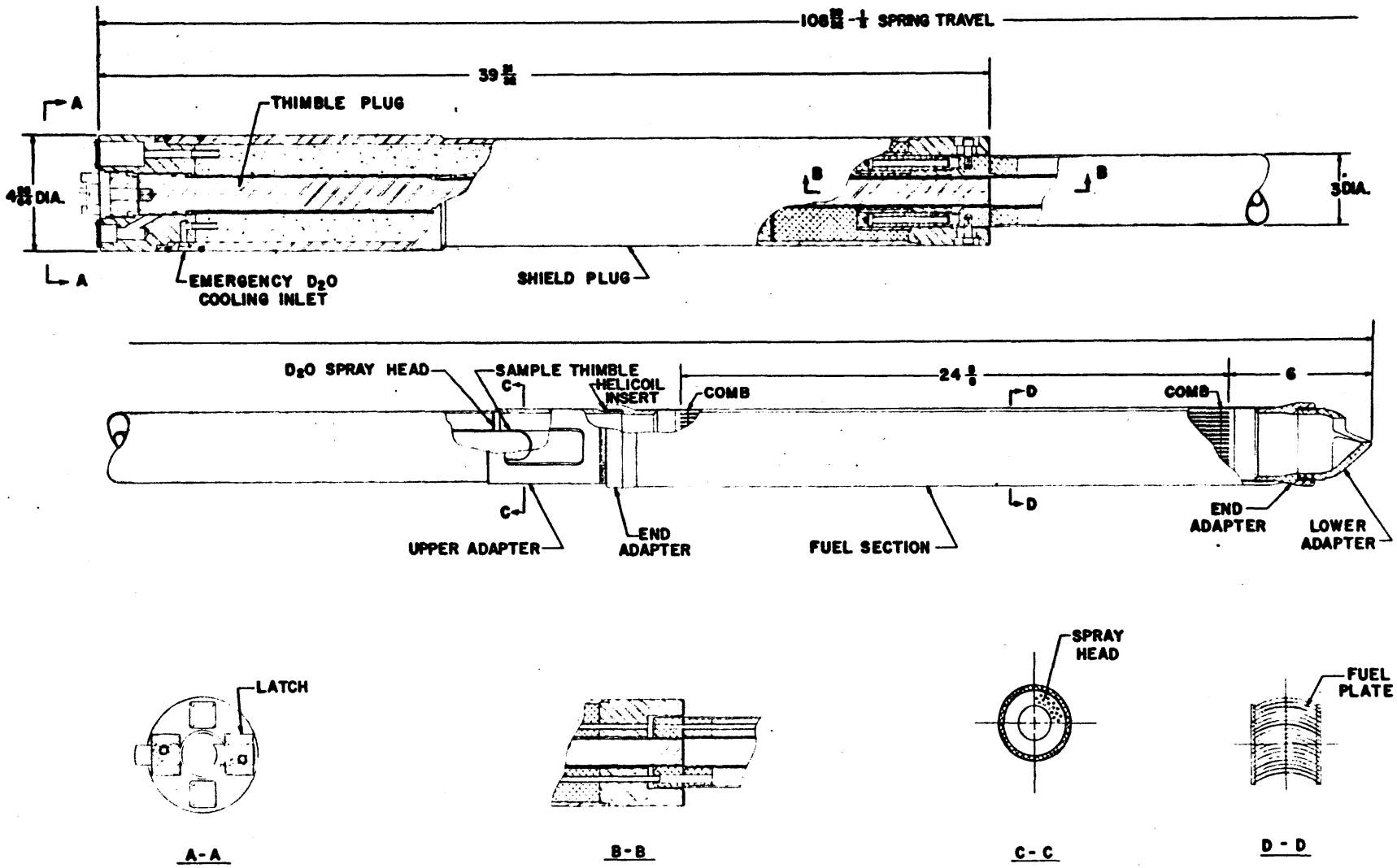

FUEL ELEMENT ASSEMBLY

FIGURE 4

ture, and the assembly is raised out of the core. The shim rods can be moved vertically over a distance of 27.2 ± .2 in. In the event that a quick reactor shutdown is required, the current to the magnets can be interrupted letting the absorber sections fall back by force of gravity. In this manner the reactor may be completely shut down in about .4 sec. Each of the control rods moves vertically inside a 5-in. diameter perforated aluminum guide tube. These sleeves hold the absorbers in a vertical position when they free fall into the core. A control rod assembly is illustrated in figure 5.

The regulating rod absorber is similar in construction to the control rods except that the cadmium "meat" covers only 1/3 of the circumference of the cylinder on the thermal column (least reactive) side. The regulating rod absorber is permanently connected to its drive mechanism so that it serves no immediate function in a reactor "scram." Its primary function is to effect minor changes in reactivity to provide a constant power level. It can be connected to an automatic power-sensing and compensating circuit.

[2-5] PRIMARY COOLANT SYSTEM

The heavy water in the MITR acts not only as a moderator, but also as the primary coolant. It is circulated

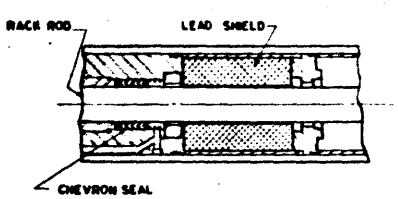

MIDDLE CASING DETAIL

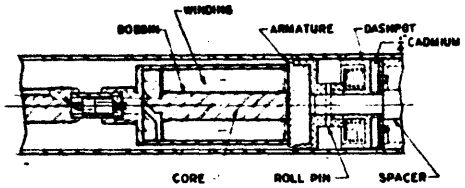

MAGNET DETAIL

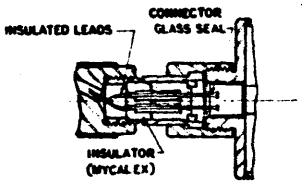

COUPLING DETAIL

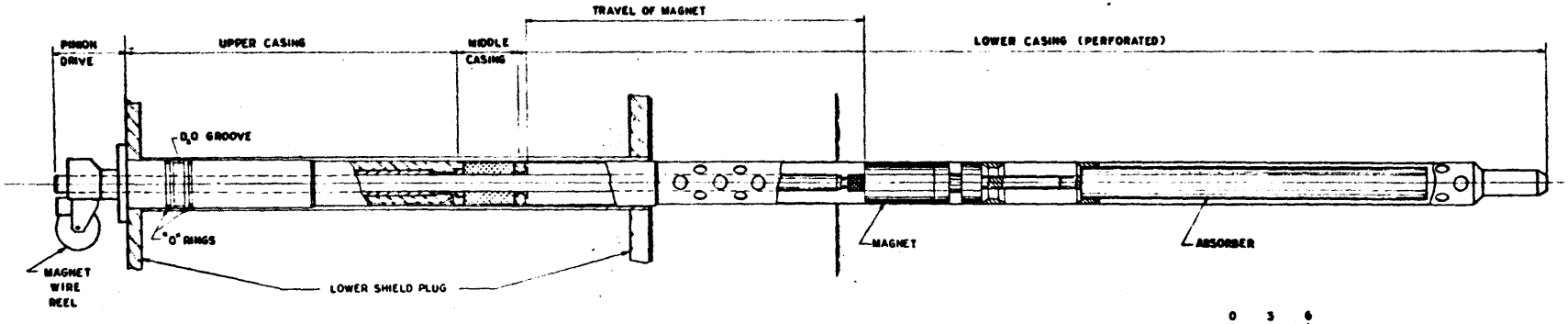

MODIFIED SHIM SAFETY ROD ASSEMBLY

FIGURE 5

at a rate of 875 GPM (at two megawatts) and exchanges the heat with a secondary coolant system of light water. The secondary coolant system then exhausts the heat to the atmosphere through evaporation in a cooling tower. Figure 6. shows the complete primary coolant system and figure 7. shows the complete secondary coolant system as they exist at 2 MW.

DM-1 is the main D_2O circulating pump. It has a capacity of 1000 GPM at 110 ft. head and is powered by a 40 HP motor. Normal exit pressure is 38 psi. After passing through the pump the coolant enters the tubes of Heat Exchanger No. 1. This heat exchanger is composed of 885 tubes of 3/8 in. O.D. and is of the single pass type. The tubes are 18 BWG thick and are constructed of stainless steel. They are mounted on a 1/2-in. square pitch and are 14 ft. 2 in. long. The outside area of the tubes is approximately 1230 sq. ft. The shell itself is 18 in. in diameter and incorporates 9 baffles. It is designed for a free area flow of 67 sq. in. The pressure at the outlet of the tube side of the heat exchanger is 33 psi. Design specifications for the heat exchanger call for 700 GPM of D_2O to be cooled from $103^{\circ}F$ to $94^{\circ}F$ by 720 GPM of H_2O rising from $80^{\circ}F$ to $90^{\circ}F$. This gives a nominal capacity of 3×10^6 BTU/hr.

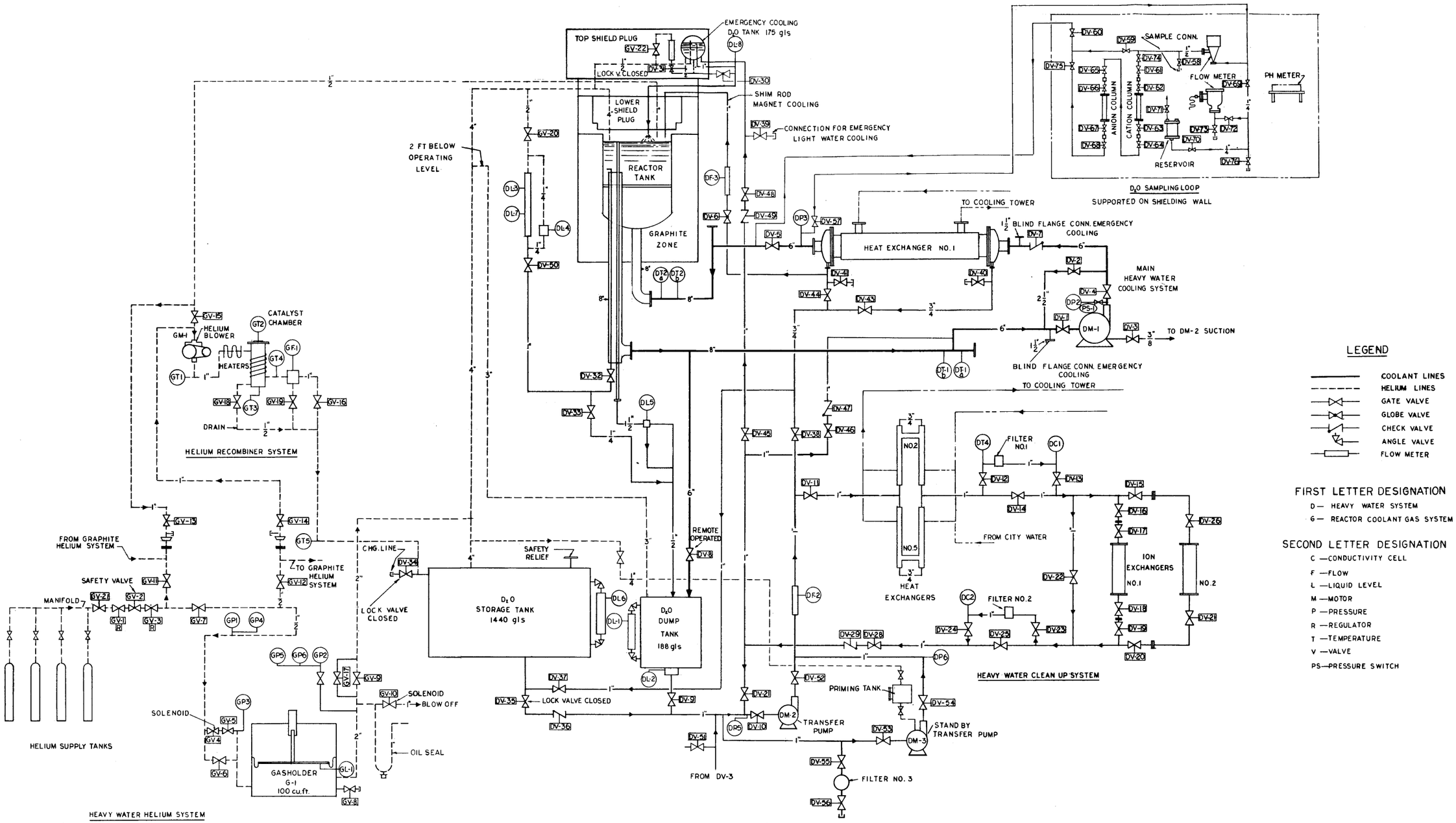

FIGURE 6

PRIMARY FLOW DIAGRAM

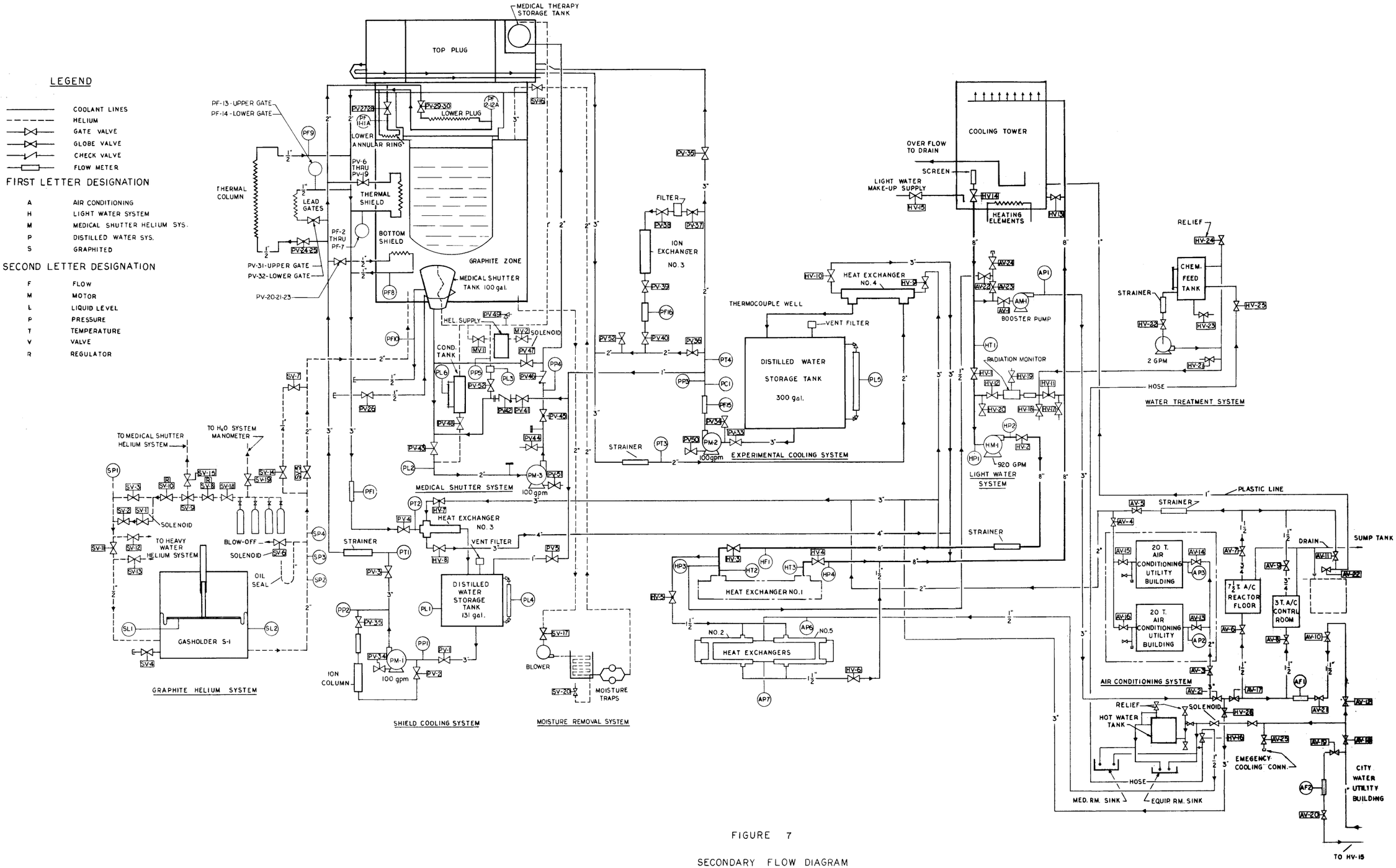

FIGURE 7

SECONDARY FLOW DIAGRAM

From the heat exchanger the heavy water flows into the plenum head of the reactor at a pressure of 10.5 psi. Here it is distributed approximately equally among the occupied fuel positions. The control rods and sample changers are closed off so that no heavy water flows into the reactor tank except via a fuel element. The coolant passes up through the lower adaptor and then through the 17 cooling channels between the fuel plates. At the lower end of the upper adaptor there is a hole through which the coolant enters the bulk volume of the reactor tank. The coolant then flows out through a pipe entrance near the plenum head and returns to the pump. Pump suction pressure is 5 psi.

Two other branches of the primary coolant loop are also important here. The transfer pump, DM-2, draws from the dump tank and supplies a cleanup system and the emergency cooling system with approximately 7 GPM at 24 psi. The cleanup system is composed of Heat Exchangers Nos. 2 and 5 in parallel. These are single-pass concentric-tube heat exchangers of local fabrication and undetermined efficiency. The flow then encounters a filter, a mixed bed resin ion exchanger, another filter, and returns to the bulk of the coolant via the emergency cooling system. The flow through this loop is approximately 2.5 GPM.

The efficiency of the cleanup system is monitored by cells that measure the electrical resistance of the water. The resistivity as measured by this means is usually about 5×10^6 ohms/cm. The remainder of the flow from the transfer pump, about 4.5 GPM, goes to the emergency cooling tank on the equipment shelf near the top of the reactor. The outlet of this tank is controlled by a lock valve so adjusted that in the event of the failure of all utilities and the simultaneous loss of all the primary coolant, the tank can feed by gravity a trickle of heavy water to each element for approximately 20 minutes to provide enough cooling to prevent melting due to decay heat.

An overflow pipe in the main reactor tank connected directly to the dump tank keeps flow separation between the two systems so that each maintains a constant volume. It also maintains an exact level of top reflector. In an emergency the top reflector can be dumped directly into the dump tank. The volume so dumped is regulated by the level of the D_2O stored in the dump tank. This level is kept at such a point that the dump will not uncover the active section of the fuel elements with the accompanying danger of meltdown. Additional D_2O is maintained in a storage tank which is large enough, when necessary, to accommodate all 10,000 pounds of D_2O in the system.

[2-6] SECONDARY COOLANT SYSTEM

HM-1 is the main pump in the secondary system. It has a capacity of 920 GPM at a head of 85 ft. and is powered by a 25-HP motor. The amount of flow in the secondary system depends on the portion of flow diverted to the top of the cooling tower with its accompanying head loss. When no flow is diverted to the top of the tower, total flow is approximately 980 GPM. When all flow is to the top of the tower, flow is approximately 880 GPM. Pump discharge pressure is 33.5 psi. A constant flow of approximately 185 GPM is diverted from the main heat exchanger to Heat Exchangers Nos. 2, 3, 4, and 5. The main flow enters the shell side of Heat Exchanger No. 1 at a pressure of 29.2 psi and leaves at a pressure of 22.5 psi. This water then joins the flow from the secondary side of all the other heat exchangers which flows to the evaporation tower for cooling.

The cooling tower is provided with a bypass valve so that the amount of water fed to the top of the tower for evaporation is continuously variable from zero to full flow. Varying the amount of tower bypass controls the equilibrium temperature of the entire system during different seasons of the year. A large fan mounted in the top of the tower also assists in the water evaporation process. The design specifications for the cooling

tower establish a capacity of 1000 GPM of light water to be cooled from 103°F to 80°F at a wet-blub temperature of 72°F and 0-10 MPH wind.

These parameters combine to give a capacity of approximately 3 1/3 MW under these adverse conditions. It must be remembered that this H_2O flow services not only the main heat exchanger, but also the shield coolant system, the experimental coolant system, the cleanup cooling system, and the entire reactor air-conditioning system. Therefore, much more heat is present than the nominal thermal output of the reactor itself.

The light water system was operated for more than two years with no form of algae or corrosion control. During this time, scale deposits built up in all parts of the system. This scale is of particular importance on the shell side of Heat Exchanger No. 1. For the past year an inhibitor has been continually added to the system and it is hoped that this has reduced the scale deposits, however, no means of inspection short of a prolonged shutdown is available in the heat exchanger to determine the exact effectiveness.

[2-7] SHIELD COOLANT SYSTEM

It has been determined that approximately 1.4 per cent of the nominal reactor power is carried away by the

shield coolant. (See Section VI.) This system is also detailed in figure 7. The system is operated by pump PM-1 with a nominal rating of 100 GPM at a head of 80 ft. It normally operates at a flow of about 75 GPM and an outlet pressure of 35 psi. The system has several branches. The first branch was designed to cool the water shutter for the medical facility, however, it developed a leak during initial operation and has been completely closed off without ill effects on the shutter operation. The next branch services the cooling coils in the bottom portion of the thermal shield. Other branches cool the lead shutter and the thermal shield in the vicinity of the thermal column. Another branch supplies the cooling coils in the annular thermal shield itself. Another branch goes to the lower annular ring of shielding, and still another cools the thermal shield portion of the lower shield plug. Many of these coils were constructed in duplicate since they are poured into the lead and concrete of the shielding and a leak or blockage would probably render the faulty coil useless.

In this system, the heat exchanger, which transfers heat from the distilled water primary coolant to the common light water system, is of a special double pass type. The distilled water flows through 438 U-shaped tubes with a total length of 3.0 ft. The tubes are

1/4-in. I.D. and 24-guage thick. The outside area of the tubes is about 101 sq. ft. This heat exchanger, referred to as Heat Exchanger No. 3 in the MITR system, is a Ross model 803 HCF and design specifications call for a capacity of 3.5×10^5 BTU/hr at a δT_{LM} of 15.6°F. Primary coolant is contained in an integral distilled water storage tank which can be further augmented through connection to a 300-gal. storage tank contained in the experimental coolant system.

The above paragraphs outline the properties of those sections of the MITR with which this paper is primarily concerned.

GENERAL INTRODUCTION TO THE PROBLEM

The objectives of this study, stated more specifically than in section I, are as follows:

For five megawatt operation:

1. To examine the upper limit on the maximum temperature of the hottest spot on any fuel plate.

2. To study the upper limitations on the maximum temperature of the bulk primary coolant at the outlet from the reactor.

3. To set a lower limit on the flow rate of the D_2O primary coolant consistent with 1 and 2 above.

4. To investigate the arrangement of fuel elements among the lattice positions in the MITR, and the uranium content allowable in each of these positions consistent with 1, 2, and 3 above.

5. To find the maximum temperature to be expected in the H_2O secondary coolant at the outlet from the cooling tower on the hottest summer day.

6. To calculate the minimum necessary H_2O secondary coolant rate consistent with all of the above.

7. To calculate the amount of heat to be removed by the shield coolant system and the primary and

secondary shield coolant flow rates necessary to accomplish this.

The accomplishment of these objectives was complicated by the following factors:

1. Operational cores of five megawatts must contain large amounts of excess reactivity. This will necessitate full power operation with the shim bank partially inserted into the core. As the core configurations to be calculated were changed, the reactivity and shim bank positions also changed. This in turn also altered the axial flux shape and the position and magnitude of the heat generation at the hot spot. Each change in these factors also changed the maximum plate wall temperature, the reactor outlet temperature, and the necessary primary coolant flow rate.

   All these factors are therefore completely interdependent and any change in core configuration necessitated a change in all of them.

2. Engineering measurement of the parameters necessary to calculate the above and other dependent variables was, in many cases, a problem. Some of the flow rates are inaccurately known. In the case of the shield primary coolant there are no

means available to calibrate the flow recorder, and in the H_2O secondary coolant system there is no direct means of accurate measurement of the total flow rate, or the flow rates through several of the branches. The principal temperatures involved were generally measured by Thermohm resistance thermometers and read on the six-point recorder. Careful calibration of this instrument on two occasions produced substantially different results and lead to suspicions about its accuracy.

3. In some cases the physical condition of the equipment involved is unknown. For example, in Heat Exchanger No. 1 the existence of scaling on the H_2O side of the tubes was postulated. There was no convenient means, however, of determining the amount or distribution of this scale.

The General method used to accomplish the objectives of this study was as follows:

1. A method for calculating neutron flux distributions was devised so that changes in fuel element loading, lattice arrangement, and control rod position could be easily incorporated.

2. The resulting heat generation distribution and the position and magnitude of the maximum heat flux was established.

3. A reasonable limit was placed on the maximum fuel element plate wall temperature and the bulk temperature of the primary coolant at the reactor outlet.

4. The flow rate of primary coolant necessary to maintain these temperatures was established.

5. Steps 1-4 were iterated for several core configurations until the variation of the upper limit on the uranium content of the fuel positions with core configuration was obtained.

6. The H_2O secondary coolant flow rate necessary to remove the reactor heat load under extremely adverse weather conditions was established.

7. The primary and secondary flow rates necessary to remove the shield heat load within reasonable temperature limitations was established.

Steps 1 and 2 above are reported in section III. Steps 3, 4, and 5 are reported in section IV. Step 6 is reported in sections V and VII, and step 7 is reported in section VI.

SECTION III

POWER PRODUCTION DISTRIBUTION

INTRODUCTION:

The objective of this section is to determine the power production distribution within the core as a whole and within a single fuel element, as a function of core configuration. The general method followed was to investigate the neutron flux distribution and power production using a model core. Later in the study the model core was altered, principally by changing the amount of uranium in particular fuel elements and the arrangement of the elements among the 30 available positions, so that realistic core arrangements in terms of reactivity requirements and equipment limitations were created. The methods evolved in this section were then used to evaluate these more difficult configurations.

The calculations in this section for determination of the flux distribution and the proportional heat distribution in the reactor core at five megawatts are based on the methods developed by Larson[1] and Steranka[2] and the experimental work of Mathews.[3]

The analysis procedure first homogenized the core in three regions and determined the properties of the unit cells in each of these three regions. Using the homogenized properties, the radial and axial flux shapes

were determined. Each unit cell was then examined and the disadvantage factors were calculated using a fuel region homogenized within the fuel element box. The flux variations were then normalized so that the total power output of the core was five megawatts. With the flux normalized, the power produced in each separate fuel region was calculated. The hottest element was then found and the absolute magnitude of its heat generation established.

Shifting from the homogeneous models to the heterogeneous reality, the heat production distribution among the plates of the element was established and the hottest fuel plate was found and its power production calculated.

[3-1] HOMOGENIZED CORE PROPERTIES

The core was assumed to be homogenized in three regions with the origin of coordinates at the center point of the core. The height of the core was taken as the height of the fuel plates, i.e. 24.625 in. Therefore, the boundary between the core and the upper reflector was at $h = H_1 = 31.274$ cm. [4] The boundary between the core and the radial reflector for 19-element cores was taken as 41.75 cm. for the following reasons.

The inner seven elements have a center-to-center spacing of 6.375 in. With these one might associate a

fuel cell of radius 6.375 in./2 = 3.1875 in. (See figure 8.) The outer ring of 12 elements is 13.25 in. from the center of the reactor. If one assumes the same cell radius for the cells in the annular ring, the outer radius of the 19-element core will be the distance from the core center to the center of the annular ring, i.e. 13.25 in. plus the cell radius, i.e. 3.1875 in. Hence, the core radius of R_c = 13.25 + 3.1875 = 16.4375 in. = 41.75 cm.

The effective outer radius of the radial reflector was taken as R_o = 79.0 cm. as the result of a calculation which homogenized the heavy water and graphite reflectors into a single effective heavy water reflector.[5] As has been stated, the inner seven elements have a center-to-center spacing of 6.375 in. and form a hexagonal lattice of unit cell 227.27 cm^2. The elements in the annular ring of twelve have a center-to-center spacing of 6.86 in. The area of the inner core is then 7 x 227.27 = 1590.9 $cm.^2$ corresponding to a circle of radius R_i = 22.50 cm. If the outer core radius for 19-element cores is taken as 41.75 cm., each of the elements in the ring of twelve would be associated with a unit cell with an area of 323.80 $cm.^2$ These differences in cell size gave rise to property differences, hence, the regional calculations. In addition, larger cores have elements

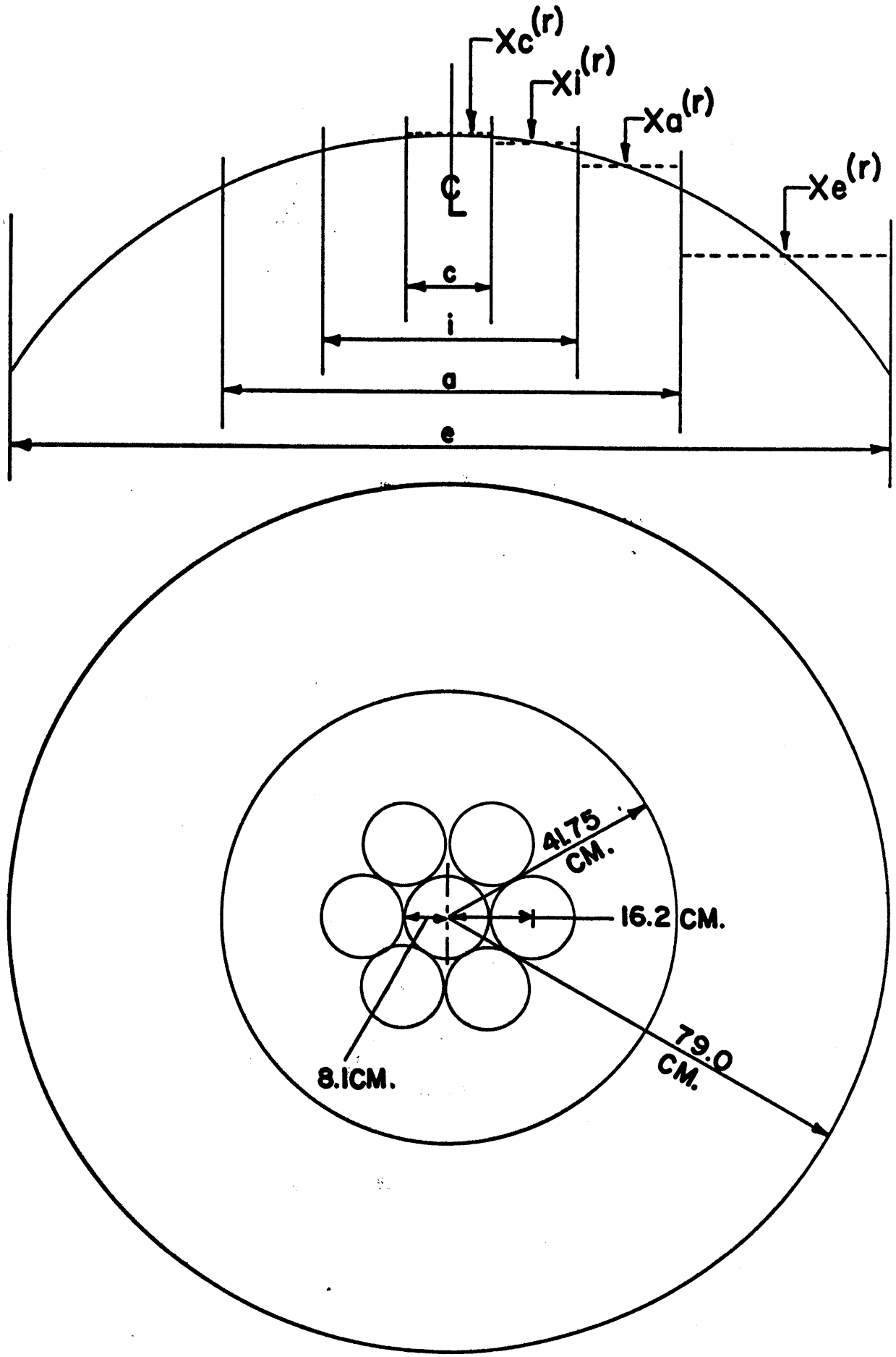

MITR CELL CONFIGURATION

FIGURE 8

placed in the outer ring of eleven fuel positions. The cell size for each of these elements is so large (2360 $cm.^2$ for six elements in the outer ring) that the reflector equations were assumed to apply in this region as far as general flux variation is concerned for calculations involving the larger cores.

The model core assumed for these calculations was a compact 19-element arrangement which utilized no fuel elements in the outer ring of eleven fuel positions. All elements were assumed to be fresh with a 162-gram fuel loading.

The core herein described is very similar to core IV computed by Larson.[6] The only major difference is that core IV had 105-gram elements in the inner seven positions and 162-gram elements in the twelve annular positions. Core IV was also extended by Larson to include 162-gram elements in the outer ring. The assumption of core IV as a model for this calculation was not unreasonable since only burned elements are used in the inner region and the actual uranium content is probably as close to 105 grams as to 162 grams. Therefore, the equations for thermal flux distribution as derived by Larson for core IV were utilized.

Σ_f was calculated for the volume of a fuel element box by:

$$\Sigma_f = \frac{V_{25} N_{25} \sigma_{25}}{V_{\text{equiv. region}}} = \frac{M_{25} N_{25} \sigma_{25}}{A_{25} V_{\text{equiv.}}} \qquad (3.1)$$

Therefore:

$$\Sigma_f = \frac{M_{25}(6.02\times10^{23})(502\times10^{-24})}{(235)(62.55)(59.305)} = 3.47\times10^{-4} M_{25} \frac{cm^2}{cm^3}$$

The inner region is designated by the subscript i and the annular region by the subscript a. The outer or extended core ring of eleven fuel positions is designated by the subscript e. The fuel region of each unit cell occupies a cross-sectional area of 59.305 cm.^{2} [7] and is designated by the subscript F. In the fuel region the volume reaction of aluminum alloy is .4415 and that of the D_2O is .5585. Some unit cell properties are given in Table I. [8]

TABLE I

PROPERTIES OF CORE UNIT CELLS

PROPERTY	INNER CORE	ANNULAR CORE
Σ_f(Fuel region) ($x10^2$)	5.621	5.621
$\bar{\varphi}_M/\bar{\varphi}_F$	1.3175	1.4163
V_M/V_F	2.8319	4.4595

[3-2] CALCULATION OF $\bar{R}(0)$, THE FLUX NORMALIZING FACTOR

A basic formula for power in a homogenized core is

$$P = K \int_{vol.} \Sigma_f \varphi \, dv \qquad (3.2)$$

where:

$$K = 3.2035 \times 10^{-17} \frac{\text{MW-sec}}{\text{fission}}$$

This constant was computed using a fission yield of 200.22 Mev. which includes 7.22 Mev./fission of capture gammas.[9]

Σ_f is known to be zero everywhere except in the fuel regions. The integral was therefore approximated by a summation over the individual fuel regions.

$$P = K \sum_{j=1}^{n} \Sigma_{f_j} V_j \bar{\varphi}_{F_j} \qquad (3.3)$$

In this expression the Σ_f is defined for the volume of the fuel element box. $\bar{\varphi}_{F_j}$ is therefore the volume averaged flux in the j^{th} fuel element box. As a volume average $\bar{\varphi}_{F_j}$ contains both radial and axial factors. It was assumed that these factors are separable. It was also assumed that the thermal flux shape in the axial direction in the fuel region is identical for all fuel positions, therefore, the axial flux factor may be separated out of the expression and independently calculated. Thereafter it was assumed to be a constant and independent of r.

Thus:

$$\varphi(r,h) = R(r)\, Z(h) \qquad (3.4)$$

Where $\varphi(r,h)$ is a generalized thermal flux at any point in the reactor. R(r) is the radial flux factor and Z(h) is the axial flux factor.

The average flux in the j^{th} fuel element box, $\bar{\bar{\varphi}}_{F_j}$ is defined as:

$$\bar{\bar{\varphi}}_{F_j} = \bar{R}_F(r) \quad \bar{Z}_F \tag{3.5}$$

where:

$$\bar{Z}_F = \frac{\int_h Z(h)\, dh}{h} \tag{3.6}$$

and is calculated for the fuel region of the unit cell. The axial flux factor is evaluated in section 3-3.

In order to find $\bar{\bar{\varphi}}_{F_j}$ an expression was first found for the average radial flux factor in the fuel region at position r, i.e. $\bar{R}_F(r)$. Larson has computed an equation for radial flux variation on the basis of a core homogenized in three regions. This expression relates the flux at any radial <u>point</u> in the core to the flux at the radial center. Since the radial flux shape is fairly flat across the core Larson's assumption [10] was employed which states that this same expression may also be used to relate the average radial flux in any <u>unit cell</u> to the average flux in the center unit cell. This assumption also includes the tacit assumption that the flux at a point on the centerline is the same as the average flux in the center unit cell.

If the radial flux variation is nearly flat this assumption is fairly good. If the distribution is not flat, the average flux assumed in the center unit cell is too high. A greater power production is therefore assumed in the center cell than actually exists, hence, the assumption is conservative.

Returning to the radial flux factor variation:

$$\bar{R}(r) = X(r)\ \bar{R}(0) \qquad (3.7)$$

where $\bar{R}(r)$ is defined as the radial flux factor in the unit cell centered at r averaged in the radial direction and $\bar{R}(0)$ is the flux normalizing factor and represents the radially averaged flux in the center unit cell. The X(r)'s are evaluated in section 3-5 according to Larson's expression discussed above. (Also see figure 8.)

The X(r)'s have been shown to relate the average flux factor in any <u>unit cell</u> with the average flux factor in the center unit cell. Within the unit cell disadvantage factors were then calculated to relate the average flux factor in the <u>fuel region</u> to the average flux factor in the cell.

For any unit cell:

$$\bar{\varphi}\ V_T = \bar{\varphi}_M V_M + \bar{\varphi}_F V_F \qquad (3.8)$$

$$\bar{\varphi} = \frac{\bar{\varphi}_M V_M + \bar{\varphi}_F V_F}{V_M + V_F}$$

where the symbols have their usual meaning.(see appendix A)
Dividing both sides by $\bar{\varphi}_F$ and rearranging:

$$\frac{\bar{\varphi}_F}{\bar{\varphi}} = \frac{1 + V_M/V_F}{1 + \dfrac{\bar{\varphi}_M V_M}{\bar{\varphi}_F V_F}} = Y(r) \qquad (3.9)$$

where all variables are functions of r.
This expression defines Y(r).

$$Y(r) = \frac{\bar{\varphi}_F(r)}{\bar{\varphi}(r)} = \frac{\bar{R}_F(r)\ \bar{Z}_F}{\bar{R}(r)\ \bar{Z}_F} \qquad (3.10)$$

The axial flux factors cancel out.

Knowing the moderator to fuel flux and volume ratios, one is able to obtain the ratio of the average flux in the fuel region of the cell to the average flux in the entire unit cell.

Combining the above results:

$$\bar{R}_F(r) = \bar{R}(0)\ X(r)\ Y(r) \qquad (3.11)$$

$$\bar{\bar{\varphi}}_{F_j} = \bar{R}(0)\, X(r)\, Y(r)\, \bar{Z}_F \qquad (3.12)$$

Thus the average flux in the fuel region of each individual unit cell can be related through the appropriate X(r) and Y(r) to the flux in the central unit cell. The total power produced in the core is then:

$$P = K \sum_{j=1}^{n} \Sigma_{f_j} V_j \bar{R}(0)\, X_j(r)\, Y_j(r)\, \bar{Z}_F \qquad (3.13)$$

The next step in the calculation was to compute all quantities on the right side of equation 3.13 with the exception of $\bar{R}(0)$, which is, of course, independent of j. Knowing the reactor power, P, to be five megawatts one could then solve for the appropriate $\bar{R}(0)$. Once $\bar{R}(0)$ was established, the power produced in each element could be determined by simply multiplying out the correct set of parameters for the j^{th} position. In this manner one is able to prove the intuitive knowledge that the central element produces the most power. More importantly, one is able to establish the absolute magnitude of the power in the central element at a reactor operating level of five megawatts.

[3-3] AXIAL FLUX VARIATION

Calculations of the axial flux variation can be carried out in a number of ways. Three methods were utilized in this study. First, the equations from Larson's two group analysis were used for the calculation on the model core. Second, the AIM-6 code of Flatt and Baller for the IBM 7090 was used for the calculations involving control poisons in the core. Third, experimental measurements were carried out at present power levels to produce distribution for use in normalizing the computer code.

The major complication in determining the axial flux variation was that as operational core fuel loadings are approached, there will be times when the reactor will be at full power with the shim bank partially inserted into the core. It has been estimated that fuel loadings having an excess reactivity of between 15β and 20β will be needed at a power level of five megawatts.[11] This amount is necessary to compensate for xenon equilibrium, xenon override, negative temperature coefficient, variable experiments, and fuel burnup, as well as fission product poisons in the core. It was also anticipated that, in the worst case, no more than 15β would have to be compensated by the shim

rod bank. For this case the bottom of the shim bank would be inserted ten in. below the top of the core. This large amount of absorption in the upper fuel region would, of course, radically alter the axial flux shape in the core.

In order to observe the change in flux shape, experimental flux measurements were taken with the shim bank as far inserted as possible and as far withdrawn as possible. These measurements were then used as a basis for adjusting the parameters of the computer code so that the code predicted the same flux shape for the same shim bank position as the experimental measurements produced. Once the code was thus normalized to the reactor it was used to predict flux shapes for which shim bank positions were not possible at the then present operating levels.

Accordingly two flux measurements were carried out by Enstice and Knotts in the central fuel element position using cobalt wires. At the time of the experiment the central element was a 162-gram element which had the center eight fuel plates removed reducing its loading to 81 gms. An inpile loop was inserted into the center of the element. There was also a guide tube available for insertion of wires, etc.

To obtain the widest variation in shim bank posi-

tion without altering the core, the two occasions were picked which would show the most and the least reactivity being neutralized by the shim bank. For the "rods out" measurement a Friday evening just prior to shutdown was chosen.

Xenon poisoning was at equilibrium, the reactor was allowed to heat up to near its temperature limit, and the regulating rod was inserted into the core. With this configuration the shim bank was even at 4.57 cm. above the top of the fuel with the reactor at power.

For the "rods in" measurement a Monday morning just after reactor startup was chosen. Xenon poisoning had essentially died away, the reactor was cooled down as far as possible, and the regulating rod was removed as far as possible. With this configuration the shim bank was level at 10.54 cm. below the top of the core. That is, the bottom of the shim rods was 10.54 cm. below the top of the fuel region. A reactor power of 20 KW was used for this measurement. The wires were then counted by a wire scanner with the results as shown in figure 9.

A computer prediction of the axial flux shape with the shim bank in the same area, i.e. 14.6 cm. below the top of the core, was then made. Both curves are plotted in figure 9 for comparison.

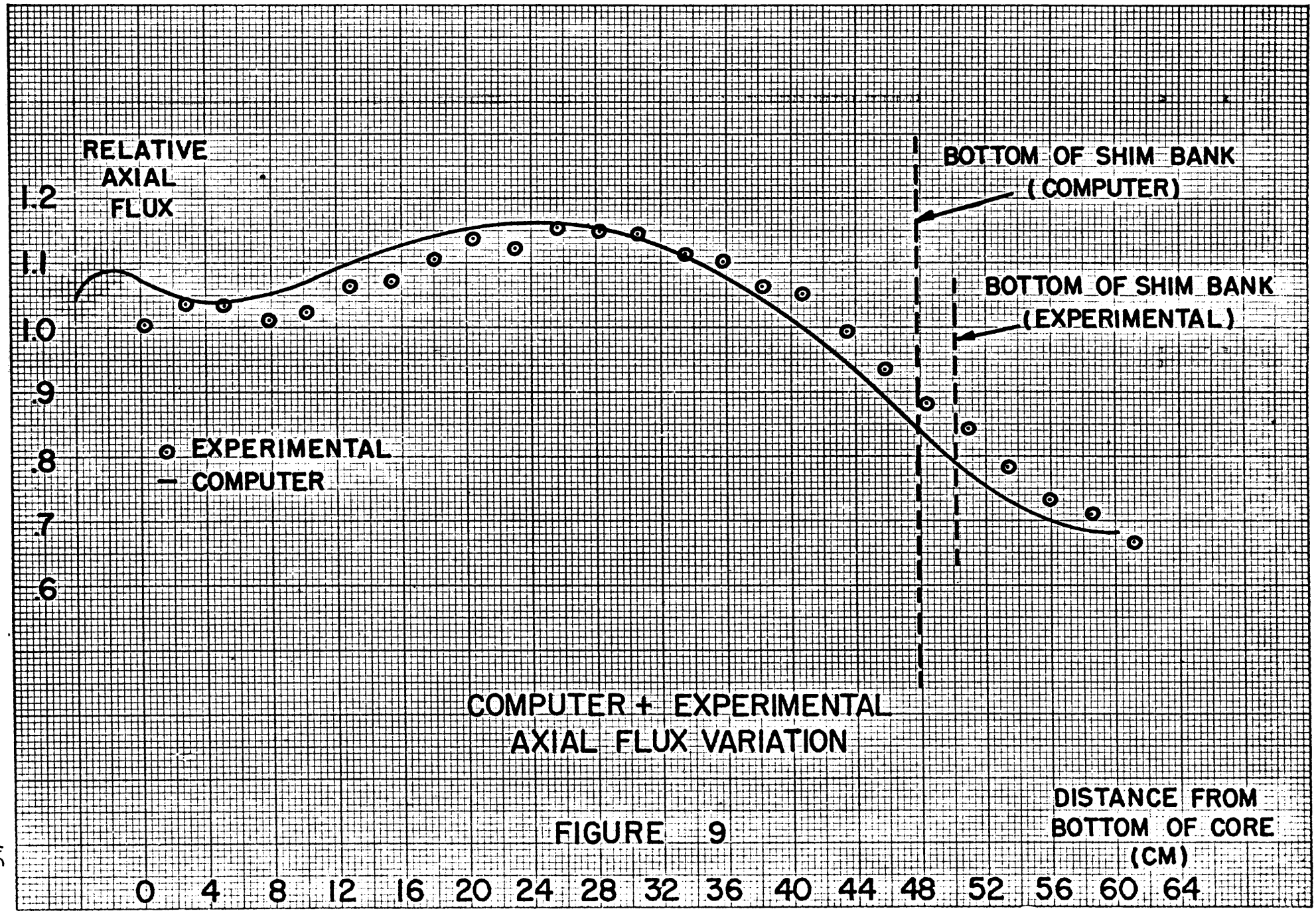
RELATIVE AXIAL FLUX
1.2
1.1
1.0
.9
.8
.7
.6
EXPERIMENTAL
COMPUTER
BOTTOM OF SHIM BANK (COMPUTER)
BOTTOM OF SHIM BANK (EXPERIMENTAL)
COMPUTER + EXPERIMENTAL AXIAL FLUX VARIATION
DISTANCE FROM BOTTOM OF CORE (CM)
0 4 8 12 16 20 24 28 32 36 40 44 48 52 56 60 64

FIGURE 9

The AIM-6 code used to produce this plot is a one-dimensional, multigroup diffusion code written for the IBM 7090 by Atomics International. For the present problem two energy groups and 101 space points were used to investigate the axial flux distribution. A four-region slab reactor was used to represent the axial dimension and transverse (radial) buckling accounted for radial leakage. Cross sections and radial buckling for the desired reactor loading were obtained from Larson's thesis.[12] Absorption cross sections for regions containing homogenized control rods were calculated using Larson's adaptation of Arnold's method.[13] To obtain a critical reactor the size of the homogenized control rod region, i.e. the control rod position, was varied. To obtain a desired control rod position the absorption in the core was changed slightly, thus simulating the presence of fission products. The k_{eff} searched for in all cases was $1 \pm .001$. The axial flux plots thus produced were normalized so that the average axial flux was unity to facilitate comparison. Both curves in figure 9 are normalized in this manner.

The computer plots were utilized in the calculations of section IV and their use will be explained more fully in that section.

Using Larson's equations the calculation of the axial flux factor proceeds as follows:

Recalling equation 3.6:

$$\bar{Z}_F = \frac{\int_h Z(h)\, dh}{h}$$

$\bar{Z}_F$ is then simply the flux factor averaged in the axial direction.

Now:

$$Z(h) = .9960 \cos(\mu_h h) + .00397 \cosh(\eta_h H) \qquad (3.14)$$

where $\mu_h = .029988$ and $\eta_h = .141723$ [14]

Since a fresh model core was utilized, a symmetrical flux shape in the axial direction was assumed with the shim bank withdrawn into the upper reflector.

Therefore:

$$\int_{-H}^{H} Z(h)\, dh = 2 \int_{0}^{H} Z(h)\, dh \qquad (3.15)$$

where $H = H_1 = 31.274$ cm.

$$2 \int_{0}^{H} Z(h)\, dh = 2 \int_{0}^{H_1} [.9960 \cos(\mu_h h) + .00397 \cosh(\eta_h h)]\, dh \qquad (3.16)$$

Therefore:

$$\int_{-H_1}^{H_1} Z(h)\, dh = 50.78 \text{ cm.} \qquad (3.17)$$

and:

$$\bar{Z}_F = \frac{50.78}{62.55} = .8118 \qquad (3.18)$$

This value of the flux factor was used in the calculation of the model core.

To insure uniformity of application of the various methods of computing the axial flux factor, all flux shapes have been normalized so that $\bar{Z}_F$ is unity. Since $\bar{Z}_F$ is constant for all fuel positions this operation was not important in the present instance, however, it assumed a major role in the hot spot calculations of Section IV. In this case the normalization factor is:

$$\frac{1.0000}{.8118} = 1.2318 \qquad (3.19)$$

All fluxes and heat generation rates for this flux shape in the following sections, other than averages, were normalized by this factor.

[3-4] UNIT CELL DISADVANTAGE FACTORS

From equation 3.9:

$$Y(r) = \left[\frac{1 + \frac{V_F}{V_M}}{1 + \frac{\varphi_M V_M}{\varphi_F V_F}}\right] r$$

The only parameters needed to calculate the Y(r)'s for the various core regions were the moderator to fuel volume and flux ratios. These values have been collected in Table I for the inner and annular core regions. It was assumed, with Larson,[15] that the flux depression for elements in the outer ring is the same as for elements in the annular ring.

$$Y(r)_i = \frac{1 + 2.8319}{1 + (1.3175)(2.8319)} = .8100$$

$$Y(r)_a = \frac{1 + 4.4595}{1 + (1.4163)(4.4595)} = .7462$$

$$Y(r)_e = Y(r)_a = .7462$$

[3-5] RADIAL FLUX VARIATION

Using Larson's equations for radial flux variation in Core IV.[16]

For the center element:

$$X(0) = 1.0000$$

For the ring of six elements: $r \leq 22.5$ cm.

$$X_i(r) = .9918\, J_o(\mu_r r) + .00822\, I_o(\eta_r r) \qquad (3.20)$$

where $\mu_r = .033072$ and $\eta_r = .148564$

For r = 16.1925 cm. :

$$X_i(r) = .9219 + .0252 = .9471$$

For the annular core: 22.50 cm. < r < 41.75 cm.

$$X_a(r) = 1.1179\, J_o(\alpha_r r) + .1010\, Y_o(\alpha_r r) + .002961\, I_o(\beta_r r) - 1.285\, K_o(\beta_r r) \qquad (3.21)$$

where $\alpha_r = .037287$ and $\beta_r = .147369$

For r = 33.655 cm. :

$$X_a(r) = .7194 + .0264 + .0778 - .0050 = .8186$$

For the outer core: $r \geq 41.75$ cm.

$$X_e(r) = 6.791\,[K_o(.031362\, r) - .01980\, I_o(.031362\, r)] - 71.08\,[K_o(.093997\, r) - 1.07\times10^{-6} I_o(.093997\, r)] \qquad (3.22)$$

For r = 53.1876 cm. :

$$X_e(r) = 6.791\,[.1723 - .0362] - 71.08\,[.003696 - .000029] = .6639$$

[3-6] CALCULATION OF $\bar{R}(0)$

Let $C_1 = K\ V \Sigma_f$ (3.23)

$K = 3.2035 \times 10^{-17}$ MW-sec/fission

$V = 3.709 \times 10^{3}$ cm.^{3}

$\Sigma_f(162) = 5.621 \times 10^{-2}$ cm.^{2}/cm.^{3}

Therefore:

$$C_1 = 6.679 \times 10^{-15}$$

Region	Number of elements	Y(r)	X(r)	$\bar{Z}_F$	N C_1 Y(r) X(r) $\bar{Z}_F$
c	1	.8100	1.0000	1.00	5.410×10^{-15}
i	6	.8100	.9471	1.00	30.743×10^{-15}
a	12	.7462	.8186	1.00	48.958×10^{-15}
					$= 85.111 \times 10^{-15}$

From section 3-2 then:

$$\bar{R}(0) = \frac{\text{Power (MW)}}{N\ C_1 Y(r)\ X(r)\ \bar{Z}_F} = \frac{5.0000}{85.111 \times 10^{-15}} = 5.875 \times 10^{13} \frac{\text{neutrons}}{\text{cm}^2\text{-sec}}$$

(3.24)

[3-7] POWER PRODUCED PER ELEMENT

Using the value computed above for $\bar{R}(0)$, the power produced per element was calculated using equation 3.13:

$$P = K\ V\ \Sigma_f\ \bar{R}(0)\ X(r)\ Y(r)\ \bar{Z}_F$$

Let:

$$C_2 = K\ V\ \Sigma_f\ \bar{R}(0)\ \bar{Z}_F \qquad (3.25)$$

$$C_2 = 392.39 \text{ KW}$$

Region	Number of elements	Y(r)	X(r)	Power/element	Power/region
c	1	.8100	1.0000	317.84	317.84
i	6	.8100	.9471	301.02	1806.13
a	12	.7462	.8186	239.69	2876.24
				Total Power	= 5000.21 KW

Due to flux peaking at the center of the core, the center element produces the most power and, therefore, will sustain the highest temperatures.

[3-8] THE HOTTEST PLATE IN THE FUEL ELEMENT

The flux disadvantage factors as calculated in section 3-4 gave us the average flux in the homogenized fuel element as compared with the average flux in the surrounding moderator. The calculation then shifted from the homogeneous model of the fuel element to the heterogeneous reality to pick out the hottest fuel plate. It would have been possible, using the method of section 3-4, to compute the flux distribution within the fuel element box. However, two sets of experimental measure-

ments were available to supply more accurate values.

Experimental work by Mathews[17] produced some flux maps of the MITR core. These measurements were made at a power level of 100 watts and have been extrapolated by Stevens to a power of one megawatt. Of particular interest is a radial and tangential flux plot at the centerline of a 105-gram element in core position No. 1. The results of these traverses are given in table II and figure 10.

The radial direction is perpendicular to the fuel plates. The tangential direction is parallel to the fuel plates. $\bar{\varphi}_F$ is the average flux in the fuel region. φ_{max} is the maximum flux at the surface of the fuel element box. φ_{Fmax} is the maximum flux in the fuel-bearing portion of the fuel element box.

TABLE II

FLUX VARIATION IN A 105 GM. FUEL ELEMENT IN CORE POSITION NO. 1 AT 1 MW

Parameter	Radial($\times 10^{13}$)	Tangential($\times 10^{13}$)
$\bar{\varphi}_F$	1.727	1.725
φ_{max}	2.000	2.000
φ_{Fmax}	1.8875	1.8125
$\varphi_{Fmax}/\bar{\varphi}$	1.093	1.051

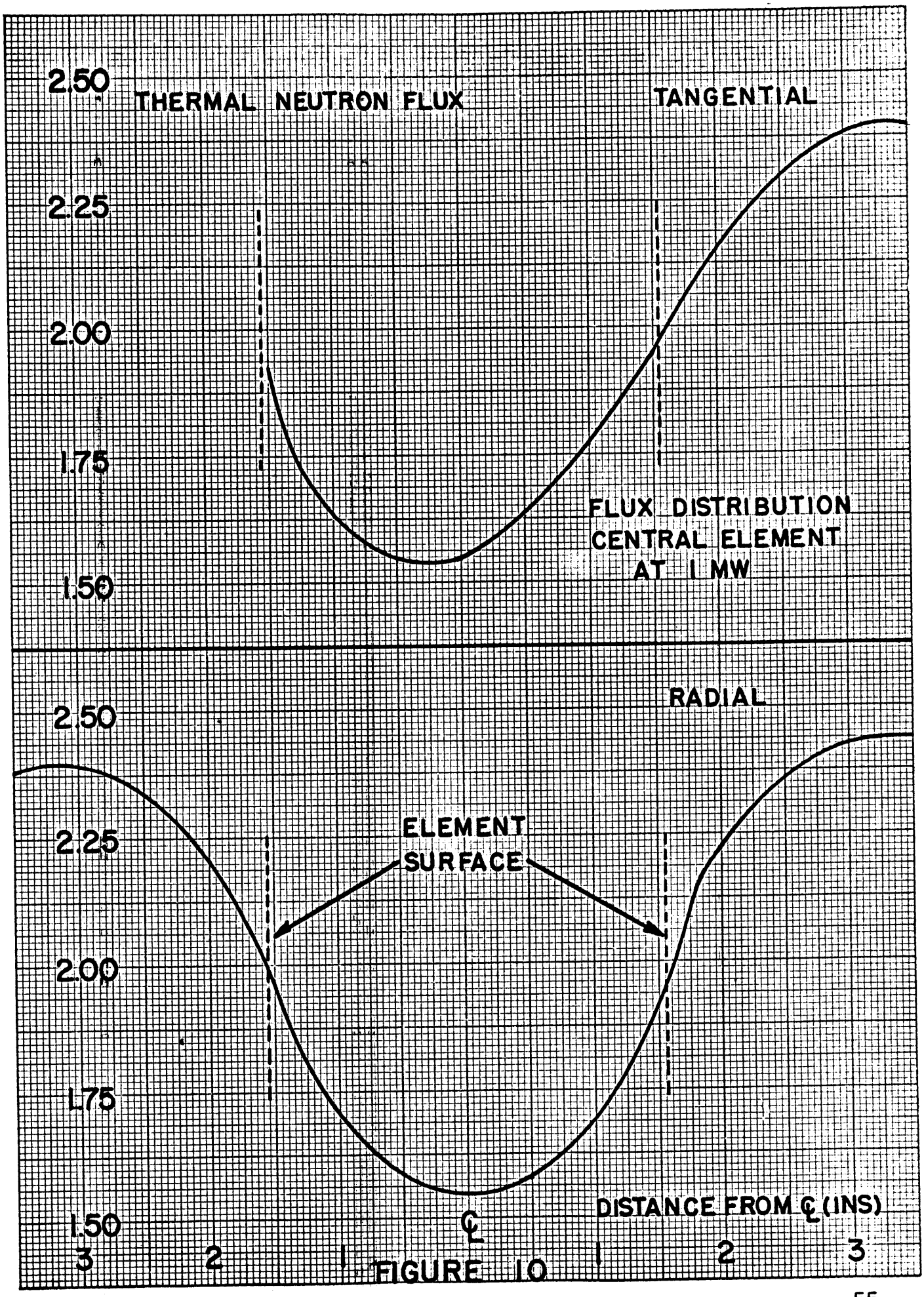
THERMAL NEUTRON FLUX
TANGENTIAL
2.50
2.25
2.00
1.75
1.50
FLUX DISTRIBUTION
CENTRAL ELEMENT
AT 1 MW
RADIAL
2.50
2.25
2.00
1.75
1.50
ELEMENT
SURFACE
DISTANCE FROM ℄ (INS)
3
2
1
℄
1
2
3

FIGURE 10

The heat produced by a fuel plate is directly proportional to the flux seen by that plate. As the neutrons proceed toward the center of an element from the moderator, many are absorbed by the fuel plates encountered along the way, hence, the flux in the center of the element is much lower than at its surface. For this reason it is the outside fuel-bearing plates that produce the greatest amount of heat. Carrying this further, the outside of the outer plate is the hottest fuel surface. Therefore, to prevent local boiling in the reactor it is sufficient to prevent it at this point. If the outside plate in the hottest element does not cause local boiling, there will be none.

As stated above, the average flux in the fuel region is known from the homogeneous case. The transition must now be made from the average flux in the fuel element to the flux in the hottest plate. From table II it is seen that Mathew's flux plots give a value of 1.093 for this ratio.

The fuel plate temperature is directly proportional to the flux seen by the plate. Marto[18] has made a temperature traverse across the fuel element in the radial direction at two megawatts. His results show that the ratio of maximum temperature to average temperature is 1.086.

From these results it appears that a conservative value of the ratio of maximum power production in the hottest plate to the power production in the average plate is in the vicinity of 1.10.

Since all the calculations which follow are aimed at removing the heat from this hottest plate and limiting its temperature, the results of the entire study are directly proportional to this ratio. This has been chosen as a convenient place to introduce a safety, or hot channel, factor. The ratio has, therefore, been increased from 1.10 to 1.25 to cover the following sources of inaccuracies:

1. Flow distribution among the coolant channels. Studies by the builders of the MITR, ACF Industries, indicate that the flow distribution among the elements does not vary more than ± five per cent.[19] There is no information available, however, on flow distribution among the interplate channels in a fuel element.

2. Non-uniform dispersion of the uranium in the fuel plates.

3. Eccentricity in the construction of the fuel plates and the resulting non-uniformity of the flow channels.

4. Warpage of fuel plates causing flow channel non-uniformity.

This hot channel factor of about 15 per cent is somewhat lower than those recommended in the literature.[20] However, there are many factors working in our favor which should be recognized.

The major factors are:

1. The outside plates of the fuel element box are pure aluminum and contain no fuel. The outside coolant passages are, therefore, available exclusively to carry away the heat produced on the outside of the outer fuel plate. This means the hottest fuel surface has access to twice as much coolant as any other surface. This tends to reduce greatly the maximum fuel plate temperature.

2. The convective heat transfer coefficient is a strong function of temperature (see figure 20). As the temperature of the coolant in the hottest channel rises, the heat is transferred away from the surface at a greater rate. This condition also tends to reduce the comparative maximum fuel plate temperature as the coefficient is evaluated at the average bulk temperature of the coolant along the length of the channel.

3. Due to the flux depression and its resulting

temperature profile, there is a diffusion of heat from the outer regions of the element toward the center. This factor is probably small, but it does work for us in reducing the maximum fuel plate temperature.

4. In the tangential direction direct conduction along the width of the fuel plates tends to produce a substantial diffusion of heat toward the center of the element. This diffusion also tends to reduce the equilibrium temperature of the corners of the fuel plates.

Some of these factors are already included in the results of Marto's experiment and tend to explain why his ratio is lower than Mathews.

The above factors, when coupled with other conservatisms mentioned specifically in the first chapter and generally throughout the study, make up a safety factor far in excess of the nominal 15 per cent included in the above paragraphs.

[3-9] POWER PRODUCED IN THE HOTTEST FUEL PLATE

Section 3-7 shows that the central element is the hottest, producing 317.84 KW at a reactor power of 5 MW.

The average plate then produces:

$$\frac{317.84}{16} = 19.865 \text{ KW}$$

For the reasons outlined in the above paragraphs it is, therefore, assumed that the hottest fuel element plate produces:

$$1.25(19.865) = 24.831 \text{ KW}$$

SECTION IV

PRIMARY COOLANT FLOW

INTRODUCTION

As stated in the general introduction to the problem, all parameters from the core configuration through the reactor temperatures to the primary flow rate are completely interdependent. Section IV assumes the power production in the hottest fuel plate from section 3-9 and proceeds to investigate the limitations on fuel plate and bulk coolant temperatures. Once reasonable ranges of values of these parameters were established, the necessary flow rate of primary coolant was calculated. Computations were first carried out for the model core, followed by application of the same methods to the general problem.

[4-1] GENERAL METHOD

The temperature difference between the maximum wall temperature and the reactor inlet is made up of two parts. The film temperature drop is made up of the difference between the maximum wall temperature, Tw_{max}, and the bulk temperature of the coolant at that point in the channel, T_c.

$$\delta T_f = Tw_{max} - T_c \qquad (4.1)$$

The coolant temperature drop is made up of the difference between T_c as described above and the reactor inlet temperature T_i.

$$\delta T_c = T_c - T_i \qquad (4.2)$$

Therefore:

$$\delta T_{tot} = Tw_{max} - T_i = (Tw_{max} - T_c) + (T_c - T_i) = \delta T_f + \delta T_c \qquad (4.3)$$

For convective heat transfer in the film drop:

$$q_1 / A = h\, \delta T_f \qquad \text{or} \qquad (4.4)$$

$$\delta T_f = q_1/hA$$

and from the energy equation:

$$q_2 = w_{ch} c_p\, \delta T_c \qquad \text{or} \qquad (4.5)$$

$$\delta T_c = q_2/w_{ch} c_p$$

q_1/A is the specific heat flux at the hottest point and q_2 is the total rate of heat transferred to the coolant from the channel entrance up to the hottest spot. As can easily be seen in equation 4.1, these calculations were actually based on the reactor inlet temperature which is much more uniform than the reactor outlet. However, since the outlet temperature recorder is the first monitor encountered by the coolant after it leaves the core, it is the logical place in the circuit to

install the various alarm and scram signals. For this reason the outlet temperature, which is recognized as an incompletely mixed bulk temperature, was used as the variable. The outlet temperature used was simply the inlet temperature plus the δT_D necessary across the core to yield 5 MW at the particular flow rate in question. For the reactor as a whole:

$$q_R = w_T\, c_p\, (T_o - T_i) \quad \text{or} \tag{4.6}$$

$$T_i = T_o - (q_R / w_T\, c_p)$$

Substituting these values in equation 4.3:

$$Tw_{max} - T_o = \frac{q_1}{hA} + \frac{q_2}{w_{ch} c_p} - \frac{q_R}{w_T c_p} \tag{4.7}$$

This was the basic equation used, however, h is also a function of flow rate and temperature.

[4-2] DETERMINATION OF THE CONVECTIVE HEAT TRANSFER COEFFICIENT

From the Colburn Equation for turbulent flow in confined passages,

$$Nu = \frac{h\, De}{k} = .023\, Re^{.8} Pr^{1/3} \tag{4.8}$$

The Prandtl Number is a temperature constant and was combined with the .023 coefficient for a particular

temperature range. In effect, this gave h as a function of flow rate.

The Reynolds Number is defined as:

$$Re = \frac{G\ De}{\mu} = \frac{w\ De}{\mu\ Ax} \qquad (4.9)$$

Therefore:

$$h = C_3(t)\ w^{.8} \qquad (4.10)$$

where:

$$C_3 = .023\ Pr^{1/3}\ (De/\mu\ Ax)^{.8} \qquad (4.11)$$

The Reynolds Number is the same whether computed for the full element or an individual channel as long as consistent parameters are used. In this case the computation was based on a single interplate flow channel. Using an average D_2O temperature of 30^oC for the fluid properties:

$$C_3 = 1.77 \times 10^{-2}\ \frac{BTU}{ft^2\ {}^oF\ lb.}$$

The validity of the Colburn relation in this application has been tested by two separate experiments. At a power level of one MW measurements were made of the temperature distribution on a fuel plate seeing the average flux in the element. Steranka then calculated the temperature distribution for this particular plate and compared the values. The experimentally measured temperatures were higher than the predicted ones by a

factor of 5.4 per cent. This indicated that the value of the heat transfer coefficient as used in the theoretical calculations was too high. Forcing the calculations to fit to observed data by varying h, Steranka obtained a value of .0168 for C_3 at 30°C, hence, the equation:

$$h = .0168\ w^{.8} \qquad (4.12)$$

More recent experiments at 500 Watts, one Megawatt, and two Megawatts by Marto[22] confirmed this value of C_3 with a surprisingly good correlation. They also indicate the magnitude of the temperature correction to be applied if the fluid temperature varies from the original 30°C value. As the temperature of the fluid rises, h increases, due mainly to a decrease in viscosity.

[4-3] CORE TEMPERATURE LIMITATIONS

The principal factor affecting the allowable temperatures at various points in the core is the requirement that the melting point of the fuel plates not be approached under any conceivable circumstances. To give this accident as wide a berth as possible, thus far in the history of the MITR, all specifications have been written so that no boiling of any type is allowed to occur. In effect, this means that no nucleate boiling is allowed at the surface of the fuel plates. The wall

temperature at the hottest spot of the hottest plate of the central element must therefore be limited.

In the treatment of nucleate boiling, Rohsenow[23] says, "Some experiments have shown that at a heated surface in water at atmospheric pressure, boiling begins at around 30°F (16.6°C) above the saturation temperature." He points out, however, that this amount of superheat may be reduced by nucleation centers, such as cavities on the heated surface. The amount of superheat of the D_2O in immediate contact with the fuel plate must be sufficient to overcome the surface tension effects to allow bubble formation. Although the exact magnitude of this amount of superheat is unknown, there is, nevertheless, a conservatism here which should not be ignored.

The hot spot on the fuel plate is close to the axial centerline of the element and is under a pressure of approximately three feet of heavy water. At this pressure the saturation temperature is 103.4°C. Taking these factors together we find that boiling actually would begin somewhere between 103°C and 120°C.

The question next asked was what happens if the saturation temperature is exceeded slightly and a limited amount of nucleate boiling occurs. Since the bulk liquid is highly subcooled, vapor bubbles formed at the

surface will either collapse in place or will leave the wall and collapse a short distance away in the cooler fluid. The net effect on the heat ransfer is a marked increase in the convective heat transfer coefficient.[24] Therefore, in case the wall temperature temporarily exceeds the boiling point of the coolant, the higher rate of convection acts to reduce the wall temperature.

Only briefly will it be mentioned that the reactor has a negative void coefficient which also tends to reduce power in the vicinity of bubble formation and helps to bring the wall temperature below the saturation temperature. The present study of primary coolant flow rate was conducted using three values of Tw_{max} from $95^{o}C$ to $105^{o}C$.

[4-4] REACTOR OUTLET TEMPERATURE LIMITATION

As the average temperature of the primary coolant is raised, more efficient heat transfer is obtained between the primary coolant and the secondary coolant, whose minimum value is relatively fixed. However, as the D_2O temperature is raised, additional flow is required to maintain a prescribed Tw_{max}. The increase in the flow required is relatively large for a small increase in primary coolant temperature. Therefore, the efficiency of the heat exchanger must be balanced

against the primary flow requirements to determine an optimum operating point. For the purposes of this study a range of reactor outlet temperatures between $40^{o}C$ and $70^{o}C$ was considered.

[4-5] REACTOR HEAT LOADS

Once a range of values for Tw_{max} and T_o was established, the remainder of the required parameters in equation 4.7 were computed.

q_R was defined as the total heat release rate of the reactor and is nominally five megawatts. Studies and measurements at one and two megawatts indicate that approximately 1.4 per cent of the total heat produced is carried away by the shield coolant. (See section 6-1.) This, in effect, reduces the heat load on the primary coolant to 98.6 per cent of five megawatts or $1.682 \times 10^{7} \frac{BTU}{hr}$.

All the heat released in the primary coolant is not transferred through the walls of the element. The case of the shield coolant which carries away heat produced by gamma ray capture in the thermal shield has already been treated. There is also some heat produced directly in the moderator by the fission neutrons and by γ capture in the D_2O, both in the core region and in the surrounding D_2O annular reflector. Wolak[25]

has determined the fission energy absorption distribution as shown in Table III.

TABLE III

FISSION ENERGY ABSORPTION DISTRIBUTION

FUEL ELEMENTS		Mev/Fission	Per Cent
K.E. of fission fragments		168.0	
K.E. of Beta particles		7.0	
Gamma Energy		4.29	
		179.29	90.5
MODERATOR			
K.E. of fast neutrons		5.0	
Gamma energy	Core	9.57	
	Annular	.67	
		15.24	7.7
SHIELD			
Gamma energy		3.69	1.8
		198.22	100.0

To determine the amount of this energy which is absorbed in various regions of the core for our purposes the procedure is as follows:

Total area (radial cross section) of a 19-element core	5476 cm.^{2}
Total area (radial cross section) of 19 fuel element boxes	1126.7 cm.^{2}
Total area (radial cross section) of free D_2O outside fuel boxes	4349.3 cm.^{2}
Total area (radial cross section) of D_2O inside fuel element boxes	629.3 cm.^{2}
Total area (radial cross section) of D_2O in core	4978.6 cm.^{2}
Per cent of free D_2O outside fuel element boxes	87.4 per cent

Since 9.57 Mev./Fission are released in the D_2O in the core, it was assumed that .874(9.57) = 8.36 Mev./Fission is absorbed in the free D_2O outside the fuel element cooling channels. It was also assumed that all of the .67 Mev. absorbed in the annulus is absorbed outside the fuel element boxes.

Some of the fast neutron energy is also deposited in the free D_2O. In this case, however, a simple volume ratio is not believed to be valid and it was assumed that one half of the 5 Mev. is deposited in the free D_2O.

Therefore, 11.53 Mev. or 5.82 per cent of the fission energy is deposited directly in the free moderator and not transferred through the walls of the fuel element plates. There is also an additional 3.71

Mev., which is deposited in the moderator within the fuel element coolant channels and which is not transferred through the plate walls.

This energy deposit must be included in the q_2 calculation, but since it is not transferred through the wall it need not be considered in the q_1/A calculations. Thus, the heat flux affecting the coolant temperature rise was reduced to 92.78 per cent of the total and the specific heat flux at the hot spot was reduced to 90.91 per cent of its computed value.

[4-6] HOT SPOT CALCULATIONS

In order to find q_1/A and q_2 the hot spot was first located. Experimental data reported by Steranka indicated that the hot spot occurs at approximately 15 cm. above the axial centerline of the fuel plate at a power level of 500 KW and at approximately 12 cm. above the centerline for a one MW power level. His calculations predicted a hot spot at 10 cm. above the centerline for two MW power.[26] Later experiments by Marto[27] gave values of 15.24 cm. above the centerline for 500 KW, 13.21 c.m above the centerline for one MW, and 11.43 cm. above the centerline for 2 MW operation. These values are plotted in figure 11. Depending on the method of extrapolation, figure 11 predicts values

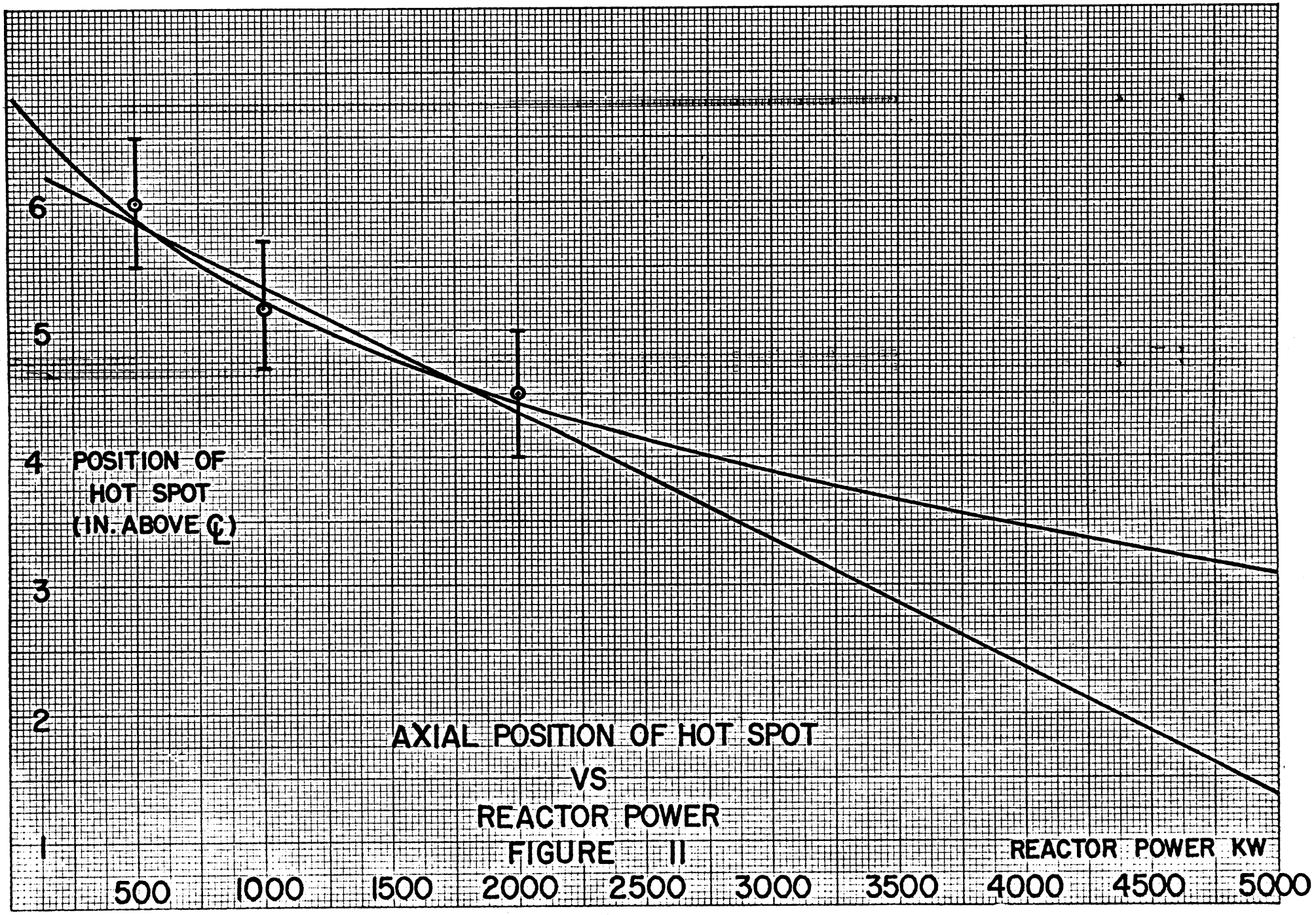

AXIAL POSITION OF HOT SPOT
VS
REACTOR POWER
FIGURE 11

between 3.4 cm. and 7.9 cm. above the centerline for the position of Tw_{max} at five megawatts.

These hot spot locations were computed using the full unshadowed length of the fuel plates. Lowering the shim bank forces the flux peak lower into the core and changes the position and magnitude of the hot spot. In these cases the information must be determined experimentally or through some other method. (See section 4-9.)

As the specific heat flux (power) increases one would expect the hot spot to move toward the centerline of the element. Decreased flow however, would tend to push the hot spot away from the centerline. The position of the hot spot for the model core at five megawatts with the rods in the upper reflector was calculated as follows:

A mathematical expression was found for each of the temperature drops which make up the difference between Tw_{max} and Ti. These expressions were then combined and differentiated to find the point of inflection, in this case a maximum, at the hot spot. The method is thoroughly outlined in the reference and will only be summarized here.[29]

$$(Tc_x - Ti) = \frac{\gamma h s_h}{w c_p} \int_o^x (Tw - Tc)\, dL \qquad (4.13)$$

Where:

Tc_x is the bulk temperature of the coolant at the position of the hot spot, x, which is unknown.

γ is the ratio of heat released in the coolant to the heat transferred through the plate walls.

The other symbols have been previously defined. (See appendix A.)

In order to evaluate this expression the axial variation of temperature along the fuel plate must be known. For the model core there are two choices for this expression. Equating the temperature and flux distributions, a simplified chopped cosine flux distribution or the more sophisticated model fitted by Larson to his experimental data can be used.

Larson's expression is:

$$\varphi_2 = \varphi_o[.9960 \cos(\mu_h L) + .00397 \cosh(\eta_h L)] \quad (4.14)$$

where

$\mu_h = .029988$ and $\eta_h = .141723$ [28]

The calculation has been worked out both ways and the agreement is within one-half of one per cent with the simplified version on the conservative side. The simplified chopped cosine has been chosen for inclusion here.

Larson's value of π/L', or μ_h as he calls it, was selected as being the best available. This calculation was made recognizing that the control rods were in the upper reflector.

Substituting the chopped cosine and integrating:

$$Tc_x - Ti = \frac{q_o s_h}{wc_p A \mu_h} \left[\sin(\mu_h x) + \sin(\mu_h \tfrac{L}{2})\right] \qquad (4.15)$$

Now:

$$q/A = \gamma h(Tw-Tc) = \frac{q_o}{A} \cos \mu_h l \qquad (4.16)$$

Therefore:

$$Tw-Tc = \frac{q_o}{\gamma h A} \cos \mu_h l \qquad (4.17)$$

and:

$$(Tw-Ti) = (Tw-Tc_x) + (Tc_x-Ti) \qquad (4.18)$$

Therefore:

$$\frac{(Tw-Ti)}{q_o s_h / wc_p A \mu_h} - \sin \mu_h \tfrac{L}{2} = \sin \mu_h x + \frac{wc_p \mu_h}{\gamma h s_h} \cos \mu_h x \qquad (4.19)$$

The left side of equation 4.19 was set equal to P and C_4 was defined as:

$$C_4 = \frac{wc_p \mu_h}{\gamma h \ s_h} \qquad (4.20)$$

Equation 4.19 was differentiated and set equal to zero with the result:

$$\mathrm{Cot}(\mu_h x) = C_4 \quad \text{at the hot spot.} \qquad (4.21)$$

C_4 was calculated as follows:

$$w = \frac{9.885\times10^6 \text{ lb/hr}}{(19 \text{ elements})(17 \text{ channels/element})} = 3.06\times10^3 \frac{\text{lb}}{\text{hr-channel}}$$

$$\mu_h = .029988/\text{cm} = .914/\text{ft}$$

$$c_p = 1.004 \text{ BTU/lb } ^\circ\text{F}$$

$$\gamma = 186.69\text{Mev}/182.98\text{Mev} = 1.021$$

$$s_h = 6.00 \text{ in} = .5 \text{ ft}$$

$$h = (.02047)(9.885\times10^5)^{.8} = 1277 \text{ BTU/hr ft}^2 \,^\circ\text{F}$$

Therefore:

$$C_4 = \frac{(3.06\times10^3)(1.004)(.914)}{(1.021)(1277)(.5)} = 4.307$$

$$1/C_4 = \mathrm{Tan}(\mu_h x) = .2322$$

$$\mu_h x = .2282$$

$$x = .2282/.029988 = 7.61 \text{ cm above the centerline.}$$

This value falls inside the span predicted by Marto's data and is on the high (conservative) side. The actual position of the hot spot is relatively immaterial as the final temperature difference between Tw_{max} and Ti is relatively insensitive to the temperature rise in the coolant up to the hot spot, δTc.

[4-7] SPECIFIC HEAT TRANSFER RATE AT THE HOT SPOT

Recalling equation 3.13 and applying it to the center element:

$$q = K \Sigma_f V \bar{R}(0) X(r) Y(r) \bar{Z}_F \qquad (4.22)$$

$$q = C_5 \int_{-H_1}^{H_1} Z(h)\, dh \qquad (4.23)$$

$C_5 = 6259.17$ watts/cm and has been normalized according to section 3-3.

Since there are sixteen plates per fuel element the average plate produces:

$$\bar{q} = \frac{1}{16}(6259.17)\int_{-H_1}^{H_1} Z(h)\, dh \text{ watts} \qquad (4.24)$$

$$\bar{q} = 391.20\int_{-H_1}^{H_1} Z(h)\, dh \text{ watts}$$

Applying the hot channel factor from section 3-8 the hottest plate produces:

$$q = 1.25(391.20)\int_{-H_1}^{H_1} Z(h)\, dh \text{ watts} \qquad (4.25)$$

$$q = 489.0\int_{-H_1}^{H_1} Z(h)\, dh \text{ watts}$$

Now:

$$A = s_h\, dh = 15.27\, dh \text{ cm}^2 \qquad (4.26)$$

Where s_h is the fuel plate perimeter and h is the height above the centerline.

q/A at a point is:

$$\frac{(489)\, Z(h)\, dh}{(15.27)\, dh} = 32.02\, Z(h) \text{ watts/cm}^2 \qquad (4.27)$$

Using equation 3.14 at 7.61 cm above the centerline:

$$Z(h) = .9960 \cos(\mu_h h) + .00397 \cosh(\eta_h h) \quad (4.28)$$

where:

$$\mu_h = .029988 \text{ and } \eta_h = .141723$$

Therefore:

$$Z(h) = .9767$$

and:

$$q_1/A = (.9767)(32.02) = 31.27 \text{ watts/cm}^2 \quad (4.29)$$
$$= 9.916 \times 10^4 \text{ BTU/hr ft}^2$$

It has been shown that not all of this heat is transferred through the walls of the fuel plate. Section 4-5 states that only 92.78 per cent is transferred by convection. Therefore:

$$q_1/A = (.9278)(9.916 \times 10^4) = 9.200 \times 10^4 \text{ BTU/hr ft}^2 \quad (4.30)$$

[4-8] COOLANT HEATING RATE UP TO THE HOT SPOT

q_2 is the total rate of heat transfer to the coolant from the place where it enters the element up to the hot spot on the hottest plate.

From equation 4.25:

$$q_2 = 489.0 \int_{-H_1}^{x_1} Z(h)dh \text{ watts} \quad (4.31)$$

where the integral is in units of centimeters.

$$\int_{-H_1=-29.7cm}^{x=7.61cm} Z(h)\, dh = 34.33 \text{ cm} \qquad (4.32)$$

Using equation 4.28 for Z(h)

Therefore:

$$q_2 = 489(34.33) = 16.787 \text{ KW} \qquad (4.33)$$
$$= 5.729 \times 10^4 \text{ BTU/hr}$$

This quantity is also reduced by the fact that some heat is released directly in the free moderator. Section 4-5 gives the appropriate factor for this case as 90.91 per cent of the total.

Therefore:

$$q_2 = 5.208 \times 10^4 \text{ BTU/hr} \qquad (4.34)$$

[4-9] D_2O FLOW RATE

Recalling equation 4.7:

$$Tw_{max} - To = \frac{-q_R}{wc_p} + \frac{q_1/A}{h} + \frac{q_2}{wc_p}$$

For the range of D_2O temperatures investigated in this calculation an average bulk temperature of 50°C was assumed.

At this temperature: (See figure 20)

$$h = 1.2185(.0168)\ w^{.8} = .02047\ w^{.8}$$

Inserting the numbers found in the last two sections:

$$Tw_{max}-To = \frac{-1.682\times10^{7}}{1.004\ w} + \frac{9.200\times10^{4}}{.02047\ w^{.8}} + \frac{5.208\times10^{4}}{1.004\ w/17\times19} \quad (4.35)$$

$$Tw_{max}-To = \frac{4.494\times10^{6}}{w^{.8}}.$$

This was the final equation for D_2O flow. This equation illustrates an unusual situation where the temperature rise of the coolant from the reactor inlet to the hot spot was exactly equal to the δT across the reactor for the bulk coolant. The first and third terms of equation 4.35 cancel out completely. This was, of course, due to the fact that the coolant emerging from the hottest channel will be above To. To is a mixed bulk temperature. (See figure 13.) The limits of Tw_{max} variation have already been discussed. Preliminary calculations indicated that to obtain a To of about 55°C, flow rates were of the order of 10^6 lb/hr. The flow rate was, therefore, varied from $.8\times10^6$ to 1.4×10^6 lb/hr. The results of these calculations are given in Table IV.

TABLE IV

VARIATION OF To AND Tw_{max} WITH CHANGING FLOW RATE

Flow rate		Tw_{max}-To	To_1	To_2	To_3
lb/hr	GPM	°C	°C	°C	°C
$.8x10^6$	1457	47.18	57.73	52.73	47.73
$1.0x10^6$	1821	39.43	65.51	60.51	55.51
$1.2x10^6$	2185	34.10	70.85	65.85	60.85
$1.4x10^6$	2550	30.16	74.82	69.82	64.82

Where:

To_1 is To for $Tw_{max} = 105°C$

To_2 is To for $Tw_{max} = 100°C$

To_3 is To for $Tw_{max} = 95°C$

This data is displayed graphically in figure 12. For reasonable values in the upper ranges of operating temperatures, such as $Tw_{max} = 100°C$ and $To = 55°C$, the minimum flow rate required is shown to be $8.58x10^5$ lb/hr = 1580 GPM.

Figure 13 is drawn using $Tw_{max} = 95°C$, $To = 55°C$, and $w_D = 1800$ GPM, fitted into the theoretical temperature distribution shape. Note that the coolant bulk temperature at the top of the element box is higher than 55°C, the assumed reactor outlet bulk temperature.

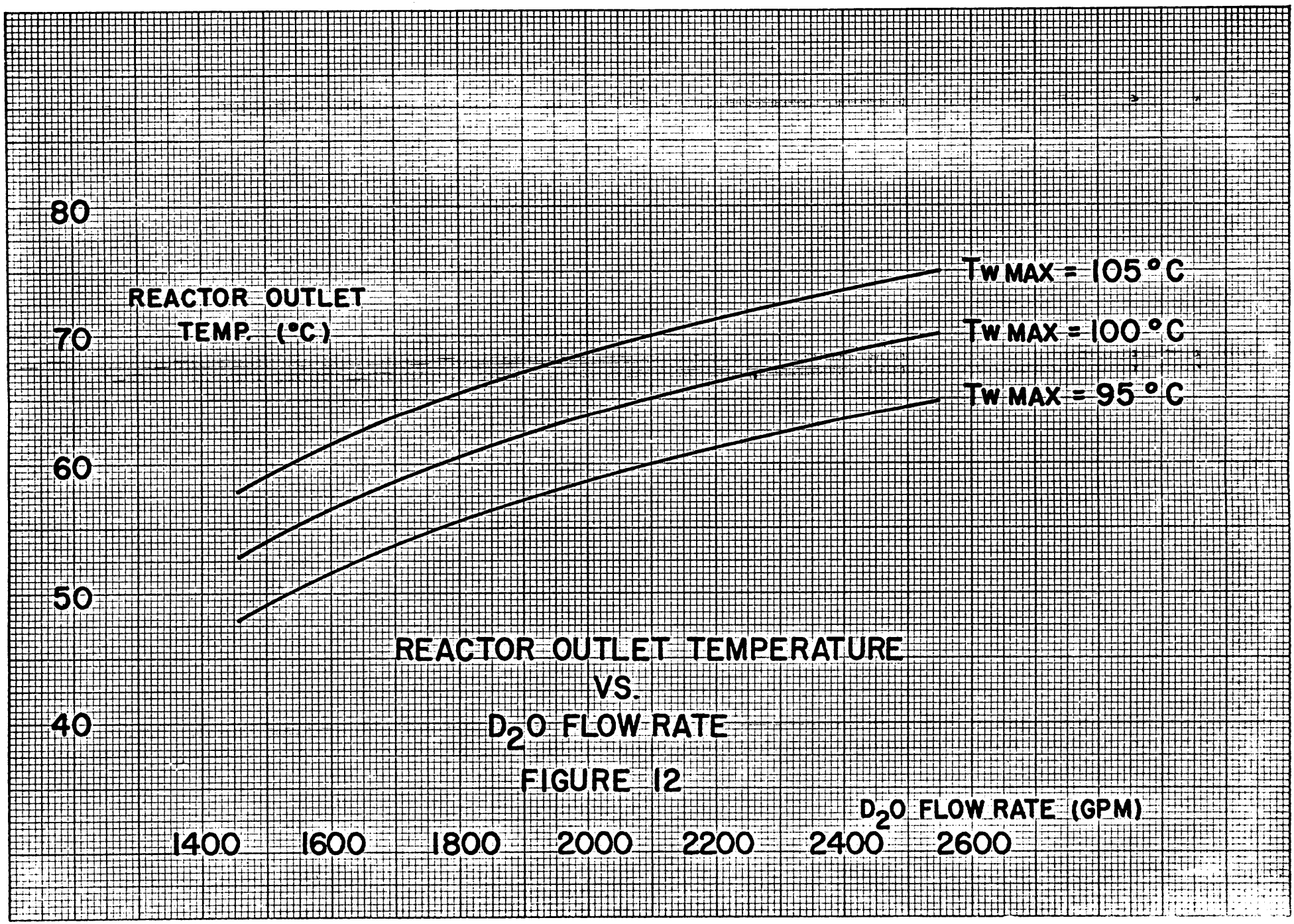

REACTOR OUTLET TEMPERATURE
VS.
D_2O FLOW RATE

FIGURE 12

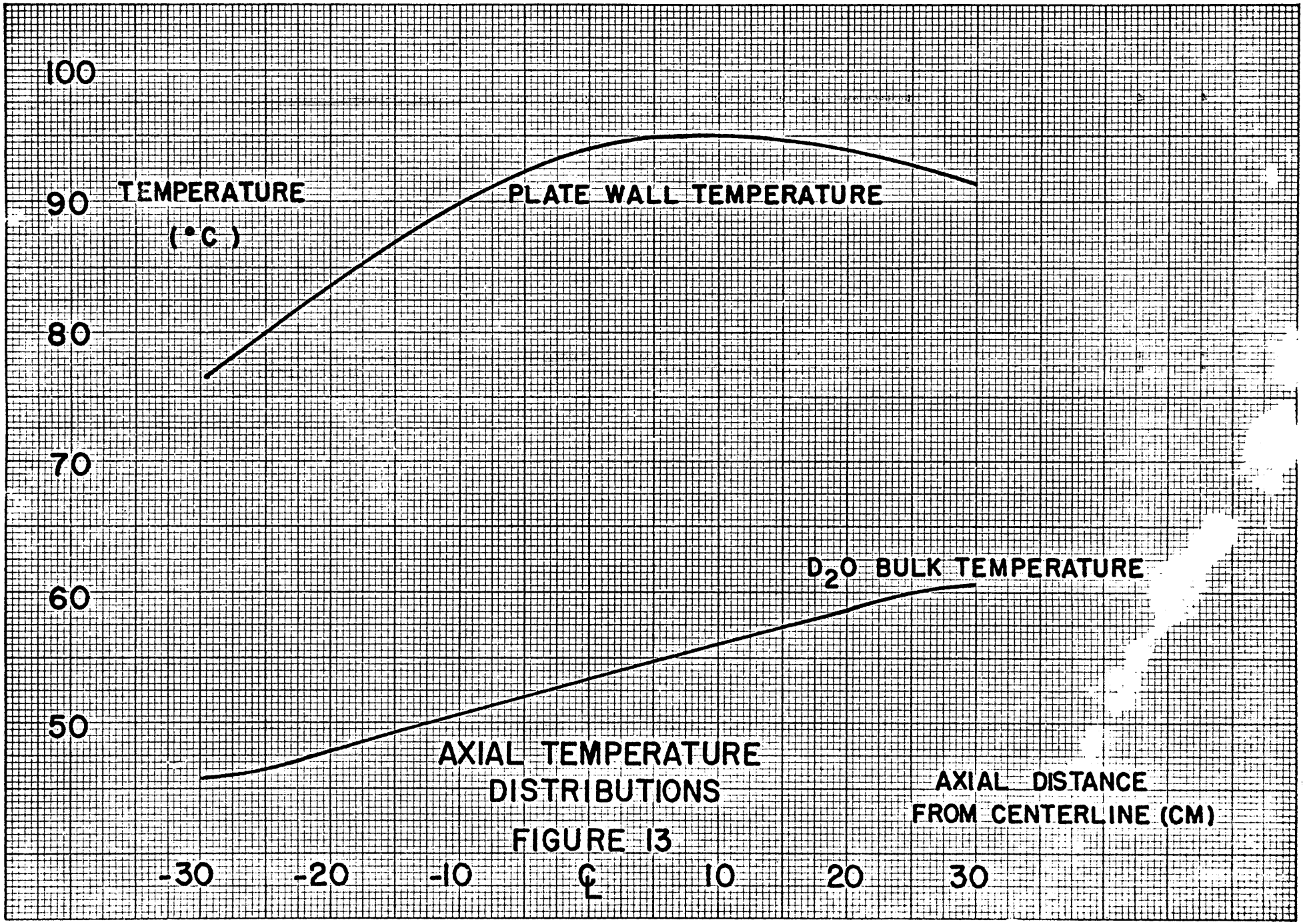
100
90
80
70
60
50
TEMPERATURE
(°C)
PLATE WALL TEMPERATURE
D2O BULK TEMPERATURE
AXIAL TEMPERATURE
DISTRIBUTIONS
AXIAL DISTANCE
FROM CENTERLINE (CM)
-30
-20
-10
℄
10
20
30

FIGURE 13

This is due to the fact that we are considering the limiting case, that is, the hottest channel. Other channels in this element and all channels in other elements will have outlet temperatures considerably lower, hence, the overall average bulk temperature at the reactor outlet is 55°C. The curve for the temperature distribution on the hottest plate does, in fact, peak at 95°C at a point 7.6 cm. above the centerline of the fuel element.

Thus, for the model core where the fuel elements are fresh and unburned, the control rods are in the upper reflector, and the axial flux shape is assumed to be a cosine symmetric about the axial centerline, the hot spot was easily found and the calculation could proceed smoothly. In the actual case where the flux shape is skewed to the bottom portion of the element, where the fuel is unevenly burned over its axial length, and where the picture is complicated by the presence of the control rods deep in the core at times, the problem was not so straightforward.

A major assumption was made here which simplified the problem somewhat. The hot spot was assumed to be at the point of maximum flux. Actually, the hot spot may be several centimeters above the point of maximum flux since the hot spot is a summation of the flux-induced temperature profile in the plate and the bulk coolant

temperature profile. The assumption is very conservative in that moving from a point of lesser neutron flux to the point of maximum neutron flux increases the specific heat flux and the resulting δT_f much more than the change affects δT_c. In fact, the entire δT_c is generally much smaller than δT_f, and δT_f is the controlling term in equation 4.7.

This assumption made it unnecessary to formulate a mathematical expression (for use in equation 4.13) to fit the experimental and computer calculated flux shapes. Direct numerical integration could then be used and ratios of maximum to average flux obtained from these more realistic flux pictures used in the calculations which follow.

[4-10] METHOD FOR ESTIMATING ALLOWABLE CENTRAL FUEL ELEMENT LOADINGS

The total power generated in a reactor core may be calculated by a numerical integration of equation 3.2, i.e.:

$$P = K \int_{vol} \varphi \Sigma_f \, dv$$

This equation relates the flux, the fuel loading, and the effective volume of the core to the total power produced. If the power level and the fuel loading per average unit

volume remain constant as the effective core volume decreases, the flux must increase. If the volume remains constant, the equation says that the general flux level must increase if the fuel level is decreased. However, this equation does not take into account the restriction placed on the system by criticality requirements. If the fuel loading per unit volume is also a variable, as it is in this case, the situation is even more complex. A general reduction in fuel loading coupled with a high loading in the center element will tend to maximize the power density in the center element. This is the worst or limiting case as far as core configuration is concerned. However, the problem also implies its solution. By limiting the amount of fuel loaded in the center element for various core configurations, and insuring that the product of $\varphi \Sigma f$ for any other element does not exceed this product in the center element, one can insure that the heat generation is kept within limits which can be effectively controlled by the amount of coolant flow available.

For the assumed limiting values of the maximum plate wall temperature, the reactor outlet temperature, and the minimum D_2O flow rate, the following calculations produce a curve of allowable center fuel element loading vs. core configuration (in terms of excess reactivity) which will

insure safe operation within these limits.

[4-11] OPERATIONAL LIMITATIONS

Due to the considerations of section 4-3 and the results of the calculation in section 4-9, a maximum wall temperature limit of 100°C can be safely utilized. This is a suggested upper limit and probably should not be the operating level, however. That is, it appears from the foregoing calculations that it would be reasonable to operate the reactor so that Tw_{max} will not exceed 95°C. If necessary, however, the reactor could be operated with a Tw_{max} of 100°C without danger of melting the fuel.

Due to the considerations mentioned in section 4-4 and the results of section V which follow, a reasonable limit for the reactor outlet temperature would appear to be 55°C. Again this is a suggested upper limit and should be approached only on the mythical "hottest day" postulated for the calculation in section V and section VII. At all other times Tr_o should be well under this temperature.

A low flow limitation of 1800 GPM of heavy water would appear to be reasonable. Although it is anticipated that the planned pumps and associated equipment will be able to produce a flow rate of the order of

2400 GPM, the calculations have been based on a minimum limit of 1800 GPM flow rate. Normal operation should easily exceed 2200 GPM, however.

[4-12] CENTRAL FUEL ELEMENT LOADING LIMITATIONS

When plotting central fuel element loading against core configuration, a careful choice must be made as to what parameter best represents the core configuration. Preliminary calculations were carried out using both total weight of uranium in the core and excess reactivity to express this variable. Both plots gave similar results for the compact 19-element core case, but when a 20th element was added to the outer ring of 11 fuel positions, the results of the two plots differed. The total core weight calculations gave too much importance to the addition of this element, hence, the limit on the loading of the center element was too high and an unsafe condition might exist. Addition of this same weight of fuel to interior fuel positions, however, would produce a safe condition. The plot using the excess reactivity available in the core in question, βex, as the parameter, takes into account the importance of the placement of the fuel and provides a much more reliable indicator. A particular amount of fuel, placed in a cell in the central

position or the ring of six positions where fuel to moderator ratios and fluxes are high has a greater capacity to produce power than the same fuel placed in the ring of 11 positions. Excess reactivity is a measure of this capacity, hence, using it as the variable instead of total core weight takes into account one more factor, i.e. the placement of the fuel. βx above the cold clean critical core was, therefore, used in the following calculations. It has been estimated that between 15β and 21β excess reactivity will be necessary for normal operation at five megawatts.[30] This estimate gave an upper limitation on the fuel loading for the following calculations.

As the amount of excess reactivity is increased, the amount the shim bank will be lowered into the core is increased. This factor is critical, especially during startup before xenon poisoning and the temperature coefficient have neutralized some of the excess reactivity. Therefore, the case was considered where all the excess reactivity must be covered by the control rods. The worth of the fuel elements in particular positions was taken from Table V.[31] The worth of the shim bank was taken from figure 14.[32] The minimum critical mass of the MITR has been taken as 1958 grams.[33] This amount was calculated using the original brazed fuel elements. The present elements are not brazed. It has been estimated[34]

TABLE V

MITR FUEL ELEMENT WORTH

Fuel position	Center position	ring of 6 elements	ring of 12 elements	outer positions
162 gm. element	3990	(3650)	2440	897
105 gm. element	2590	(2250)	1590	754 (595)
Brazing on 105 gm. element	-282	(-245)	(-174)	(-103)
One gm. U-235 uniformly spread over 105 gm. element	28.6	(24.8)	(17.5)	(10.4)

Numbers in parentheses were not directly measured, but inferred from other measurements.

Reactivity worths in units of mβ.

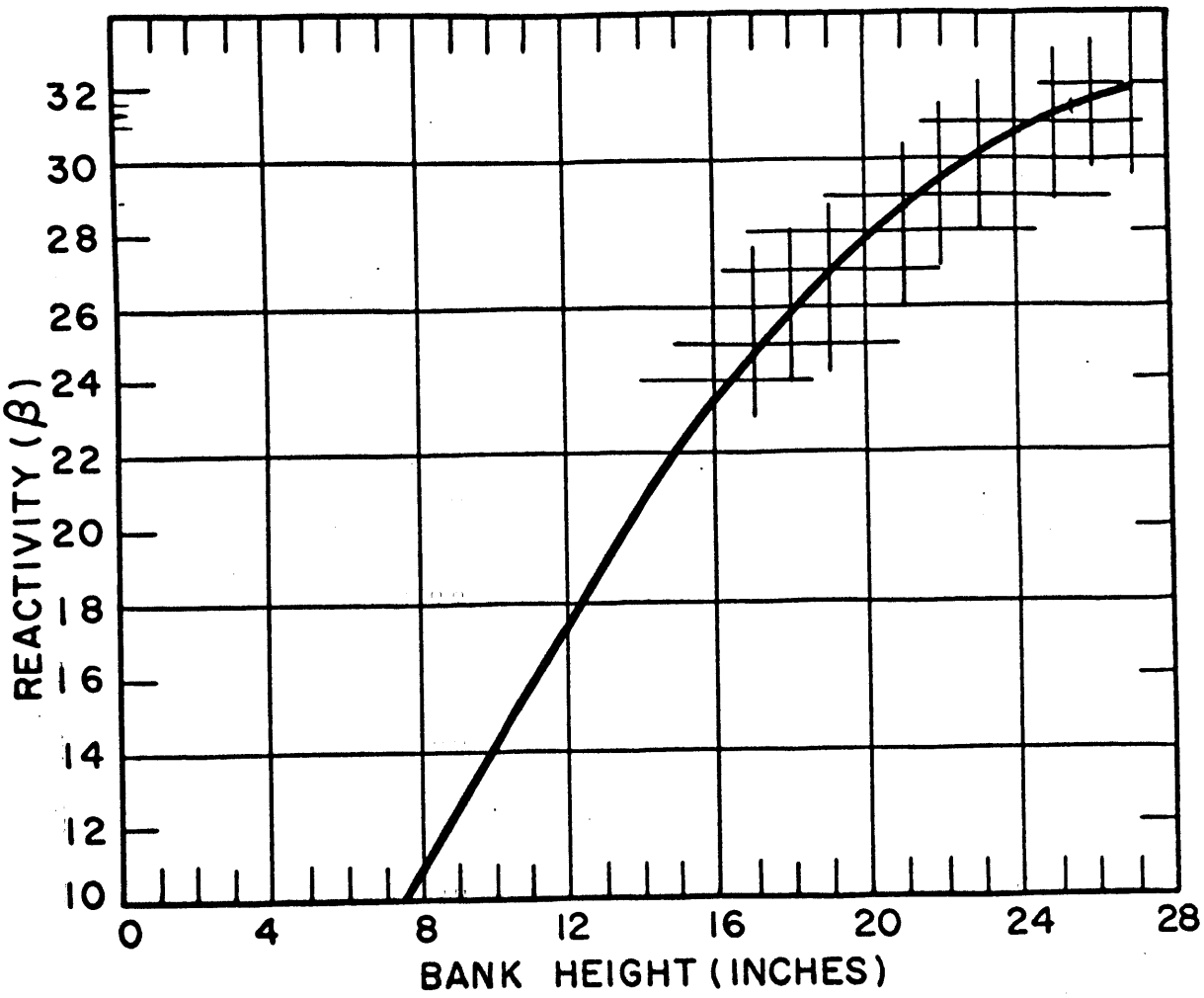

FIGURE 14

SHIM BANK WORTH

that the reactivity effect of the removal of the braze is worth 3.833 β. Therefore, it was assumed that a 1958 gm. core is critical with 3.833 β excess reactivity. Subtracting the amount of fuel represented by this amount of βex , the minimum critical mass using unbrazed elements is 1770 gms.

The procedure was then as follows:

1) A certain configuration of fuel element loading and arrangement was postulated.
2) The βex was figured according to Table V.
3) The shim bank position necessary to just neutralize this βex was taken from figure 14.
4) Knowing the shim bank position the experimentally normalized computer flux plots were utilized.

In order to calculat the specific heat flux at the hot spot, q_1/A, for use in equation 4.7 the maximum to average flux ratio in the axial direction, $Z_{Fmax}/\bar{Z}_F$, must be known. (See section 4-7) Since the position of the shim bank will vary according to the core configuration, $Z_{Fmax}/\bar{Z}_F$ must be known as a function of shim bank position. This information was obtained using the normalized computer code described in section 3-3. Axial flux plots were obtained from the computer program for shim bank positions

where the bottom of the shim bank was 6.2 cm.,14.60 cm., 22.90 cm., and 31.25 cm., below the top of the fuel plates. Each of these plots was numerically integrated so that $\bar{Z}_F$, the average value of the flux, could be found. The maximum point was also located and the ratio of $Z_{Fmax}/\bar{Z}_F$ was established for each plot. Figure 15 was then plotted showing the variation of $Z_{Fmax}/\bar{Z}_F$ with shim bank position. Shim bank position is expressed as unshadowed core length, that is, the length of core which does not contain any control rods.

The axial position of the point of maximum flux was established for each of the four plots. This parameter was also plotted as a function of unshadowed core length. (See figure 16.)

The amount of the axial flux plot from the bottom of the core up to the hot spot was again numerically integrated and the average flux in this region found. The ratio of average flux in this region to the average flux in the entire core length was then established for each of the shim bank positions. This ratio is plotted against unshadowed core length in figure 17.

Figures 16 and 17 were used to obtain the information necessary to calculate q_2, the total heating rate of the

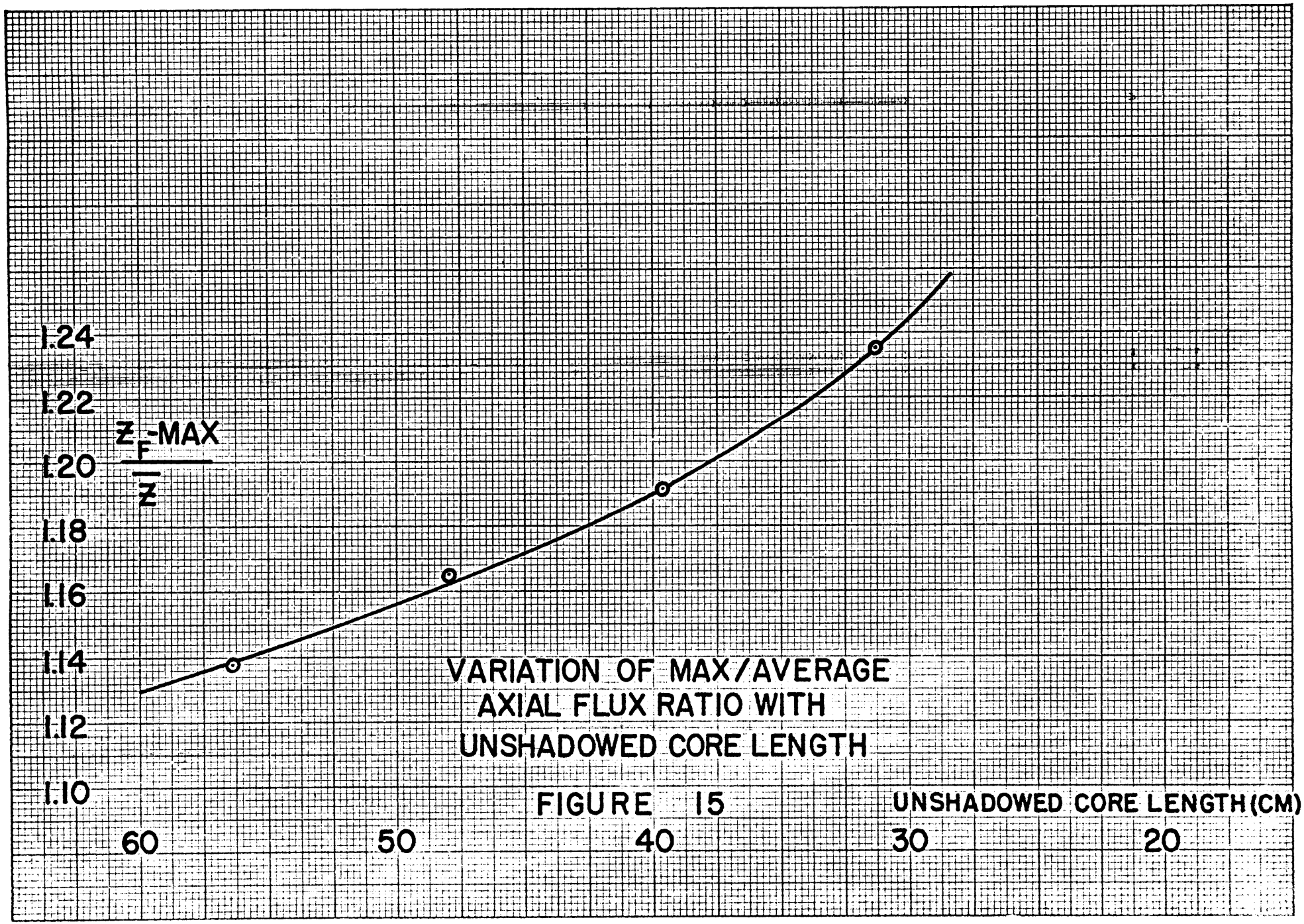

VARIATION OF MAX/AVERAGE AXIAL FLUX RATIO WITH UNSHADOWED CORE LENGTH

FIGURE 15

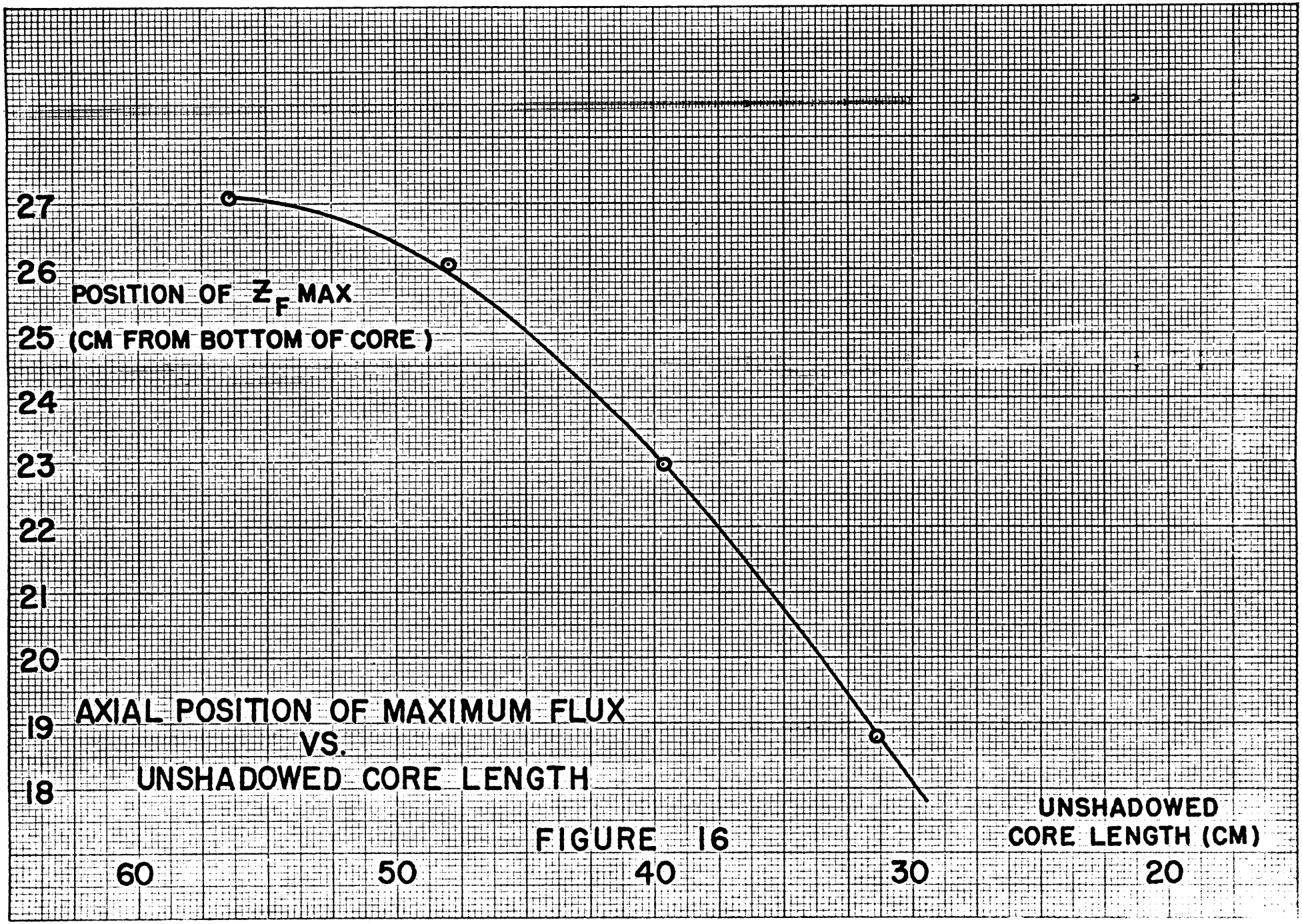

AXIAL POSITION OF MAXIMUM FLUX
VS.
UNSHADOWED CORE LENGTH

FIGURE 16

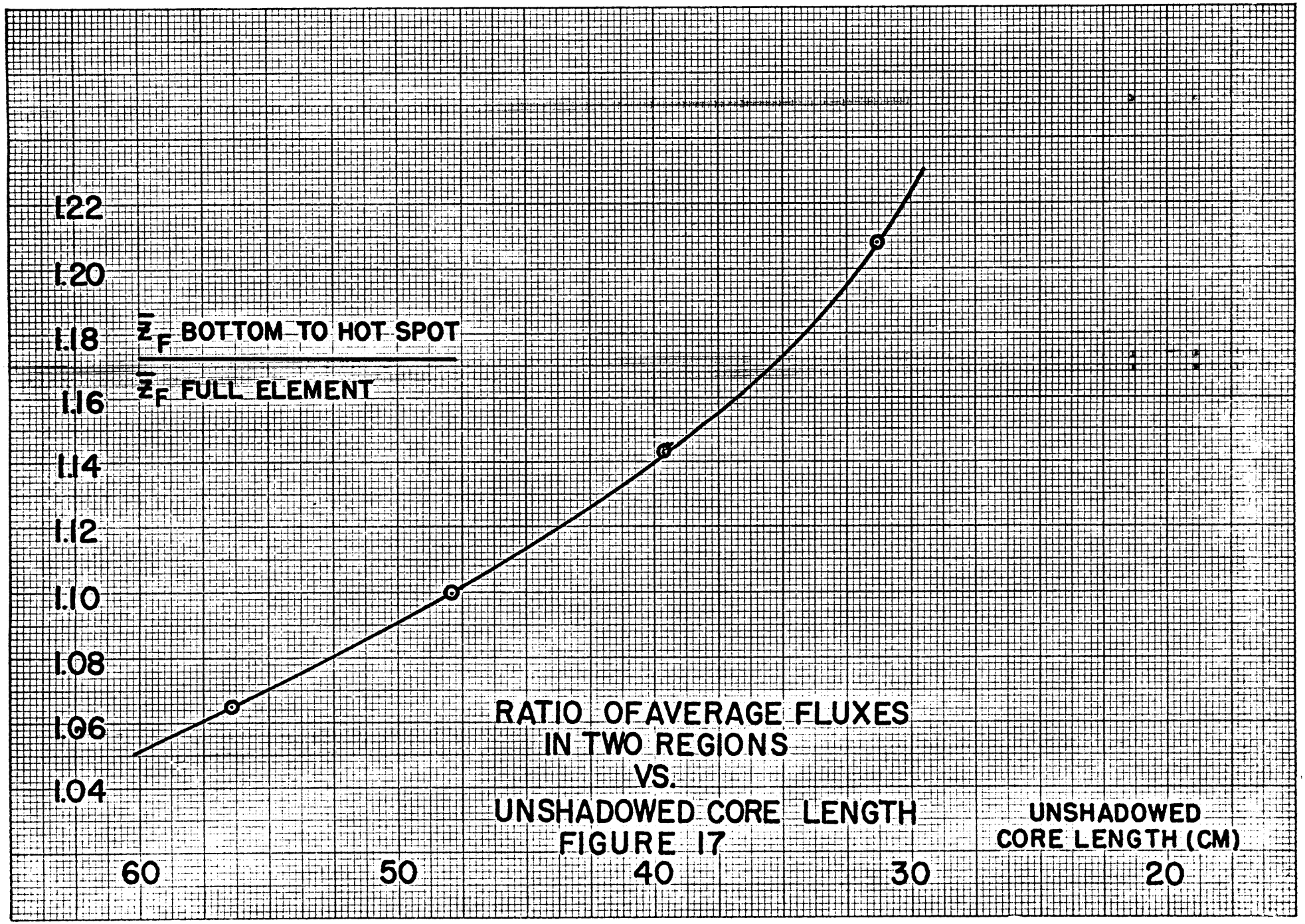
1.22
1.20
1.18
1.16
1.14
1.12
1.10
1.08
1.06
1.04
$\frac{\bar{z}_F \text{ BOTTOM TO HOT SPOT}}{\bar{z}_F \text{ FULL ELEMENT}}$
RATIO OF AVERAGE FLUXES
IN TWO REGIONS
VS.
UNSHADOWED CORE LENGTH
60
50
40
30
20
UNSHADOWED
CORE LENGTH (CM)

FIGURE 17

bulk coolant from the bottom of the channel up to the hot spot, for use in equation 4.7. This information was used in a calculation similar to that found in section 4-8.

Once q_1/A and q_2 were established by this method, equation 4.7 was used to calculate the temperature difference between the maximum wall temperature and the reactor outlet. The fuel loading in the central element was then varied so that the Tw_{max}-To for 1800 GPM flow rate was exactly equal to 100 - 55 = 45°C as established in section 4-11. Each change in fuel loading caused a change in βex, shim bank position, and all of the information taken from figures 15, 16, and 17. The fuel loading which caused Tw_{max}, To, and the D_2O flow rate to be just tangent to their limits was picked as the upper limit on fuel loading for the central position for the amount of excess reactivity present in the configuration under study. This limit is projected to the other fuel positions through the X(r)'s of section 3-5. The product of Σ_f X(r) for any fuel position must not exceed that in the central position when Σ_f of the central element is at its limiting value.

[4-13] TYPICAL CALCULATIONS OF THE CENTRAL FUEL ELEMENT LIMITATION

An analysis of the four 162 gm. elements which have been through the complete burnout cycle in the MITR shows that fresh 162 gm. elements are, on the average, burned to 138 gms. in the ring of twelve before being moved to the ring of six where they are burned to 118 gms. before being removed from the reactor. For this sample calculation an approximately average operating core was postulated in which the center element was fresh at 162 gms. The elements in the ring of twelve were chosen to have an average burnup of 12 gms. to 150 gms, one-half of the usual total burnup in this position. The elements in the ring of six were chosen to have an average burnup of 34 gms. to 128 gms. A sample calculation was then carried out to check that it is safe to place a 162 gm. fresh element in core position number one for this configuration.

TABLE VI

CORE CONFIGURATION

Region	Fuel Elements No.-Loading	Wt. of U for criticality	Total U	Excess Reactivity
c	1-162 gm.	162 gm.	162 gm.	0
i	6-128 gm.	768 gm.	930 gm.	0
a	6-150 gm.	900 gm.	1830 gm.	0
a	1-150 gm.	128 gm.	1980 gm.	0.331 β
		1958 gm.		
a			2730 gm.	11.295 β
Braze				3.833 β
				15.459 β

TABLE VII

FISSION CROSS SECTIONS

Region	Unburned fuel/element	$\Sigma_f \times 10^2$
c	162 gm.	5.621
i	128 gm.	4.441
a	150 gm.	5.205

The procedure follows section 3-6. The only parameter which is changed is C_1 through Σ_f and this is a direct proportionality, therefore:

Region	From sect. 3-6 $N\ C_1\ Y(r)\ X(r)\ \bar{Z}_F$		Present case $N\ C_1\ Y(r)\ X(r)\ \bar{Z}_F$
c	5.410×10^{-15}	(162/162) =	5.410×10^{-15}
i	30.743×10^{-15}	(128/162) =	23.946×10^{-15}
a	48.958×10^{-15}	(150/162) =	45.331×10^{-15}
		Σ =	74.610×10^{-15}

Therefore:

$$\bar{R}(0) = \frac{5.000}{74.610\times10^{-15}} = 6.702\times10^{13}\ \frac{\text{neutrons}}{\text{cm}^2\text{-sec}}$$

The power in the central element is:

$$P = 6.702\times10^{13}\ (5.410\times10^{-15}) = .35742\ \text{MW}$$
$$= 357.42\ \text{KW}$$

From figure 14, for a β_{ex} of 15.459 β the shim bank must be 28.3 cm. into the core. The unshadowed core length is then 62.55 - 28.3 = 34.25 cm. At this shim bank position the maximum/average flux ration is 1.217 from figure 15 and the position of maximum flux is at 20.3 cm. above the bottom of the core from figure 16. The ratio of average flux between the bottom of the core and the hot spot to the average flux in the whole element was found to be 1.179 from figure 17. The calculations then follow section 4-7:

In the center element:

$$q = 357.42\ \text{KW}$$

The average plate produces:

$$\bar{q} = 357.42/16 = 22.339 \text{ KW}$$

The hottest plate produces:

$$q_{hp} = 1.25(22.339) = 27.924 \text{ KW}$$

The surface area of a fuel plate is:

$$A = 62.55\ (15.25) = 953.89 \text{ cm}^2.$$

The average specific heat flux in the hottest plate is:

$$q/A = 29.273 \text{ watts/cm}^2.$$

The maximum specific heat flux was then simply the ratio of maximum to average flux found in figure 15 times this number, i.e.:

$$q_1/A = 1.217(29.273) = 35.625 \text{ watts/cm}^2.$$
$$= 1.130 \times 10^5 \text{ BTU/hr ft}^2.$$

This number number can be reduced by the factor found in section 4-5 for the heat which is not transferred through the plate walls.

Therefore:

$$q_1/A = .9091\ (1.130 \times 10^5) = 1.027 \times 10^5 \text{ BTU/hr ft}^2.$$

The heat deposited in the coolant channel up to the hot spot was found as follows:

In the center element:

The heat deposited in an average coolant channel is:

$$q = \frac{357.42}{17} = 21.205 \text{ KW}$$

The average heat deposited in the outer coolant channel is:

$$q = 1.25\ (21.205) = 26.281\ KW$$

Since the hot spot is 20.3 cm. from the bottom of the channel, (from figure 15) the heat deposit up to the hot spot is:

$$q = \frac{20.30}{62.55}\ (26.281) = 8.529\ KW$$

This number was then adjusted for the difference between the average flux in this region and the average flux in the entire axial channel. This ratio is found in figure 17. Therefore:

$$q_2 = 1.179\ (8.529) = 10.056\ KW$$
$$= 3.432 \times 10^4\ BTU/hr.$$

This number was also adjusted to account for the direct γ and neutron heating in the free moderator, as outlined in section 4-5.

Therefore:

$$q_q = .9278\ (3.432 \times 10^4) = 3.184 \times 10^4\ BTU/hr.$$

Recalling equation 4.7:

$$Tw_{max} - To = \frac{q_{1/A}}{h} + \frac{q_2}{w_{ch}\ c_p} - \frac{q_R}{w\ c_p}$$

For a flow of 1800 GPM (9.882×10^5 lb/hr) and a To of 55°C:

$$q_R = 1.682 \times 10^7\ BTU/hr = w\ c_p\ \delta T$$

Therefore:

$$Ti = 45.58^{\circ}C$$

$$\bar{T}_R = 50.29^{\circ}C$$

At this temperature: (from figure 20 and section 4-2)

$$h = .0168(1.2185)w^{.8}$$

$$h = .02047\ w^{.8}$$

$$w^{.8} = 6.25 \times 10^{4}\ lb/hr$$

and:

$$w_{ch} = \frac{9.882 \times 10^{5}}{19 \text{ elements (17 channels/element)}}$$

$$= 3.059 c 10^{3}\ lb/hr.$$

Therefore, substituting in equation 4.7:

$$Tw_{max} - To = 80.27 + 10.33 - 16.95 = 73.65^{\circ}F$$

$$= 40.91^{\circ}C$$

The difference between the reactor outlet temperature and the maximum plate wall temperature was found to be $40.91^{\circ}C$. Therefore if a limit on reactor outlet temperature is assumed at $55^{\circ}C$, the maximum plate temperature will be $55^{\circ} + 40.91^{\circ} = 95.91^{\circ}C$. If a limit of $100^{\circ}C$ is set for the maximum plate temperature the reactor outlet temperature can safely be allowed to rise to $100 - 40.91 = 59.09^{\circ}C$. This means that a fresh 162-gram element is

allowable in the center position for this configuration. To find the maximum allowable center element fuel loading for this configuration, the entire calculation of section 4-13 must be itereated until a value of center fuel element loading is found which gives a Tw_{max} of exactly 100°C when the reactor outlet temperature is at the assumed limit of 55°C. This procedure was carried out with several core configurations having excess reactivities in the range from 4β to 16β. The results are plotted in figure 18.

To use this figure, one first computes the excess reactivity of the core in question by the method of section 4-13. The intercept of this value of β_{ex} with the slanted line of figure 18 establishes the maximum fuel loading in the center fuel element position. This limit is then extended to the other fuel element positions through the X(r)'s as explained in section 4-12. The horizontal line represents the maximum fuel loading currently available in MITR fuel elements, i.e. 162 grams.

It can be seen that cores having an adequate operational range of reactivity, that is, 15β to 20β, may employ a fresh 162-gram element in the central position at any time without fear of meltdown. It is emphasized that figure 18 has been calculated using the temperature, flow, and power limits stated on the figure. Any change in any of these values will necessitate new calculations and the construction of a new figure.

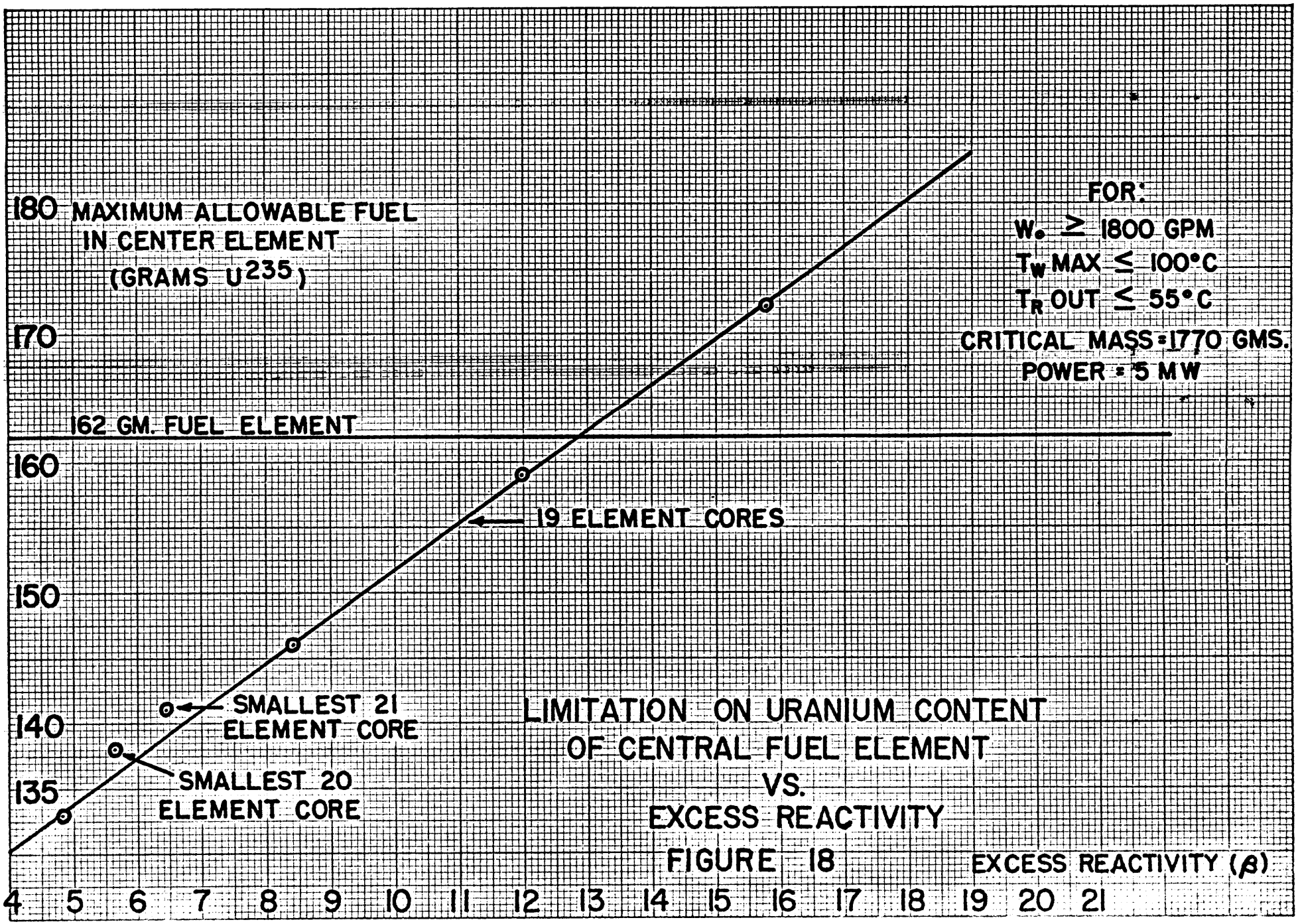
180
MAXIMUM ALLOWABLE FUEL IN CENTER ELEMENT (GRAMS U235)
170
160
150
140
135
FOR:
Wo ≥ 1800 GPM
TW MAX ≤ 100°C
TR OUT ≤ 55°C
CRITICAL MASS = 1770 GMS.
POWER = 5 MW
162 GM. FUEL ELEMENT
19 ELEMENT CORES
SMALLEST 21 ELEMENT CORE
SMALLEST 20 ELEMENT CORE
LIMITATION ON URANIUM CONTENT OF CENTRAL FUEL ELEMENT VS. EXCESS REACTIVITY
FIGURE 18
EXCESS REACTIVITY (β)
4 5 6 7 8 9 10 11 12 13 14 15 16 17 18 19 20 21

SECTION V

H_2O FLOW RATE

[5-1] METHOD

The general method of this section is to assume two parallel heat removal systems, each handling one half of the gross heat load of the reactor and its associated systems. In this situation the present heat exchanger system must be so operated as to remove 2.5 MW. To determine the required flow rate of secondary coolant for five megawatt operation, it was first necessary to investigate the efficiency of the heat exchanger at its present operating level. Using this information as a base, one is able to extrapolate the system to five megawatt operating parameters.

The most important characteristic of the heat exchanger is its overall resistance to heat flow, 1/UA.

$$\frac{1}{UA} = \frac{1}{h_o A_o} + \frac{1}{h_i A_i} + \frac{1}{h_{sc} A_{sc}} + \frac{\ln(r_o/r_i)}{2\pi k L N} \qquad (5.1)$$

where $\frac{1}{h_o A_o}$ is the convective resistance on the outside of the heat exchanger tubes. $\frac{1}{h_i A_i}$ is the convective resistance on the inside of the tubes. $\frac{1}{h_{sc} A_{sc}}$ is the resistance of the scale on the outside of the tubes, and

$\frac{\ln r_o/r_i}{2\pi kLN}$ is the conduction resistance of the stainless steel walls of the tubes. In this equation, h_i can easily be calculated by a well-correlated expression and the conduction term is well known. The principal unknowns were then h_o and h_{sc}. A_{sc} might also be considered unknown, but it can be approximated fairly accurately from the dimensions of the heat exchanger. According to McAdams,[35]

$$h_i = \frac{k}{D}(.023\ Re^{.8}\ Pr^{.33}) \qquad (5.2)$$

and h_o can be approximated by,

$$h_o = K(k\ Re^{.6}\ Pr^{.33}) \qquad (5.3)$$

Fortunately for out analysis, the constant in the expression for h_i is well defined. The constant K in the expression for h_o was here determined experimentally. The most significant point in these expressions is that:

$$h_i = K_1(T)\ w_i^{.8} \qquad \text{and} \qquad h_o = K_2(T)\ w_o^{.6}$$

The first step toward the solution of equation 5.1 was the calculation of h_i according to equation 5.2. The conduction term, $\frac{\ln(r_o/r_i)}{2\pi kLN}$, was then calculated.

Neglecting for a moment the effects of temperature, if the D_2O flow rate inside the tubes is kept constant, $1/h_iA_i$ is also constant. $1/h_{sc}A_{sc}$ was assumed independent of flow rate and is, therefore, also a constant. Regrouping equation 5.1:

$$\frac{1}{UA} = C_6 + \frac{1}{h_oA_o} \tag{5.4}$$

where

$$C_6 = \frac{1}{h_iA_i} + \frac{1}{h_{sc}A_{sc}} + \frac{\ln(r_o/r_i)}{2\pi kLN} \tag{5.5}$$

however:

$$h_o = .33\ Re^{.6}\ Pr^{.33}$$

Regrouping this expression:

$$h_o = C_7\ w_o^{.6} \tag{5.6}$$

where

$$C_7 = .33\ Pr^{.33}\ (De/A_x\mu)^{.6} \tag{5.7}$$

Substituting equation 5.6 into equation 5.4

$$\frac{1}{UA} = C_6 + \frac{1}{C_7A_ow_o^{.6}} \tag{5.8}$$

or, incorporating the area into the constant:

$$\frac{1}{UA} = C_6 + C_8 (1/w_o^{.6}) \qquad (5.9)$$

The general heat transfer relation

$$q = UA\ \delta T_{LM} \qquad (5.10)$$

was also employed here.

$$UA = q/\delta T_{LM} \qquad (5.11)$$

where

$$\delta T_{LM} = \frac{\delta T_{D_2O} - \delta T_{H_2O}}{\ln \left[\frac{T_{D_1} - T_{H_2}}{T_{D_2} - T_{H_1}} \right]} \qquad (5.12)$$

An experiment was then conducted to determine the constants in equation 5.9. At constant power and D_2O flow rate, and in as nearly constant temperature ranges as possible, the H_2O flow rate was varied and the following quantities were observed for each variation: T_{D_1}, T_{D_2}, T_{H_1}, T_{H_2}, and w_o. δT_{LM} was then found by equation 5.12 and UA by equation 5.11. Plotting 1/UA vs. $1/w_o^{.6}$, the extrapolated value of the line at the point where $1/w_o^{.6}$ is zero gave C_6 and the slope of the line yielded C_8. A linear least squares fit was used so that the extrapolation

was as exact as possible.

Once C_6 was known, $1/h_{sc}A_{sc}$ was available, and C_8 easily gave us h_o as a function of flow rate. After these base values were determined, it remained only to correct each for flow rate and temperature in order to extrapolate 1/UA to the conditions of five megawatt operation. Knowing UA and q at the new operating point one then finds δT_{LM} by equation 5.10. At this point another factor must be considered, namely, the cooling tower.

The cooling tower will be considered at length in section VII which describes an experiment designed to measure its efficiency.

Suffice it to say that up to this time the cooling tower has proved to be very efficient. An analysis of the MITR operating records for the summer of 1961 indicated that, even on the hottest, most humid days, the cooling tower was always able to deliver H_2O at less than 76°F. These records are for 1.8 MW operation and total H_2O flow of 835 GPM. Design specifications of the tower call for 1000 GPM of H_2O to be cooled from 103°F to 80°F at a wet-bulb temperature of 72°F and 0-10 MPH wind. A quick calculation indicates a nominal design heat dissipation rate of 3.34 MW. It must be remembered, however, that this tower must service not only the reactor, but also its associated experiments and air-conditioning

equipment with their additional heat load.

Consistent with the limiting nature of this study, the H_2O flow rate was computed using conditions which would exist on the hottest day. The outlet temperature of the cooling tower was taken to be 89.25°F (see section VII) with the reactor outlet temperature at 131°F (55°C). For the established flow rate of 9.885×10^5 lb/hr, this gives a D_2O δT of 16.96°F and a reactor inlet temperature of 114.04°F.

As described above using equation 5.10 we were able to arrive at a δT_{LM} for the reactor at five megawatts. Using this derivation for δT_{LM} and the above assumed temperatures, we were able to establish T_{H_2} and δT_{H_2O}. With this value and using

$$q = w_o c_p \delta T_{H_2O} \qquad (5.13)$$

an approximation of the required flow rate can be computed. It must be remembered that both heat loads and flow rates must be halved in these calculations as only one half of the anticipated two parallel and identical systems is being dealt with.

Using this calculated value of the H_2O flow, one returns to the extrapolation of 1/UA and iterates the entire calculation until the required accuracy is obtained.

[5-2] CALCULATION OF h_i AT EXPERIMENTAL CONDITIONS

Using the Colburn equation and the values of the parameters listed in Table VIII, a base value of h_i was readily calculated for the conditions under which the heat exchanger experiments were conducted.

From equation 5.2:

$$h_i = .023\ Re^{.8}\ Pr^{.33}$$

The Reynolds Number was computed on the basis of one tube.

$$Re = \frac{w_i D_i}{A x_i \mu} \qquad (5.14)$$

$$w_i = \frac{4.590 \times 10^5}{885 \text{ tubes}} = 518.6 \text{ lb/hr-tube}$$

$$Re = \frac{(518.6)(2.3 \times 10^{-2})}{(3.95 \times 10^{-4})(2.439)} = 1.238 \times 10^4$$

$$Re^{.8} = 1.87 \times 10^3$$

$$Pr = \frac{c_p \mu}{k} = \frac{1.005(2.439)}{.343} = 7.146 \qquad (5.15)$$

$$Pr^{.33} = 1.925$$

$$h_i = \frac{(.343)(2.30 \times 10^{-2})(1.87 \times 10^3)(1.925)}{2.30 \times 10^{-2}}$$

$$= 1.235 \times 10^3$$

TABLE VIII

PARAMETERS FOR HEAT EXCHANGER CALCULATIONS

AT EXPERIMENTAL CONDITIONS

Tube length	L	14.17 Ft.
Inside tube radius	r_i	1.15×10^{-2} Ft.
Outside tube radius	r_o	1.56×10^{-2} Ft.
Tube wall thickness	x	4.08×10^{-3} Ft.
Outside wall area of tubes	A_o	1230.50 Ft^2.
Inside wall area of tubes	A_i	909.88 Ft^2.
Cross section of one tube	A_x	3.95×10^{-4} Ft^2.
Average bulk temperature of D_2O	$\bar{T}_D$	28.65°C
Average bulk temperature of H_2O	$\bar{T}_H$	19.77°C

μ_D	2.439	lb/hr-Ft
$C_p(D_2O)$	1.005	BTU/lb-°F
$C_p(H_2O)$	.998	BTU/lb-°F
k (D_2O)	.343	BTU/hr-Ft-°F
k (stainless steel)	9.4	BTU/hr-Ft-°F
w_i	4.590×10^5	lb/hr

[5-3] CONDUCTION RESISTANCE

The next step was the calculation of the resistance to heat flow of the stainless steel walls of the tubes. Parameters were again taken from Table VIII.

$$\frac{\ln r_o/r_i}{2\pi kLN} = \frac{\ln(1.56\times10^{-2}/1.15\times10^{-2})}{2\pi(9.4)(14.17)(885)} = 4.117\times10^{-7} \qquad (5.16)$$

[5-4] HEAT EXCHANGER EXPERIMENTS

Two separate experiments were conducted with the process system to measure the performance of the heat exchanger. In each case, with the reactor power at one megawatt and the D_2O flow rate constant, the H_2O flow rate was varied in steps of approximately 100 GPM from 700 GPM to 400 GPM. For each step the amount of evaporation in the cooling tower was adjusted so as to keep an approximately equal H_2O temperature average.

At each step the entire system was allowed to come to thermal equilibrium, and the temperatures and flow rates were recorded. The flow recorders were calibrated by means of U-tube manometers just prior to the experiments, and the temperature recorders were calibrated over the appropriate ranges on the day after the experiment. In this way, the accuracy of the experiments was increased

considerably. The corrected data from both these experiments has been summarized in Table IX. Figure 19 is a plot of the combined data points of both experiments. 1/UA, the resistance to heat flow of the heat exchanger, is plotted against the six-tenths power of the H_2O flow rate.

A standard least squares analysis performed on this data resulted in the line shown in figure 19. C_6 was found to be 2.669×10^{-6} and C_8 was 6.81×10^{-5}.
From equation 5.4

$$C_6 = \frac{1}{h_i A_i} + \frac{1}{h_{sc} A_{sc}} + \frac{\ln(r_o/r_i)}{2\pi k L N}$$ but from section 5-2,

$$1/h_i A_i = 8.896 \times 10^{-7}$$ and from section 5-3,

$$\frac{\ln(r_o/r_i)}{2\pi k L N} = 4.117 \times 10^{-7}$$

Therefore:

$$\frac{1}{h_{sc} A_{sc}} = C_6 - \frac{1}{h_i A_i} - \frac{\ln(r_o/r_i)}{2\pi k L N}$$

$$= 26.69 \times 10^{-7} - 8.896 \times 10^{-7} - 4.117 \times 10^{-7} = 13.677 \times 10^{-7}$$

This illustrates that the scale resistance is approximately equal to the inside film resistance plus

TABLE IX

HEAT EXCHANGER EXPERIMENTS - CORRECTED DATA

D_2O Flow GPM	H_2O Flow GPM	T_{D_1} °C	T_{D_2} °C	T_{H_1} °C	T_{H_2} °C	δT_{LM} °C	q_R BTU/hr x10^{-6}	1/UA x10^{6}	$\bar{w}_o^6$ x10^{-2}
835	685	29.85	25.65	16.90	22.85	14.12	3.506	4.207	2.00
835	685	29.65	25.55	16.90	22.75	13.97	3.424	4.080	2.00
835	605	30.25	26.35	17.35	23.85	13.73	3.256	4.218	2.13
835	604	30.15	26.15	17.15	23.75	13.73	3.339	4.112	2.15
835	513	30.35	26.45	16.55	24.05	14.35	3.423	4.191	2.38
835	513	30.35	26.25	16.45	23.95	14.37	3.339	4.303	2.38
835	427	29.10	25.05	13.85	22.95	15.17	3.382	4.486	2.65
835	427	29.05	25.05	13.95	23.05	14.92	3.340	4.466	2.65
836	690	28.10	24.05	15.60	21.60	13.38	3.366	3.975	1.98
836	615	29.05	25.00	16.20	22.65	13.56	3.341	4.058	2.12
831	515	33.25	29.50	19.40	27.05	14.39	3.317	4.338	2.35
831	422	31.55	27.30	16.10	25.50	15.05	3.368	4.468	2.65

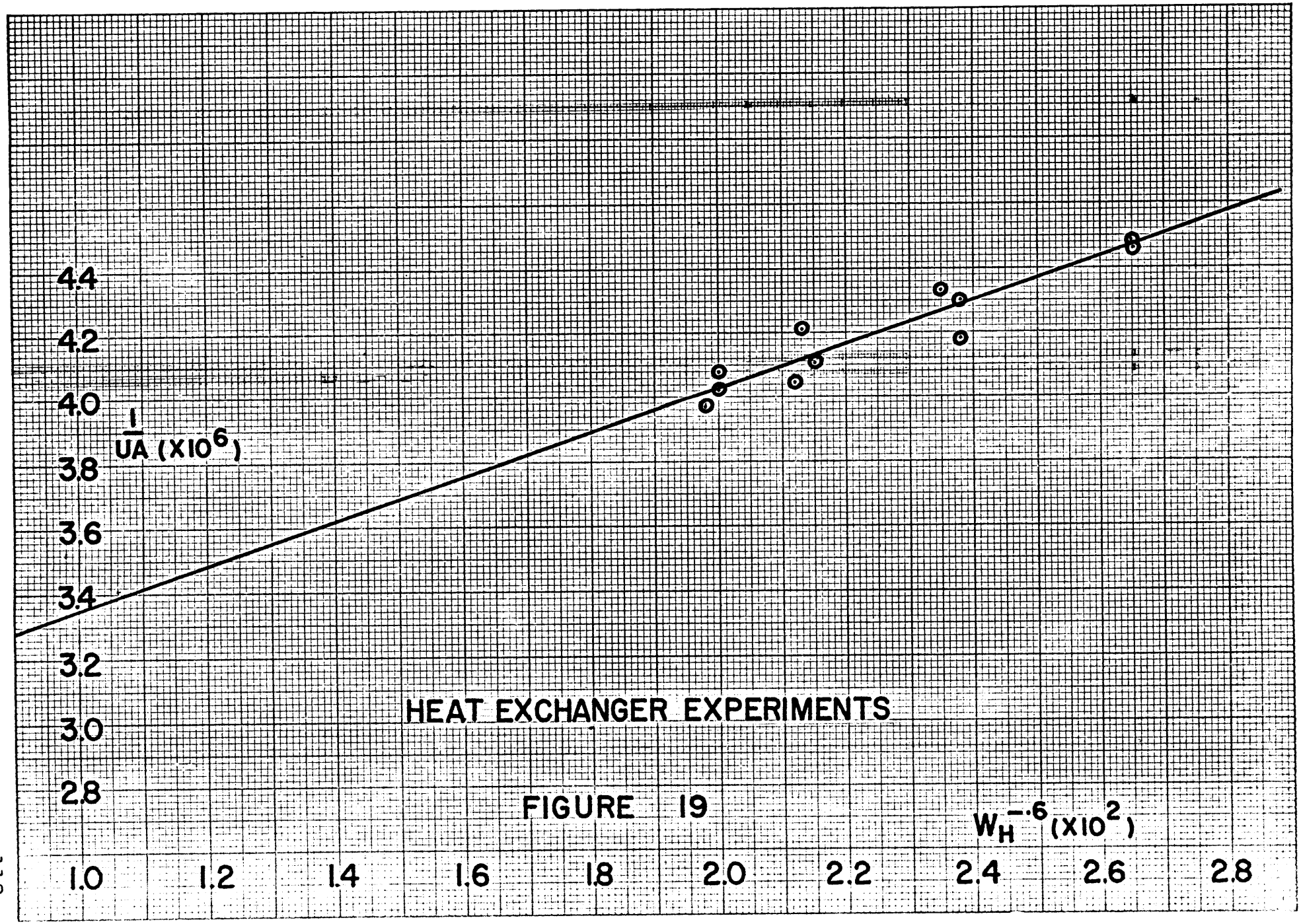
4.4
4.2
4.0
3.8
3.6
3.4
3.2
3.0
2.8
$\frac{1}{UA}$ (X10^6)
1.0
1.2
1.4
1.6
1.8
2.0
2.2
2.4
2.6
2.8
$W_H^{-.6}$ (X10^2)
HEAT EXCHANGER EXPERIMENTS

FIGURE 19

the conduction resistance.

From equation 5.9:

$$1/h_o A_o = C_8 \, (1/w_o^{.6})$$

As a base value computed for an H_2O flow rate of 685 GPM and a $\bar{T}_H$ of 19.77°C:

$$1/h_o A_o = 6.81 \times 10^{-5} (2.00 \times 10^{-2}) = 13.62 \times 10^{-7}$$

As a quick check, these resistances should add up to 40.27×10^{-7} as found in row 1 of Table IX.

$$(8.896 + 4.117 + 13.677 + 13.62 = 40.31) \times 10^{-7}$$

These values are then the base. With appropriate temperature and flow corrections they can be extrapolated to new conditions over a reasonable range.

[5-5] TEMPERATURE CORRECTIONS

Of the four terms in the resistance to heat flow expression, equation 5.1, the conduction term is independent of temperature over the range of interest, and the scale resistance was assumed to be temperature independent over this range. The convective heat transfer coefficients, both inside and outside of the tubes, are strongly dependent on temperature, becoming

larger with higher temperatures, due largely to the decreased fluid viscosity.

From equation 5.2, clearing fractions,

h_i is directly proportional to $k^{.67} w^{.8} c_p^{.34} \mu^{-.46}$

Separating the flow rate term from the fluid density,

$$h_i = k^{.67} \varepsilon^{.8} c_p^{.34} \mu^{-.46} \qquad (5.17)$$

since,

$$w(lb/hr) = m(GPM)\varepsilon(lb/Ft^3)\ C_9(Ft^3 min/Gal)hr$$

Taking the average temperatures of the heat exchanger experiment as a base, the temperature dependence has been calculated and plotted in the form of a temperature correction factor to $1/h_i$. This correction is shown in figure 20.

In a like manner, equation 5.3 shows that h_o is directly proportional to $k^{.67} w_o^{.6} c_p^{.34} \mu^{-.26}$ or $k\ \mu^{-.6}\ Pr^{.33} w_o^{.6}$. Again separating the flow rate in gallons per minute from the fluid density term,

$$h_o = k\ Pr^{.33}\ \varepsilon^{.6}\ \mu^{-.6} \qquad (5.18)$$

The temperature correction to $1/h_o$ is illustrated in figure 21.

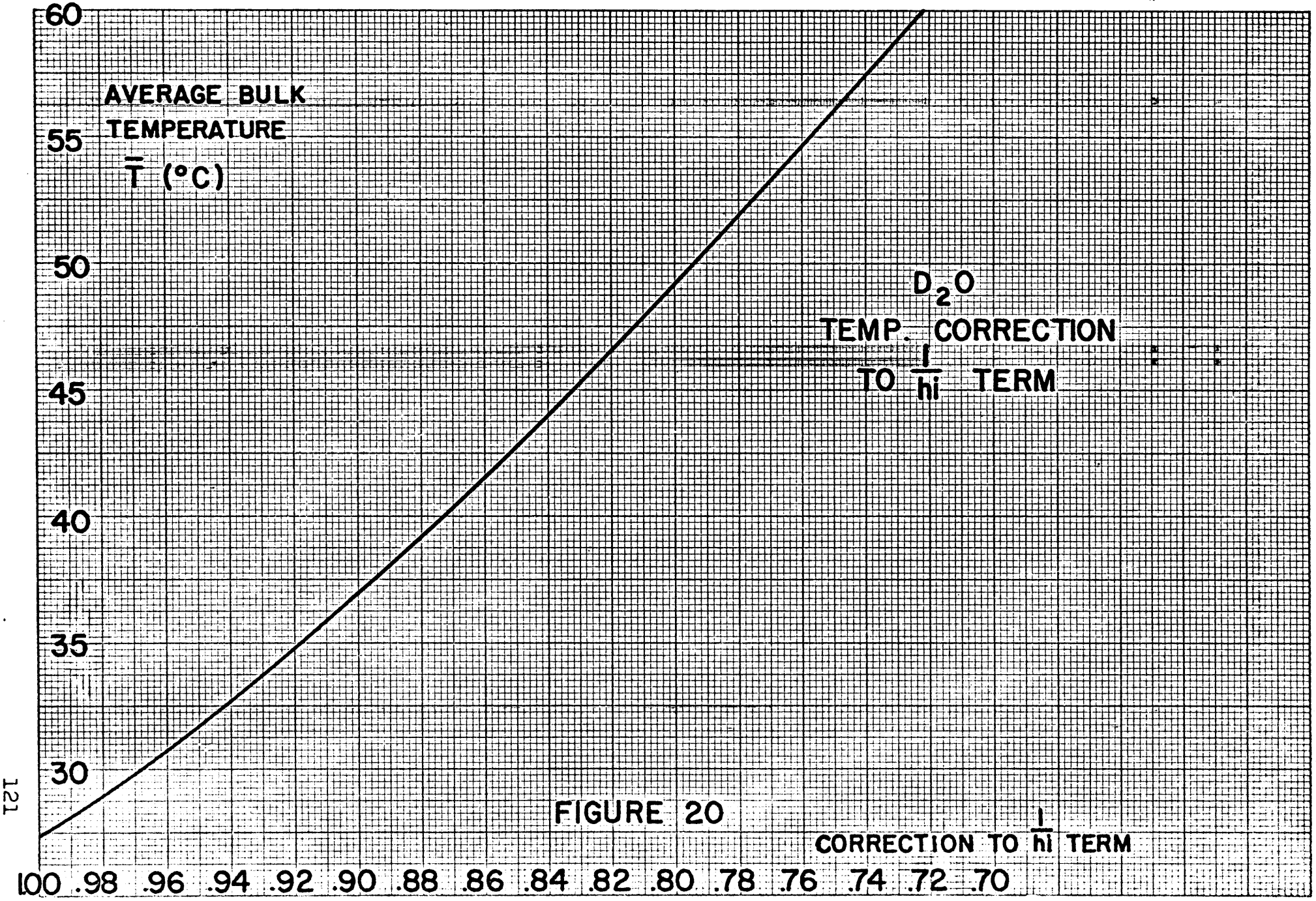
60
55
50
45
40
35
30
AVERAGE BULK
TEMPERATURE
$\bar{T}$ (°C)
D_2O
TEMP. CORRECTION
TO $\frac{1}{hi}$ TERM
100 .98 .96 .94 .92 .90 .88 .86 .84 .82 .80 .78 .76 .74 .72 .70
CORRECTION TO $\frac{1}{hi}$ TERM

FIGURE 20

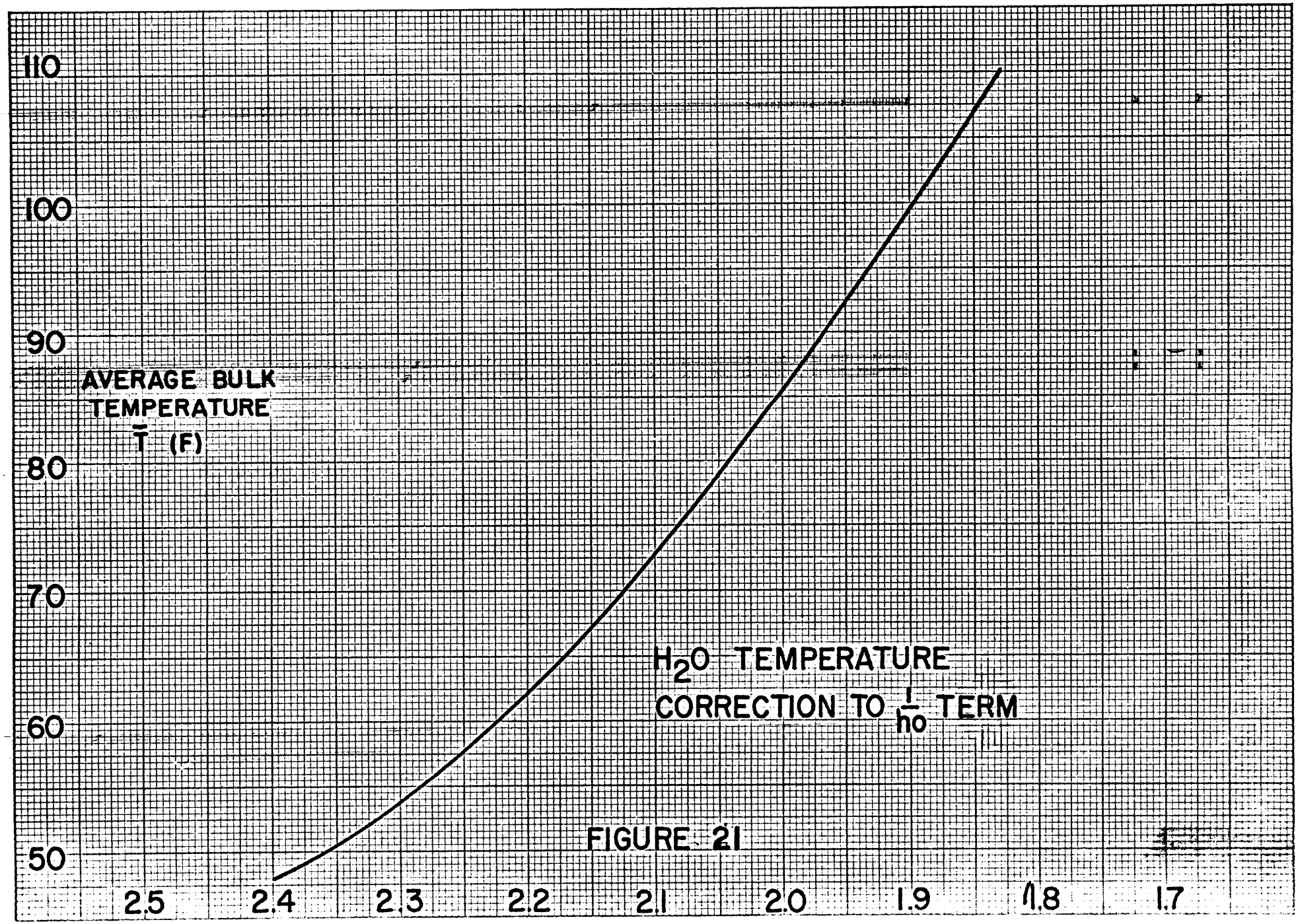
110
100
90
80
70
60
50
AVERAGE BULK TEMPERATURE
$\bar{T}$ (F)
2.5
2.4
2.3
2.2
2.1
2.0
1.9
1.8
1.7
H_2O TEMPERATURE CORRECTION TO $\frac{1}{h_o}$ TERM

FIGURE 21

[5-6] FIVE MEGAWATT RESISTANCE CALCULATION

Since the conduction term and the scale resistance have been assumed to be independent of temperature and flow rate, their values were simply brought forward unchanged. The average bulk temperature of the D_2O under the limiting conditions of the hottest day is 50.29°C and the average H_2O temperature for these conditions is 96°F. At these temperatures the fluid properties have changed somewhat from Table VIII.

The base value of $1/h_iA_i$ is 8.896×10^{-7} calculated for a flow rate of 831 GPM and at a $\bar{T}$ of 28.65°C. At five megawatts the expected D_2O flow rate will be 1100 GPM per heat exchanger and $\bar{T}$ will be 50.29°C. From figure 20 the temperature correction was then,

$$\frac{.786}{.984} = .805$$

and the flow rate correction was

$$\left(\frac{831}{1100}\right)^{.8} = .799$$

Therefore the extrapolated value was

$$1/h_iA_i = (8.897 \times 10^{-7})(.805)(.799) = 5.723 \times 10^{-7}$$

The base value of $1/h_oA_o$ was 13.62×10^{-7} at an H_2O flow rate of 685 GPM and a $\bar{T}$ of 19.77°C (67.59°F).

At five MW conditions the first trial value of the flow rate was 1000 GPM. The average temperature is 96°F, hence, from figure 21 the temperature correction was,

$$(\frac{1.908}{2.151}) = .887$$

The flow rate correction was:

$$(\frac{685}{1000})^{.6} = .797$$

The extrapolated value of $1/h_oA_o$ was then,

$$(.797)(13.62\text{x}10^{-7})(.887) = 9.628\text{x}10^{-7}$$

For five megawatt operation 1/UA is:

$$1/UA = [9.628 + 5.723 + 4.117 + 13.677 = 35.751]\ \text{x}10^{-7}$$

From section 4-5, the total heat load of the primary system is $1.683\text{x}10^7$ BTU/hr or $8.42\text{x}10^6$ BTU/hr-HE. According to equation 5.10:

$$\delta T_{LM} = q/UA = (8.42\text{x}10^6)(3.315\text{x}10^{-6}) = 27.91°F \qquad (5.19)$$

This is the δT_{LM} required in the heat exchanger to remove the heat load under the conditions specified.

Three of the four temperatures involved in δT_{LM} were defined in section 5-1 as $T_{D_1} = 131°F$, $T_{D_2} = 114.04°F$, $T_{H_1} = 89.25°F$. The unknown was, therefore, T_{H_2}.

Figure 22 is a plot of δT_{LM} vs. H_2O flow rate in GPM, for various values of T_{H_2} in the range of 100 to 110°F.

The value of δT_{LM} required in equation 5.19 is then found to necessitate an H_2O flow rate of 1160 GPM/HE from figure 22. This would require a total H_2O flow for both heat exchangers of 2320 GPM. This was the first iteration. Using the calculated value of 1160 GPM/HE, $1/h_oA_o$ was again computed. The temperature correction remained the same, but the flow correction was changed to:

$$(\frac{685}{1160})^{.6} = (.591)^{.6} = .729$$

Therefore:

$$1/h_oA_o = (13.62\text{x}10^{-7})(.887)(.729) = 8.807\text{x}10^{-7}$$

$$1/UA = 32.324\text{x}10^{-7}$$

$$\delta T_{LM} = 27.21$$

$$M_{H_2O} = 1110 \text{ GPM/HE}$$

Several iterations are illustrated in Table X.

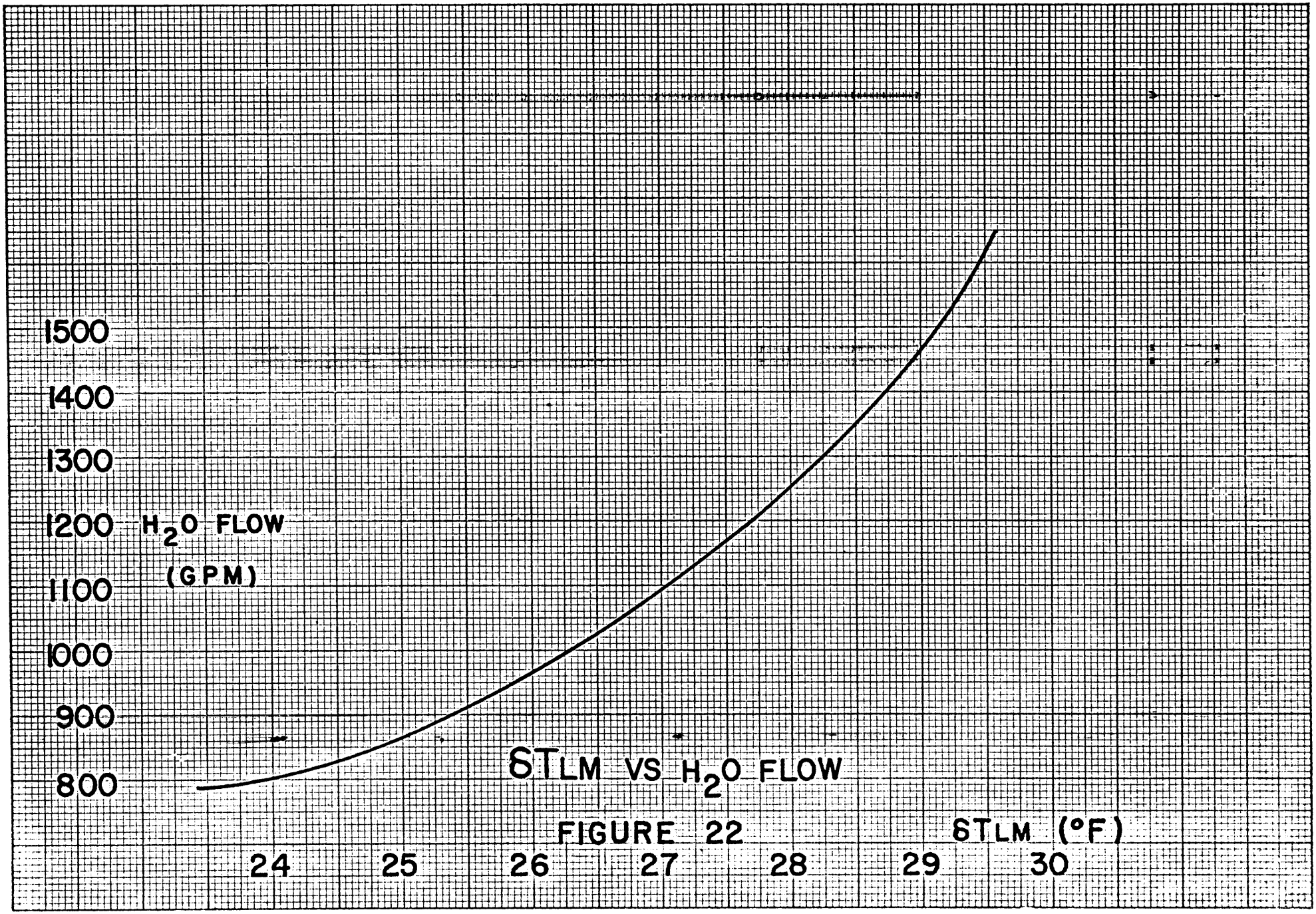
1500
1400
1300
1200
1100
1000
900
800
H2O FLOW
(GPM)
δTLM VS H2O FLOW
24
25
26
27
28
29
30
δTLM (°F)

FIGURE 22

TABLE X

H_2O FLOW ITERATIONS

Iteration	Assumed flow rate	$1/h_{o_7}A_o$ ($\times 10^7$)	$1/UA$ ($\times 10^7$)	δT_{LM} °F	Calculated flow rate (figure 22)
1.	1000 GPM	9.628	33.145	27.91	1160 GPM
2.	1160 GPM	8.807	32.324	27.21	1110 GPM
3.	1135 GPM	8.928	32.445	27.32	1130 GPM

Iteration number three is approximately closed at 1132 GPM. The total H_2O flow rate for the two main heat exchangers on the "hottest day" was established at 2263 GPM. The H_2O flow is the most dependent variable since it depends on the heat distribution calculations of Section III, the D_2O flow rate and temperature calculations of Section IV, and the cooling tower experiment of Section VII for its accuracy.

A complete error analysis was therefore carried out on the H_2O flow rate calculation. The principal results will be summarized here.

Errors assumed in the principal parameters were:

D_2O flow rate $\pm$ 20 GPM

H_2O flow rate $\pm$ 5 GPM

All temperatures $\pm$ .2 ^{o}C

These errors were propagated through the heat exchanger experiment calculations where the final error in 1/UA as calculated in section 5-6 was found to be 11.6 per cent. Proceeding with the calculation of the H_2O flow rate using values of 1/UA + 11.6 o/o and 1/UA - 11.6 o/o the actual range of variation of w_H was found to be from 892 GPM to 1530 GPM per heat exchanger.

Therefore:

$$w_H = 2264 \begin{matrix} +800 \\ -480 \end{matrix} \text{ GPM}$$

This represents a maximum error of about 35 o/o.

It should be remembered at this point that this value of w_H was calculated under extremely adverse conditions on the hottest summer day. It is anticipated that the need for flow rates of this magnitude will be extremely rare.

SECTION VI

SHIELD COOLANT SYSTEM

INTRODUCTION

The general method of this section was first to investigate the installed equipment in the shield coolant system and then to evaluate its performance at an assumed power level of five megawatts. On the basis of this investigation, recommendations were made as to the installation of any new components necessary.

[6-1] SHIELD POWER

The first requirement was to evaluate the heat load carried by the shield coolant at two megawatts.

$$q_S = w_S c_p \delta T_S \qquad (6.1)$$

In this equation q_S is the shield power dissipation, w_S is the primary shield flow rate, and δT_S is the temperature difference across the heat exchanger in the primary shield coolant. To get a good experimental average δT_S, the six point recorder was first calibrated

during a Saturday maintenance period. The following Monday the reactor was brought to an operating power of two megawatts and a twelve hour period allowed for the system to come to thermal equilibrium. The shield coolant temperatures were then recorded hourly in the operations log for the next three days. The δT's computed for these 72 sets of readings were then temperature corrected according to the calibration curves and averaged. This average δT was then used for any further calculations involving shield power. δT_S was found to be $1.877 \pm .127\ ^{o}C$ ($3.379 \pm .229\ ^{o}F$) by this method.

The shield coolant flow rate remained essentially constant throughout this experiment at 77 ± 5 GPM. Since there is no installed way of checking the calibration of the shield coolant flow recorder a small calibration correction recommended by Homeyer[36] was applied. He found by experimental measurement that at a recorded flow of 70.7 GPM the actual flow rate was 73.0 GPM. The flow rate was therefore taken to be:

$$w_S = (73/70.7)(77.0) = 79.46 \pm 5 \text{ GPM}$$

One gallon per minute of light water at this temperature was found to be equal to 497.88 lb/hr and c_p was .9974

at $35^{o}C$.

Therefore:

$$q_S = (79.46)(497.88)(.9974)(3.379) = 1.33 \times 10^5 \text{ BTU/hr} \pm 6.55 \text{ o/o}$$

The average power produced in the reactor primary coolant during this period was 6.449×10^6 BTU/hr. The total power was therefore:

$$6.449 \times 10^6 + .133 \times 10^6 = 6.582 \times 10^6 \text{ BTU/hr}$$

Shield power was then:

$$\frac{.133}{6.582} = 1.360 \pm .095 \text{ o/o}$$

of the total reactor power. While the error quoted is 7 o/o it is believed that the actual error range is probably closer to 100 o/o due to the fact that careful calibrations of the shield temperature recorder gave widely varying results on different days.

It was assumed that the main contribution to heating in the thermal shield comes from the energy deposit by γ radiation and neutron interaction in the boral, with

only a small amount of heat introduced by conduction and radiation from the graphite. The heating rate in the thermal shield should, therefore, be directly proportional to the power level of the reactor. In specific application, the percentage of the total reactor heat load removed by the shield coolant was assumed to be the same at five megawatts as it is at two. At five megawatts therefore:

$$q_S = .0136\ (1.706 \times 10^7) = 2.320 \times 10^5 \text{ BTU/hr}$$

[6-2] SHIELD COOLANT HEAT EXCHANGER

The next item of interest was the shield coolant heat exchanger. There is no direct means of measuring the flow on the secondary side of this component. It was necessary to install a well and Thermohm resistance thermometer in the secondary outlet of this exchanger to get even a secondary means of flow measurement. A glance at figure 6 shows that the secondary side of the shield coolant heat exchanger is in parallel with the main D_2O - H_2O heat exchanger across the light water circuit. The flow through these two heat exchangers will therefore distribute itself so that the pressure

drop across each will be the same. This suggested one means of obtaining an estimate of the flow on the secondary side of Heat Exchanger No. 3 at five megawatts.

Gages are available to read the pressure drop across Heat Exchanger No.1. The flow rate through Heat Exchanger No.1 is also known. These are related through the following formulas:

$$\delta P = 4 f \frac{L}{D} \frac{G^2}{2\varepsilon g} \qquad (6.2)$$

where the symbols are defined in Annex A.
For turbulent flow in a pipe:

$$f = \frac{.0792}{(Re)^{.25}} \qquad (6.3)$$

Combining these two equations one finds:

$$\delta P = K \varepsilon^{.75} \mu^{.25} w^{1.75} = K(T) w^{1.75} \qquad (6.4)$$

The pressure drop is therefore directly proportional to the flow rate to the 1.75 power and to a temperature dependent constant. Knowing both δP and w at two megawatts, K can be evaluated experimentally. Assuming the same temperature range and the previously calculated

flow rate at five megawatt conditions, the new δP for the main heat exchanger is calculated. The flow rate and δP for Heat Exchanger No.3 are also known at present operating levels. The proportionality constant for Heat Exchanger No.3 can then be calculated from this data. Since δP must be the same for Heat Exchanger No. 1 and Heat Exchanger No.3 at all power levels, and since the δP for Heat Exchanger No.1 has previously been calculated for five megawatts, the amount of coolant which would flow on the secondary side of the shield coolant heat exchanger at five megawatts under present equipment conditions can be calculated.

A typical set of corrected operating data at two megawatts is:

HE No.1 inlet pressure	30.7 psi
HE No.1 outlet pressure	23.5 psi
w_H HE No.1	678 GPM
w_S HE No.3 primary	79.0 GPM
T_{p1} HE No.3 primary inlet	32.3°C
T_{p2} HE No.3 primary outlet	30.32°C
T_{s1} HE No.3 secondary inlet	22.0°C
T_{s2} HE No.3 secondary outlet	26.8°C

δP for this data for the main heat exchanger was:

$$\delta P = 30.7 - 23.5 = 7.2 \text{ psi}$$

From equation 6.4:

$$\delta P = K_1 \, w_H^{1.75}$$

Therefore:

$$K_1 = \frac{\delta P}{w_H^{1.75}} = \frac{7.2}{(678)^{1.75}} = \frac{7.2}{8.008 \times 10^4} = 8.991 \times 10^{-5} \qquad (6.5)$$

At five megawatts H_2O flow has been calculated to be 1132 GPM/HE, therefore:

$$\delta P = 8.991 \times 10^{-5} (1132)^{1.75}$$
$$= 8.991 \times 10^{-5} (2.195 \times 10^5) = 19.74 \text{ psi}$$

In the shield coolant heat exchanger the heat on the primary and secondary sides was balanced to get the secondary flow rate.

$$w_p \, \delta T_p = w_s \, \delta T_s \qquad (6.6)$$

$$w_s = \frac{\delta T_p}{\delta T_s} w_p = \frac{1.98}{4.80} (79.0) = 32.55 \text{ GPM} \qquad (6.7)$$

Therefore:

$$K_2 = \frac{\delta P}{w_s^{1.75}} = \frac{7.2}{(32.55)^{1.75}} = \frac{7.2}{(4.182 \times 10^2)} = 1.722 \times 10^{-2} \qquad (6.8)$$

Secondary flow rate under five megawatt conditions is then:

$$w_s^{1.75} = \frac{\delta P}{K_2} = \frac{19.74}{1.722 \times 10^{-2}} = 1.146 \times 10^3 \qquad (6.9)$$

$$w_s = 53.0 \text{ GPM}$$

To remove the required heat load the secondary coolant δT must then be:

$$\delta T_s = \frac{q_s}{w_s c_p} = \frac{2.320 \times 10^5}{(53.0)(498)(.9974)} = 8.81^\circ F$$

$$= 4.89^\circ C$$

[6-3] HEAT EXCHANGER EXPERIMENT

The limiting temperature conditions of the secondary coolant system are known from Section V. The flow rates on both sides of the shield heat exchanger and the shield

power at five megawatts are known from section 6-2. Since these parameters are fixed, the only variables remaining are the temperatures on the primary side of the shield coolant heat exchanger.

From equation 5.8:

$$q = UA\ \delta T_{LM}$$

and from equation 5.1:

$$\frac{1}{UA} = \frac{1}{h_o A_o} + \frac{1}{h_i A_i} + \frac{1}{h_{sc} A_{sc}} + \frac{\ln(r_o/r_i)}{2\pi k L N}$$

These equations were applied to Heat Exchanger No.3

An initial assumption was made that the primary flow rate will be the same at five megawatts as it is at two megawatts. Therefore, except for a small temperature correction to the $1/h_i$ term, the last three terms of equation 5.1 are constant.

Changing to the notation of the shield coolant system:

$$\frac{1}{UA} = \frac{1}{h_s A_s} + C_{10} \qquad (6.10)$$

where:

$$C_{10} = \frac{1}{h_p A_p} + \frac{1}{h_{sc} A_{sc}} + \frac{\ln(r_o/r_i)}{2\pi k L N} \qquad (6.11)$$

Again following the method of section 5-1:

$$\frac{1}{UA} = C_{10} + C_{11}(1/w_s^{.6}) \qquad (6.12)$$

where:

$$C_{11} = \frac{1}{.33\ Pr^{1/3}\ A_s\ (De/A_x\mu)^{.6}} \qquad (6.13)$$

By varying the flow rate on the secondary side of the heat exchanger and observing the primary inlet and outlet temperatures, the secondary inlet and outlet temperatures, and the primary flow rate the following information is established:

$$q_p = w_p c_p \delta T_p = q_s = w_s c_p \delta T_s \qquad (6.14)$$

The primary side of the equation yields the shield heat load. A heat balance will give w_s, the secondary flow rate. Since:

$$\delta T_{LM} = \frac{\delta T_s - \delta T_p}{\ln \frac{T_{p2} - T_{s1}}{T_{p1} - T_{s2}}} \qquad (6.15)$$

and:

$$q_S = UA\ \delta T_{LM} \tag{6.16}$$

UA can be found for each variation of the flow rate and its accompanying temperature changes. Plotting 1/UA vs. $1/w_s^{.6}$ C_{10} in equation 6.7 is found at the ordinate where $1/w_s^{.6} = 0$, and C_{11} is found by the slope of the points. Establishing these two constants gave an equation which can be used to predict the heat exchanger resistance at any secondary flow rate.

Extending 1/UA to the five megawatt operating condition and knowing q_S at that power, δT_{LM} is found. T_{s1} is the same as T_{H1} on the hottest day in Section V for the limiting case. δT_s is known from section 4-2. δT_p was found to be:

$$\delta T_p = \frac{q_p}{w_p c_p} = \frac{2.320 \times 10^5}{(79)(498)(.9974)} = 5.91^\circ F \tag{6.17}$$
$$= 3.28^\circ C$$

Therefore, in effect, three of the four temperatures involved in δT_{LM} are established and the expression can be solved for the fourth. This method gave the bulk temperature in the shield coolant for the secondary flow rate in question.

Working in the other direction, the primary coolant temperature desired was specified and going back through δT_{LM} the secondary flow rate required to maintain this temperature was found.

[6-4] HEAT EXCHANGER EXPERIMENT- EXECUTION

To obtain the necessary curve of 1/UA vs. $w_s^{-.6}$ the secondary flow rate was varied via valve HV-8. With HV-8 full open the reactor was brought to power and 24 hours were allowed for the system to come to thermal equilibrium. The base point, or normal operating condition, was then calculated. All four of the shield heat exchanger temperatures were read on each of three successive cycles of the 6 point temperature recorder. The results were corrected using the previously prepared calibration curves and averaged. The shield primary coolant flow rate was read from its recorder and corrected. The secondary coolant flow rate was then calculated using the ratio of the δT's. δT_{LM} was calculated using the four heat exchanger temperatures. q_p was found according to equation 6.1 and UA was established using equation 5.1.

HV-8 was then partially closed and the system was again given 24 hours to come to thermal equilibrium. After that time another set of readings was taken and the same calculation procedure followed. This cycle was repeated until four points had been obtained. The principal experimental parameters are listed in Table XI. The results of the experiment are presented in figure 23. The line represents a linear least squares fit to the four experimental points.

For the previously calculated flow rate of 53.0 GPM for the secondary side at five megawatts, the resultant shield coolant temperatures were calculated as follows for the hottest day.

$$w_p = 79.98 \text{ GPM}$$
$$w_s = 53.0 \text{ GPM}$$
$$q_s = 2.32 \times 10^5 \text{ BTU/hr}$$
$$c_p = .9974$$
$$T_{s1} = 89.25^\circ F$$
$$T_{s2} = 98.06^\circ F$$
$$T_{p1} = \text{unknown}$$
$$T_{p2} = T_{p1} - 5.91^\circ F$$

Therefore:

$$w_s^{-.6} = (53.0)^{-.6} = .0925$$

TABLE XI

SHIELD HEAT EXCHANGER EXPERIMENT - CORRECTED DATA

w_p GPM	w_s GPM	T_{p1} °C	T_{p2} °C	T_{s1} °C	T_{s2} °C	δT_{LM} °F	q_S BTU/hr $\times 10^{-5}$	1/UA $\times 10^5$	$w_s^{-.6}$ $\times 10^2$
79.46	25.290	35.5	33.59	23.57	29.57	14.036	1.357	10.34	14.40
79.98	20.501	38.77	36.95	24.23	32.33	15,874	1.301	12.20	16.31
79.98	23.988	38.30	36.35	25.60	31.90	15.098	1.394	10.83	14.88
79.98	18.488	38.13	36.32	23.27	31.10	17.517	1.294	13.54	17.39

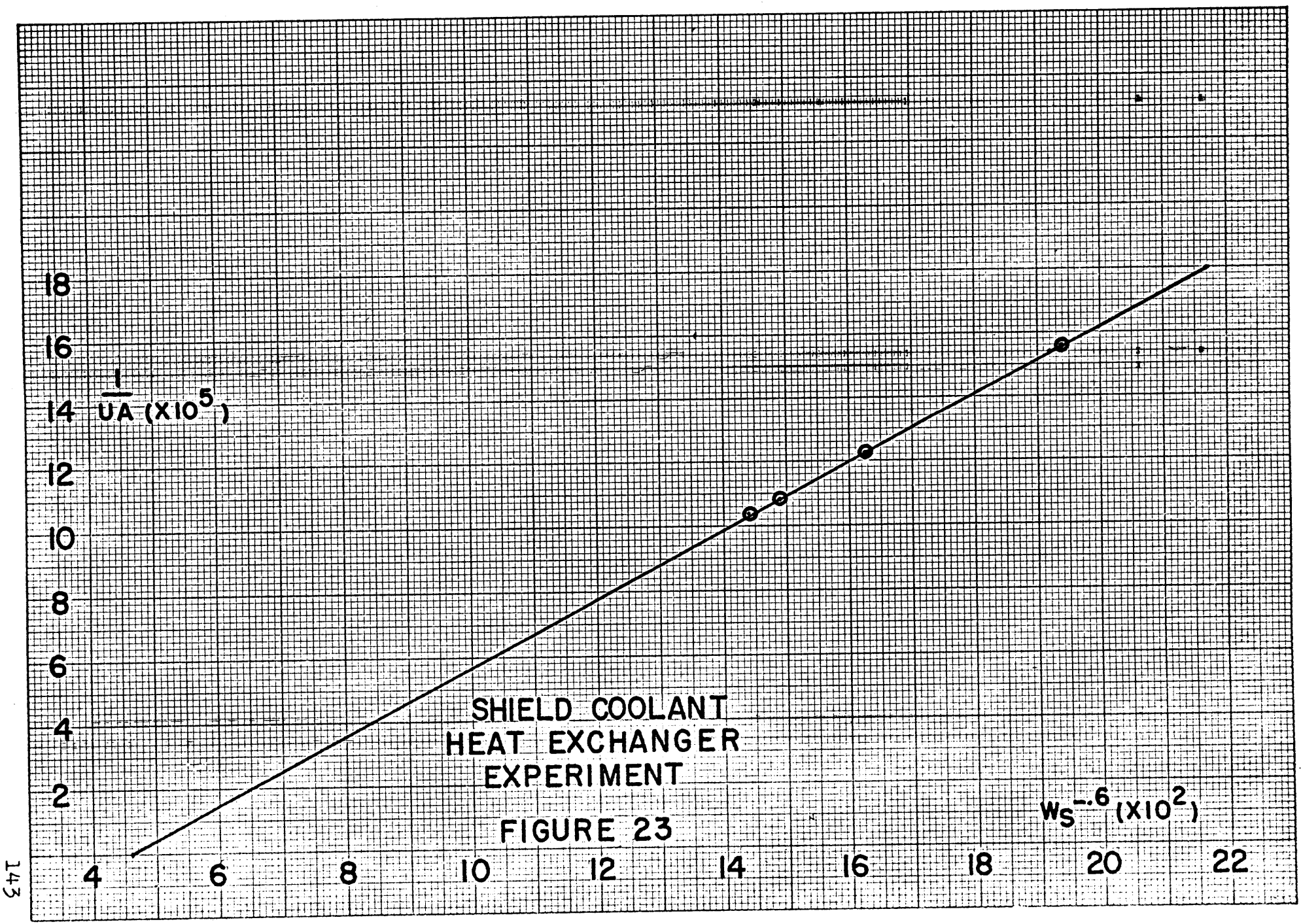
18
16
14
12
10
8
6
4
2
$\frac{1}{UA}$ (X10^5)
4
6
8
10
12
14
16
18
20
22
$W_S^{-.6}$ (X10^2)
SHIELD COOLANT
HEAT EXCHANGER
EXPERIMENT

FIGURE 23

From figure 23 at $w_s^{-.6} = .0925$:

$$1/UA = 4.95 \times 10^{-5}$$

$$\delta T_{LM} = q/UA = (2.32 \times 10^5)(4.94 \times 10^{-5}) = 11.48^\circ F$$

Therefore from equation 6.15:

$$11.48 = \frac{2.90}{\ln \frac{T_{pl}-95.16}{T_{pl}-98.06}}$$

$$\frac{T_{pl}-95.16}{T_{pl}-98.06} = e^{.2526} = 1.278$$

Therefore:

$$T_{pl} = 108.49^\circ F = 42.49^\circ C$$

This is an increase of about $5^\circ C$ above present operating levels for the shield coolant and probably represents a much larger increase in the temperature of the shield itself, including the possibility of cracking the concrete. It was concluded therefore that a means must be found of extracting heat from the heat exchanger more efficiently so that the primary coolant temperatures

could be reduced below this level.

Limiting the shield temperatures to their two megawatt levels and working back through the calculations the secondary flow rate necessary to maintain this condition was found. The calculation is an iterative one where a flow rate was picked for a start and then a better value computed.

For w_s = 100 GPM :

$$\delta T_s = \frac{q_s}{w_s c_p} = \frac{2.32 \times 10^5}{(100)(498)(.9974)} = 4.67^\circ F$$

For the hottest day:

$$T_{s1} = 89.25^\circ F$$
$$T_{s2} = 93.92^\circ F$$
$$T_{p1} = 104^\circ F \ (40^\circ C)$$
$$T_{p2} = 98.1^\circ F$$

According to equation 6.15:

$$\delta T_{LM} = 9.79^\circ F$$

Therefore:

$$1/UA = \frac{\delta T_{LM}}{q} = \frac{9.79}{2.32 \times 10^5} = 4.22 \times 10^{-5}$$

From figure 23 at this ordinate:

$$w_s^{-.6} = .086$$

Therefore:

$$w_s = 61.0 \text{ GPM}$$

Several more iterations in this manner yield a value of 68 GPM for the secondary coolant flow necessary to maintain the shield primary coolant outlet temperature at 40°C or less on the hottest day.

It is therefore recommended that a small pump of approximately 100 GPM capacity be added to the secondary side of the shield coolant system to insure that no excessive temperatures are experienced in the shield and to avoid the accompanying danger of cracking the concrete.

SECTION VII

COOLING TOWER

INTRODUCTION

The thermal equilibrium temperature of the entire reactor system is dependent on the temperature of the H_2O secondary coolant leaving the cooling tower. An evaluation of the performance of this piece of apparatus was therefore vital to this study of process system requirements.

[7-1] COMPLICATING FACTORS

Any analysis of the cooling tower is complicated by the following factors:

1. The total flow through the cooling tower is inaccurately known. The H_2O secondary coolant carries away the heat from the D_2O primary reactor coolant through Heat Exchanger No.1. The flow meter on this system is the only means of measurement of secondary coolant flow rate. Secondary coolant also flows through Heat Exchangers No.2 and No.5

which cool the clean up loop of the primary system. (See figure 7.) Although the flow rate is small no means is available to evaluate the flow through these heat exchangers.

The secondary coolant also carries away heat from Heat Exchanger No.4 in the experimental system. Again no means of obtaining accurate flow rate information is available. In Heat Exchanger No.3 in the shield coolant system, a secondary means of measurement of flow rate was established for this study. (See Section VI.)

In addition to the five main heat exchangers mentioned above, the secondary coolant system must also supply four air-conditioning units which vary in size from one and one-half to twenty tons. No means of measuring the flow rate to these units is available.

The only means of estimating the total H_2O flow is to valve off all systems except the main heat exchanger and then measure the flow through this unit. This method is inexact in that pressure drops throughout the various systems are in no way matched to the pressure drop across Heat Exchanger No.1, hence the flow conditions are somewhat changed.

2. The temperature of the H_2O entering the cooling tower is not accurately known. Since the secondary coolant system has so many branches and functions, the various outlet temperatures should be combined in a volume average to obtain the temperature of the H_2O entering the tower. This is not possible however as much of this information is not available.

3. The performance of the cooling tower itself is dependent on such quantities as wind velocity and relative humidity which are constantly changing.

The general plan for five megawatt operation includes construction of a new cooling tower of the same capacity as the installed unit to serve one of the aforementioned parallel and identical heat removal systems. In effect this will reduce the heat load on tower No.1 by one-half of the heat load of the auxiliary systems, which will then be shared between the two towers. The principal reactor input to the tower will be increased by 25 per cent from two megawatts to 2.5 megawatts however.

[7-2] COOLING TOWER EXPERIMENT

Design specifications for the cooling tower call for

1000 GPM of light water to be cooled from 103°F to 80°F at a maximum wet-bulb temperature of 72°F and 0-10 MPH wind. The total H_2O flow rate as measured by the method outlined in section 7-1 was found to be approximately 980 GPM with all the flow going to the cooling tower basin and 870 GPM with all the flow going to the top of the cooling tower. If the tower were 100 per cent efficient, one would expect that for zero power input the tower would cool the H_2O to the wet-bulb temperature.

The first cooling tower experiment was designed to find out if flow rate changes (within the design limitations) had any effect on the temperature of the H_2O coming out of the tower. At constant power level the flow rate of the H_2O through the main heat exchanger was cut from 685 GPM to 557 GPM with a corresponding increase in the H_2O δT and the temperature of the H_2O entering the tower. The wet-bulb temperature was measured with a sling psychrometer just before the flow change and the temperature of the H_2O leaving the tower was noted. The system was then allowed to come to thermal equilibrium. The wet-bulb temperature was measured again and the H_2O temperature was recorded. Neither the wet-bulb temperature of the air nor the temperature of the water leaving the tower changed during the experiment.

The conclusion was then drawn that flow rate has no effect on the temperature of the water leaving the tower within the design specifications. The water temperature is depemdent only on the power level and the wet-bulb temperature.

A second experiment was carried out to determine the amount of variation of the H_2O temperature with power level and its dependence on T_{wet}. At various intervals over a three month period from May through July 1962 measurements were made on the wet-bulb temperature and the cooled H_2O temperature as a function of power level.

T_{H1}, the H_2O temperature entering the main heat exchanger and assumed to be the temperature of the water leaving the cooling tower, and T_{wet} were plotted as a function of power level with the results as shown in figure 24. The solid lines are least squares linear fits to the zero power, one megawatt, and two megawatt experimental points. The zero power line does not coincide with the 100 per cent efficiency line because:

1. Even at zero reactor power there is still a heat load on the tower due to the experimental coolant system, the air-conditioning system, and pump heating.
2. The tower is probably not quite 100 per cent efficient.

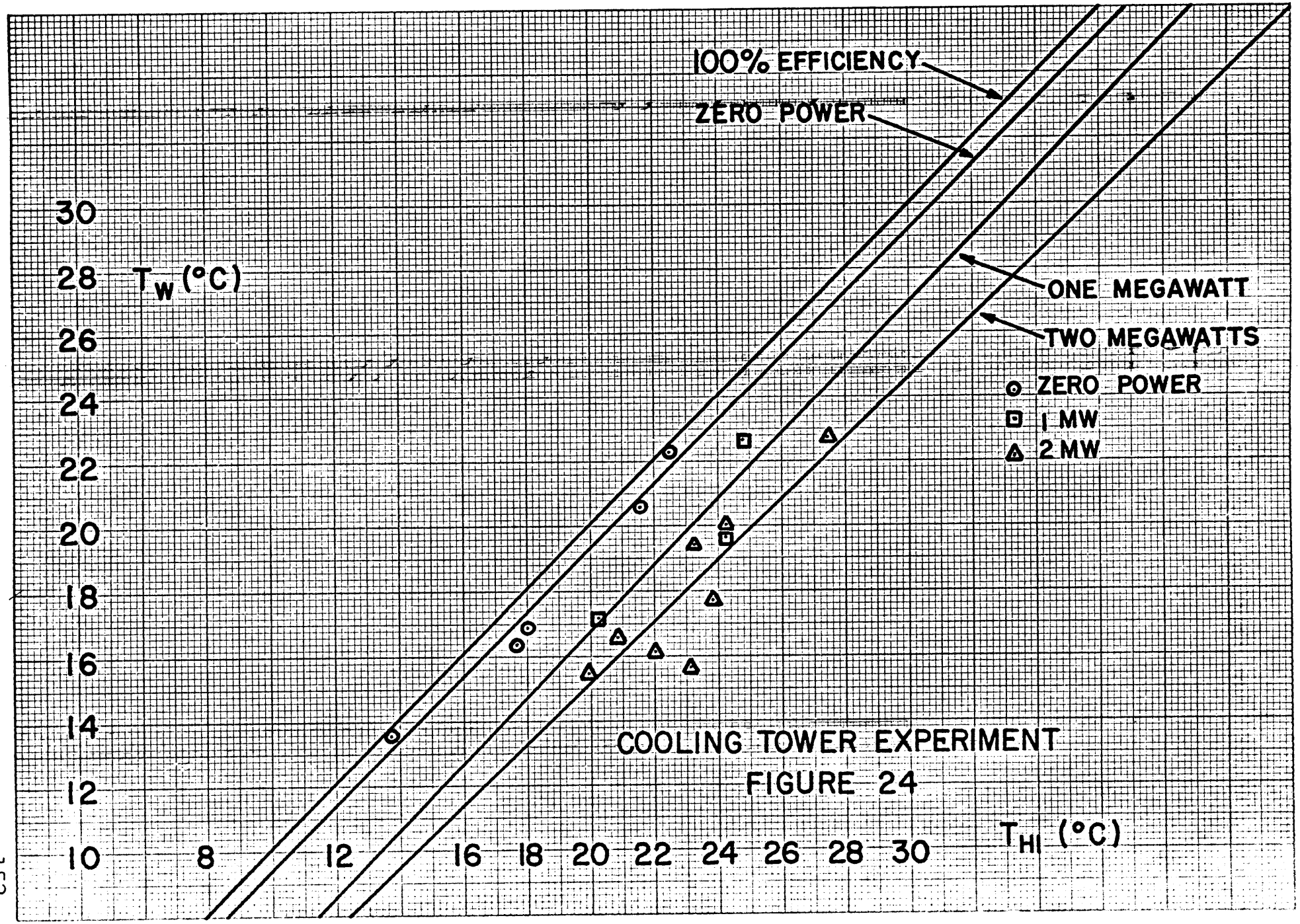

COOLING TOWER EXPERIMENT

FIGURE 24

Averaging out the two megawatt data the conclusion was drawn that the equation

$$T_{H1} = T_{wet} + C_{12}(P) \qquad (7.1)$$

can be used to evaluate the outlet H_2O temperature from the cooling tower. In this equation C_{12} was found to be $2.5^{\circ}C/MW$ and P is the reactor heat load carried by the tower in megawatts.

It should be noted that this value for C_{12} appears to be conservative in that the δT_{H1} between the one megawatt and two megawatt lines on the figure is smaller than the δT_{H1} between the zero power and one megawatt lines. This indicates a trend toward lower δT_{H1}'s at higher power levels.

Using equation 7.1 the H_2O entering the secondary cooling system in general and the main heat exchanger in particular on a day when the wet-bulb temperature is $78^{\circ}F$, will be at a temperature of:

$$\begin{aligned} T_{H1} &= T_{wet} + 2.5^{\circ}C/MW(2.5MW) = \\ &= T_{wet} + 6.25^{\circ}C \\ &= 78^{\circ}F + 11.25^{\circ}F = 89.25^{\circ}F \end{aligned}$$

A power level of only 2.5 MW was used in this equation since two cooling towers will be present with each removing one-half of the primary reactor heat load. The utility of knowing this temperature has already been aptly illustrated in Section V.

In general, one may then conclude that although the method of obtaining equation 7.1 is fairly crude, the equation probably gives fairly good results since it only has to be extended 500 KW above its base of zero to two megawatts. The 500 KW increase in power input to each tower at the new operating level is partially offset by the fact that there will be two towers to share the auxiliary systems heat load now carried entirely by the single tower.

SECTION VIII

SUMMARY AND RECOMMENDATIONS

[8-1] RESULTS

The principal results of this study are as follows:

1. From the standpoint of process system requirements the increase in reactor power to the five megawatt level is feasible and can be accomplished without major difficulties.

2. A reasonable value for the minimum allowable D_2O primary coolant flow for five megawatts was set at 1800 GPM. It was anticipated that normal operating flow rates would be in the vicinity of 2200 GPM.

3. A reasonable value for the maximum temperature of the fuel plate wall at the hottest point in the reactor was found to be 100°C, and a reasonable value for the maximum bulk temperature at the reactor outlet of the D_2O primary coolant was established at 55°C.

4. Based on the values in 2 and 3 above the fuel loading per element is limited. In the center element figure 18 defines the maximum amount of uranium fuel which can be loaded in this central position.

Figure 18, with appropriate corrections from section 3-5, also defines the maximum fuel loading allowable in the other positions in the core lattice. These limits are defined according to the amount of excess reactivity carried in the core.

5. The cooling tower was shown to be able to deliver H_2O to the secondary coolant system at a maximum temperature of 89.25°F on a postulated "hottest summer day." This temperature was found to be independent of flow rate over a reasonable range.

6. It was established that the amount of H_2O flow required in the secondary coolant system to carry the reactor heat load on the postulated "hottest day" was approximately 2300 GPM.

7. It was shown that the shield coolant system will maintain approximately the same shield temperatures at five megawatts as it does at two megawatts provided a small (100 GPM) pump is installed in the secondary side of the system.

[8-2] RECOMMENDATIONS

It is therefore recommended that:

1. An increase in the uranium content of the

fuel elements be considered so as to introduce the necessary reactivity into the core keeping approximately the same number of fuel elements.

2. An additional pump and the necessary supporting equipment be installed in the D_2O system to increase its capacity to an operating range of 2200 to 2400 GPM.

3. A heat exchanger identical to Heat Exchanger No.1 be installed in parallel with Heat Exchanger No.1 to provide sufficient heat exchange capacity to adequately remove the heat load at five megawatts. This heat exchanger should be constructed with an inspection plate so that scaling on the outside of the tube sheet can be monitored.

4. An additional pump and the necessary supporting equipment be installed in the secondary coolant system to increase the H_2O flow capacity to an operating range of 2200 to 2400 GPM.

5. A cooling tower identical to the installed unit be constructed to be operated in parallel with the existing facility.

6. The above components should be installed in two parallel but separate heat removal systems to insure at least partial power operation in the event of a major component failure. Provision for cross flow between

the two systems should also be incorporated.

7. A small pump of approximately 100 GPM capacity be installed in the secondary side of the shield coolant system.

8. A terminal board be installed near the six point temperature recorder and connected directly to the resistance thermometers so that direct measurements of the temperatures can be made. This will eliminate the uncertainty due to the mechanical inaccuracy of the recorder when highly accurate readings are desired.

9. Accessible thermocouple wells be installed in the inlet and outlet pipes to the new cooling tower to facilitate cooling tower measurements.

10. A calibrated orifice and manometer taps be installed in the secondary coolant system at a point where it will measure the total flow rate.

11. Further refinements be made on figure 18 to reflect the changing critical mass as the core size is increased. Calculations in Sections III and IV were made for cores of approximately 2500 grams. Actual operating cores at five megawatts are anticipated to contain approximately 3500 grams. Figure 18 would be highly conservative when applied to these heavier cores.

It is again emphasized that all results of this study are highly conservative. In all cases where a choice existed, the safest or most conservative alternative was selected. It is believed that the results of this study define the operating ranges of the principal process system parameters at five megawatts. Planning based on these figures will provide adequate, compatible process systems for operation of the MITR at that power level.

APPENDIX A

SYMBOLS

Those symbols referred to as general are subscripted to indicate specific applications.

a	annular core region
A	area
A	atomic weight
c	center core region
C	constant, as specified
c_p	specific heat at constant pressure
D	diameter
De	equivalent diameter
e	extended or outer core region
f	friction factor
G	specific mass flow rate, lb/hr ft^2
g	gravitational acceleration
h	vertical coordinate, general
H_1	boundary between core and upper or lower reflector
H_2	outer boundary of upper or lower reflector
i	inner core region

k	conductive heat transfer coefficient
K	constant, general
K.E.	kinetic energy
K(T)	temperature dependent constant
L	length, general
L'	extrapolated core length
m	flow rate, gallons per minute
N	number, general
No	Avogadro's number
Nu	Nussult number
P	power, general
P	pressure
Pr	Prandtl number
Q	heat, BTU
q	heating rate, general
q_o/A	specific heat flux at fuel plate axial centerline
q_1/A	specific heat flux at hot spot on fuel element plate
q_2	heating rate of primary coolant in one fuel element flow channel from the bottom of the core up to the hot spot
r	radial coordinate, general
Rc	boundary between core and radial reflector
Ri	boundary between inner and annular cores
Ro	outer boundary of radial reflector
R(r)	radial flux factor, general

$\bar{R}(r)$	radial flux factor in unit cell centered at r averaged in radial direction
$\bar{R}(0)$	radial flux factor in center unit cell averaged in radial direction
$\bar{R}_F(r)$	radial flux factor in fuel region of unit cell centered at r averaged in radial direction
Re	Reynolds number
S_h	heat transfer surface area
s_h	heat transfer perimeter
T	temperature, general
Tc	coolant bulk temperature, general
Ti	reactor inlet temperature
To	reactor outlet temperature
Tw_{max}	maximum temperature of fuel element plate wall
U	overall coefficient of heat transfer BTU/hr ft^2 ^oF
V	volume, general
w	mass flow rate, lb/hr
x	axial position of hot spot
X(r)	$\bar{R}(r)/\bar{R}(0)$ = ratio of average radial flux factor in unit cell centered at r to average radial flux factor in central unit cell
Y(r)	ratio of average flux in fuel region of unit cell to average flux in entire unit cell
Z(h)	axial flux factor
$\bar{Z}_F$	axial flux factor in fuel region of unit cell averaged over axial direction

β	delayed neutron fraction
βex	excess reactivity
γ	gamma radiation
γ	ratio of heat released in coolant to heat transferred through cladding
δT	temperature difference, general
δTc	coolant temperature difference
δT_f	film temperature difference
δT_{LM}	log mean temperature difference between fluids in a heat exchanger
ε	density lb/ft^3
μ	dynamic viscosity, lb/hr ft
σ	microscopic cross section
Σ	macroscopic cross section
$\sum$	summation
φ	thermal neutron flux, general
$\bar{\varphi}$	average flux in unit cell
$\bar{\varphi}_F$	average flux in fuel region of unit cell
φ_o	flux at center point of core
φ_{max}	maximum flux at surface of fuel element box
φ_{Fmax}	maximum flux in fuel bearing portion of fuel element box
$\bar{\bar{\varphi}}_{F_j}$	thermal neutron flux in fuel region of jth fuel element averaged in both radial and axial directions

SUBSCRIPTS

a	annular core region
c	coolant
ch	channel
D	D_2O
e	extended or outer core region
F	fuel region
f	film
f	fission
H	H_2O
i	inner core region
i	inside
i	inlet
M	moderator region
o	outlet
o	outside
p	primary
R	reactor as a whole
S	shield
s	secondary
sc	scale
T	total

w	wall
x	corss section
1	entrance to heat exchanger
2	exit from heat exchanger
25	U^{235} properties

FOOTNOTES

1. Charles L Larson, Reactivity Studies of a Heavy Water Moderated, Highly Enriched Uranium Reactor, pp. 134-139.

2. Paul Steranka, Final Two Megawatt Calculations, pp. 1-13.

3. Richard L. Mathews, Flux Data,(unpublished)

4. Larson, op cit., p. 134.

5. Ibid., pp. 249-250.

6. Ibid., pp. 150-152.

7. Ibid., p. 135

8. Ibid., p. 139.

9. Francis A. Wolak, Heat Dissipation in the MIT Reactor, p. 18.

10. Larson, op cit., pp. 190-191

11. David D. Lanning, et al., Draft Letter to the AEC Requesting Ammendment of License (unpublished), p 13.

12. Larson, op cit., p. 139.

13. Ibid., p. 251.

14. Ibid., p. 160.

15. Ibid., p.192.

16. Ibid., p. 168.

17. Mathews, op cit.,

18. Paul J. Marto, Measurement of Surface temperatures of an Irradiated MITR Fuel Element During Steady State and Transient Operating Conditions, figure 4

19. Peter Loeb and John H. Nicklas, Hydraulic Measurements and Adjustments of the MIT Reactor Vessel and Fuel Elements,

20. Harold Etherington et al, Nuclear Engineering Handbook, p. 9-87.

21. Steranka, op cit., pp. 23-40.

22. Marto, op cit., figure 5.

23. Warren M. Rohsenow, Heat Transfer with Boiling, MIT 2.521 Course Notes. p. 9.

24. Ibid, p. 5.

25. Wolak, op cit., p. 23.

26. Steranka, op cit., p. 28.

27. Marto, private communication 5/14/62.

28. Larson, op cit., p. 160.

29. Edward A. Mason, Steady State Temperature Distribution Along Coolant Channels, MIT 22.23 Course Notes, pp. 1-8.

30. Lanning, op cit., p. 13.

31. Larson, op cit., p. 84.

32. A. E. Profio, Operating Manual for the MIT Reactor,

33. Larson, op cit., p. 88.

34. Ibid, p. 76.

35. William H. McAdams, Heat Transmission, p. 425.

36. Homeyer, MIT M.S. Thesis, 1959, p. 13.

BIBLIOGRAPHY

Eckert, E.R.G. and Drake, R.M.Jr.,Heat and Mass Transfer, Second Edition (New York: McGraw-Hill Book Co.Inc., 1959).

Eshback, Ovid W. Ed.,Handbook of Engineering Fundamentals, (New York: John Wiley and Sons, 1952).

Etherington, Harold Ed., Nuclear Engineering Handbook, (New York: McGraw-Hill Book Co,Inc.,1958).

Faires, Virgil M.,Applied Thermodynamics,(New York: McMillan Co. 1952).

Homeyer, W.G., Thermal Power Calibration of the MITR, (Cambridge: MIT M.S.Thesis, 1959).

Lanning, David D., Draft Letter to the AEC, Subject: Amendment of License, Unpublished, 1962.

Lanning, David D. and Steranka, P.,Operation of the MIT Research Reactor at Power Levels up to Two Megawatts, Unpublished, 1960.

Larson, Charles L., Reactivity Studies of a Heavy Water Moderated, Highly Enriched Uranium Reactor, (Cambridge: MIT Sc.D. Thesis, 1959).

Loeb, Peter, and Nicklas, John H., Hydraulic Measurements and Adjustments of the MIT Reactor Vessel and Fuel Elements, (Washington: Nuclear Products Division of A.C.F. Industries, 1957). Unpublished.

McAdams, William H., Heat Transmission,(New York: McGraw-Hill Book Co Inc., 1954).

Marto, P., Measurement of Surface Temperatures of an Irradiated MITR Fuel Element During Steady State and Transient Operating Conditions, (MIT 22.42 Course Report, 1962). Unpublished.

Mason, E.A., Steady State Temperature Distribution Along Coolant Channels in Nuclear Reactors,(MIT 22.23 Course Notes, 1961). Unpublished.

Mathews, R.L. Experimental Relative Neutron Flux Data by Co^{60} Wire Activation (unpublished).

Profio, A.E., Operating Manual for the MIT Reactor, (Unpublished),

Rohsenow, Warren H., Heat Transfer with Boiling,(MIT 2.521 Course Notes, 1960). Unpublished.

Sokolnikoff, I.S. and Redheffer, R.M. Mathematics of Physics and Modern Engineering,(New York: McGraw-Hill Book Co. Inc., 1958).

Steranka, P., Five Megawatt Calculations,(Unpublished)

Wolak, Francis A.,Heat Dissipation in the MIT Reactor, (Cambridge: MIT M.S. Thesis, 1958).